Investigation of initial attachment and biofilm formation of mesophilic leaching bacteria in pure and mixed cultures and their efficiency of pyrite dissolution

Dissertation

zur Erlangung des akademischen Grades eines

Doktors der Naturwissenschaften

- Dr. rer. Nat. -

vorgelegt von

Bianca Michaela Florian

geboren in Mülheim an der Ruhr

Institut für Chemie

der

Universität Duisburg-Essen

2012

Die vorliegende Arbeit wurde im Zeitraum von Februar 2008 bis Februar 2012 im Arbeitskreis von Prof. Dr. W. Sand am Institut für Chemie, Biofilm Centre der Universität Duisburg-Essen durchgeführt.

Tag der Disputation: 11.05.2012

Gutachter:	Prof. Dr. W. Sand
	Prof. Dr. H-C. Flemming
Vorsitzender:	Prof. Dr. G. Jansen

to my friends…

Thought is impossible without an image
Aristoteles, 325 n. Chr.

Acknowledgments

I would like to thank:

Prof. Dr. Wolfgang Sand, for being my supervisor, for his guidance, encouragement, support and invaluable help throughout this project

Prof. Dr. Hans-Curt Flemming, for accepting the task of being my co-adviser

Vattenfall, MIBRAG and **GMB**, for financial support

Nanni, who was always been interested in my work, for her comments, cheerfulness and friendship

Andrzej, for his technical advice and assistance with the AFM

Felipe, for his professional assistance and advice

My colleagues: **Nanni, Andrzej, Anne, Mariël, Christian, Claudia, Mario, Beate, David, Igor, Petra, Tilman, Sören, Jürgen, Robert, Markus, Vanessa, Mark, Rui-yong, Agata, Cindy and Jens** for all their support and a funny good time

Christian, for his love, understanding and assistance during this project

My friends, for their cheerfulness and friendship during all the time

Carsten, who always pointed out my lack of knowledge by asking extraordinary questions

My parents, granny and brother, for understanding and all your love

Special thanks also go to Christian, Nanni, Andrzej, Mario, Susi and Anne for proofreading

… to all those who haven't believed in me…

and therewith aroused my ambition to complete this project!

Table of Contents

List of Figures

List of Tables

Glossary

A.f.	*Acidithiobacillus ferrooxidans*
A.t.	*Acidithiobacillus thiooxidans*
AFM	atomic force microscopy
AMD	acid mine drainage
ARD	acid rock drainage
ATCC	American type culture collection
Cy3	cyanine dye 3
ConA	concanavalin A (Lectin of Canavalia ensiformis)
DAPI	4’,6-diamino-2-phenylindole
DNA	deoxyribonucleic acid
DSMZ	Deutsche Stammsammlung von Mikroorganismen und Zellkulturen
EPS	extracellular polymeric substances
FISH	fluorescence in situ hybridization
FITC	fluorescein-isothiocyanate
HPLC	High-performance liquid chromatography
IC	Ion-exchange chromatography
L.f.	*Leptospirillum ferrooxidans*
M	molarity
MS	metal sulfide
n	numbers of repetition
n.d.	not detected
NAD	nicotinamid-adenin-dinucleotid
p.a.	pro analysi
PBS	phosphate buffer solution
rRNA	ribosomal ribonucleic acid
spp	species pluralis
TRITC	tetramethylrhodamine-5-isothiocyanate
xg	-times acceleration of gravity (9,81 m/s^2)

Abstract

The objective of this thesis was to investigate initial attachment and biofilm formation to pyrite surfaces of the mesophilic, acidophilic leaching bacteria *Leptospirillum ferrooxidans* DSM 2705, *Acidithiobacillus ferrooxidans* ATCC 23270 and *Acidithiobacillus thiooxidans* DSM 622 in pure and mixed cultures and their efficiency in pyrite dissolution.

The highest initial attachment of pure cultures to pyrite grains was detected for *Leptospirillum ferrooxidans* DSM 2705 and *Acidithiobacillus thiooxidans* DSM 622. However, *Leptospirillum ferrooxidans* DSM 2705 showed the highest leaching rates of pure cultures, whereas *Acidithiobacillus thiooxidans* DSM 622 is not able to leach pyrite at all. The highest attachment rate for mixed cultures to pyrite grains was detected for *Acidithiobacillus ferrooxidans* ATCC 23270 with *Leptospirillum ferrooxidans* DSM 2705. The highest leaching rates were detected for the pure culture of *Leptospirillum ferrooxidans* DSM 2705 and all mixed cultures including this strain. Contrary to the high attachment of the mixed culture composed of cells of *Acidithiobacillus ferrooxidans* ATCC 23270 and *Acidithiobacillus thiooxidans* DSM 622 to pyrite grains, leaching of pyrite grains was low. The investigation of bacterial attachment and leaching of pyrite grains indicated that high attachment rates do not necessarily correlate with high leaching rates.

In particular, initial attachment of *Acidithiobacillus ferrooxidans* ATCC 23270, *Acidithiobacillus thiooxidans* DSM 622 and *Leptospirillum ferrooxidans* DSM 2705 in pure and mixed cultures to pyrite coupons was investigated. A combination of atomic force microscopy and epifluorescence microscopy allowed the visualization of cells, biofilms and pyrite surfaces at the same side with high spatial accuracy.

Visualization of cells on pyrite coupons showed heterogeneous attachment and biofilm formation by both pure and mixed cultures. The bacteria attached as single cells or in small cell clusters to the mineral surface. Only cells of *Leptospirillum ferrooxidans* DSM 2705 showed rarely cluster formation with higher cell numbers on the pyrite surfaces. However, large areas of the pyrite surface remained cell-free, whereas, others where highly colonized. The highest attachment to pyrite coupons was determined for the pure culture of *Leptospirillum ferrooxidans* DSM 2705 and the mixed culture of *Acidithiobacillus ferrooxidans* ATCC 23070 with *Acidithiobacillus thiooxidans* DSM 622 and *Leptospirillum ferrooxidans* DSM 2705. The investigation of individual species in mixed cultures on pyrite

coupons showed heterogeneously distributed cells with no physical interspecies contact. Depending on the composition of the mixed culture individual species showed increased (*Acidithiobacillus ferrooxidans* ATCC 23270) or decreased (*L. ferrooxidans* DSM 2705) attachment to pyrite coupons.

Attachment of pure cultures of *Leptospirillum ferrooxidans* DSM 2705, *Acidithiobacillus ferrooxidans* ATCC 23270 and *Acidithiobacillus thiooxidans* DSM 622 considerable changed, if coupons were previously colonized by biofilms whose cells were heat-inactivated before secondary colonization. Increased attachment for *Acidithiobacillus ferrooxidans* ATCC 23270 and *Acidithiobacillus thiooxidans* DSM 622 and decreased attachment for *Leptospirillum ferrooxidans* DSM 2705 was detected.

However, no significant difference in leaching of virgin pyrite coupons compared to precolonized pyrite coupons by pure cultures of *Leptospirillum ferrooxidans* DSM 2705 and *Acidithiobacillus ferrooxidans* ATCC 23270 was detected.

1. Introduction

1.1. Bioleaching

Bioleaching is the dissolution of metal sulfides to soluble metal sulfates and sulfuric acid by specialized iron- and/or sulfur-compound oxidizing bacteria or archaea (Colmer and Hinkel 1947, Schippers et al. 1999a, Kelly and Wood 2000). Sulfide minerals such as pyrite (FeS_2) or chalcopyrite ($CuFeS_2$) exist in the crust of the earth in the form of ore bodies in association with metals such as copper, gold or zinc. Bacterial leaching can occur as an unwanted natural process called acid rock drainage (ARD) or acid mine drainage (AMD). These processes are accompanied with acidification and heavy metal pollution of water bodies (Barnes and Romberger 1968; Gray 1996). Acid mine drainage is a significant environmental problem worldwide.

Bioleaching is also used in industrial applications (biomining) to separate valuable metals from low grade ores. The industrial bacterial leaching processes are environmentally friendly compared to other metal winning processes based on pyro-metallurgy due to the reduced production of toxic waste (Rohwerder and Sand 2007a).

The use of microorganisms in the extraction of metals from ores can be traced back to the Romans as described by Gaius Plinius Secundus at 23 - 79 A.D (König and Winkler 1989). However, the first reports that bacteria are involved in leaching of zinc and iron sulfides did not come up until the 1920s (Waksman and Joffe 1922). The essential role of bacteria in leaching processes was unknown until the middle of the 20th century (Colmer and Hinkel 1947). Nowadays, microbial recovery of heavy metals is established in biotechnological techniques like tank or heap leaching, with significant economic impact. A diverse group of bacterial species is used in large-scale bioleaching facilities to leach metals of value such as copper, zinc, nickel, cobalt or gold from sulfide minerals (Bosecker 1997,). Biological leaching is also applied for coal depyritisation processes to produce coal with extremely low mineral- (ash), pyrite- and sulfur contents (Stevens et al. 1993).

On one hand, unwanted bacterial leaching processes have to be reduced and new strategies for mitigation and remediation of AMD and ARD are necessary. On the other hand industrial leaching processes have to be optimized with regard to increased process speed and efficiency together with reduced process cost.

1.2. Mechanisms of bioleaching

Metal sulfides can be classified into acid-soluble (e.g. chalcopyrite) and acid-insoluble (e.g. pyrite). The acid solubility, determined by the electron configuration, is the relevant criterion for the determination of the pathway of dissolution (Tributsch and Bennett 1981a, Schippers and Sand 1999a, Edelbro et al. 2003). Acid soluble metal sulfides have valence bands derived from the metal and the sulfur atom orbitals and can be attacked by protons, whereas, metal sulfides with valence bands derived from orbitals of the metal atoms cannot be attacked by protons and are acid insoluble (Grundwell 1988).

Two different reaction mechanisms for the dissolution of metal sulfides are proposed: the thiosulfate mechanism for non acid-soluble metal sulfides and the polysulfide mechanism for acid-soluble metal sulfides (Schippers 1998, Schippers and Sand 1999a, Sand et al. 2001). The pathways are named after the first intermediate generated in the processes.

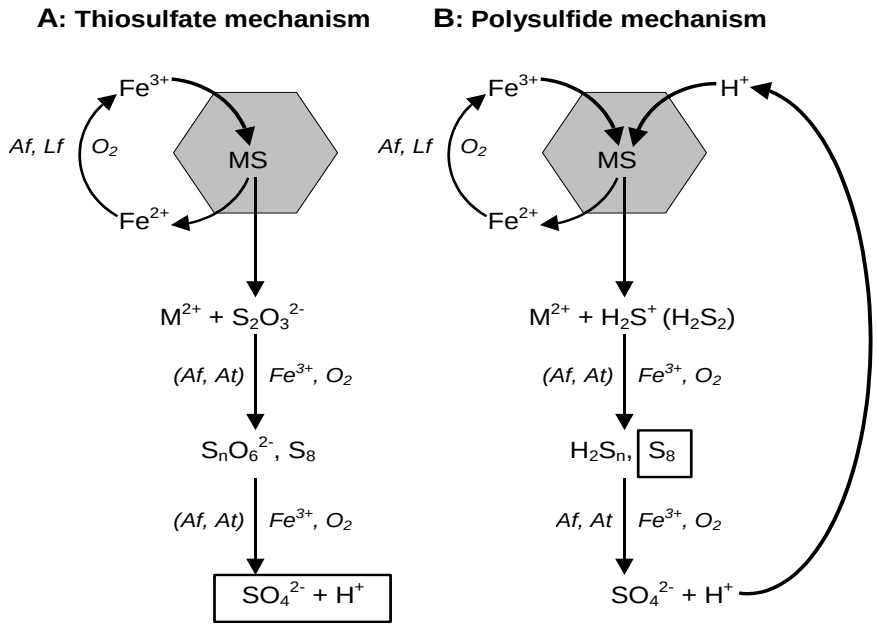

Figure 1: Schematic illustration of the two metal sulfide bioleaching pathways, the thiosulfate mechanism (A) and polysulfide mechanism (B) with intermediates and final products (Schippers and Sand 1999a)
MS = metal sulfide, M = metal cation, *Af = Acidithiobacillus ferrooxidans*, *Lf = Leptospirillum ferrooxidans*, *At = Acidithiobacillus thiooxidans*.

Acid insoluble metal sulfides such as pyrite (FeS_2), molybdenite (MoS_2) and tungstenite (WS_2) are oxidized via the thiosulfate pathway (Schippers and Sand 1999a). Oxidation processes are indispensable for the dissolution of these metals. Six successive one-electron

oxidation steps are conducted to break the chemical bonds between the sulfur- and the metal-atom. Iron(III) ions are the relevant oxidation agents and are reduced to iron(II) ions (Equation 1; Moses et al. 1987, Luther III 1987, Schippers et al. 1996, Sand et al. 2001, Rohwerder and Sand 2007a). The iron(II) ions are oxidized by acidophilic iron-oxidizing bacteria such as *Acidithiobacillus ferrooxidans* (*A. ferrooxidans*) or *Leptospirillum ferrooxidans* (*L. ferrooxidans*) and thereby regenerated as oxidizing agent (Equation 3; Temple and Colmer 1951, Kelly and Wood 2000). The first free sulfur compound in this process is thiosulfate (Equation 1). Thiosulfate is finally oxidized via tetrathionate or other polythionates to sulfate (Equation 2; Schippers et al. 1996, Schippers and Sand 1999a, Rohwerder and Sand 2007a). Bacteria or archaea such as *A. ferrooxidans*, *Acidithiobacillus thiooxidans (A. thiooxidans)* or *Acidianus brierleyi* generate energy by oxidizing sulfur or the intermediate sulfur compounds to sulfate and protons (Equation 4; Schippers, 2007). Elemental sulfur (10 to 20 %) is produced in the absence of sulfur compound oxidizing bacteria (Rohwerder et al. 1998, Schippers and Sand 1999a).

Equation 1 $FeS_2 + 6\ Fe^{3+} + 3\ H_2O \rightarrow S_2O_3^{2-} + 7\ Fe^{2+} + 6\ H^+$

Equation 2 $S_2O_3^{2-} + 8\ Fe^{3+} + 5\ H_2O \rightarrow 2\ SO_4^{2-} + 8\ Fe^{2+} + 10\ H^+$

Equation 3 $2\ Fe^{2+} + 0.5\ O_2 + 2\ H^+ \rightarrow 2\ Fe^{3+} + H_2O$

Equation 4 $0.125\ S_8 + 1.5\ O_2 + H_2O \rightarrow SO_4^{2-} + 2H^+$

Acid soluble metal sulfides such as sphalerite (ZnS), galena (PbS), arsenopyrite (FeAsS), chalcopyrite ($CuFeS_2$) or hauerite (MnS_2) are dissolved by the attack of protons and iron(III) ions. Protons can bind valence band electrons of the metal sulfide. After binding of two protons, hydrogen sulfide (H_2S) is liberated and can be oxidized by iron(III) ions to a sulfide cation (H_2S^+). This cation can spontaneously dimerise to a free disulfide (H_2S_2; Equation 5). H_2S_n can be further oxidized via higher polysulfides and polysulfide radicals to elemental sulfur (Equation 6; Streudel 1996). The liberated sulfur compounds are oxidized abiotically as well as biotically by bacteria or archaea, e.g. *Acidithiobacillus* spp. or *Sulfolobus* spp. Elemental sulfur is bacterially oxidized to sulfuric acid (Equation 7) which provides new protons for the polysulfide pathway (Schippers 1998, Schippers and Sand 1999a, Sand et al. 2001, Rohwerder and Sand 2007a).

Equation 5 $0.5\ H_2S_n + Fe^{2+}\ (n \geq 2)$

Equation 6 $0.5\ H_2S_n + Fe^{3+} \rightarrow 0.125\ S_8 + Fe^{2+} + H^+$

Equation 7 $0.125\ S_8 + 1.5\ O_2 + H_2O \rightarrow SO_4^{2-} + 2\ H^+$

1.3. Contact- and non contact-mechanism

Bacteria play a decisive role in leaching via the (re)generation of iron(III) ions and production of sulfuric acid. Two bacterial mechanisms are proposed, the non-contact and contact mechanism; a schematic overview is shown in Figure 2 (Sand et al. 2001, Rawlings 2002).

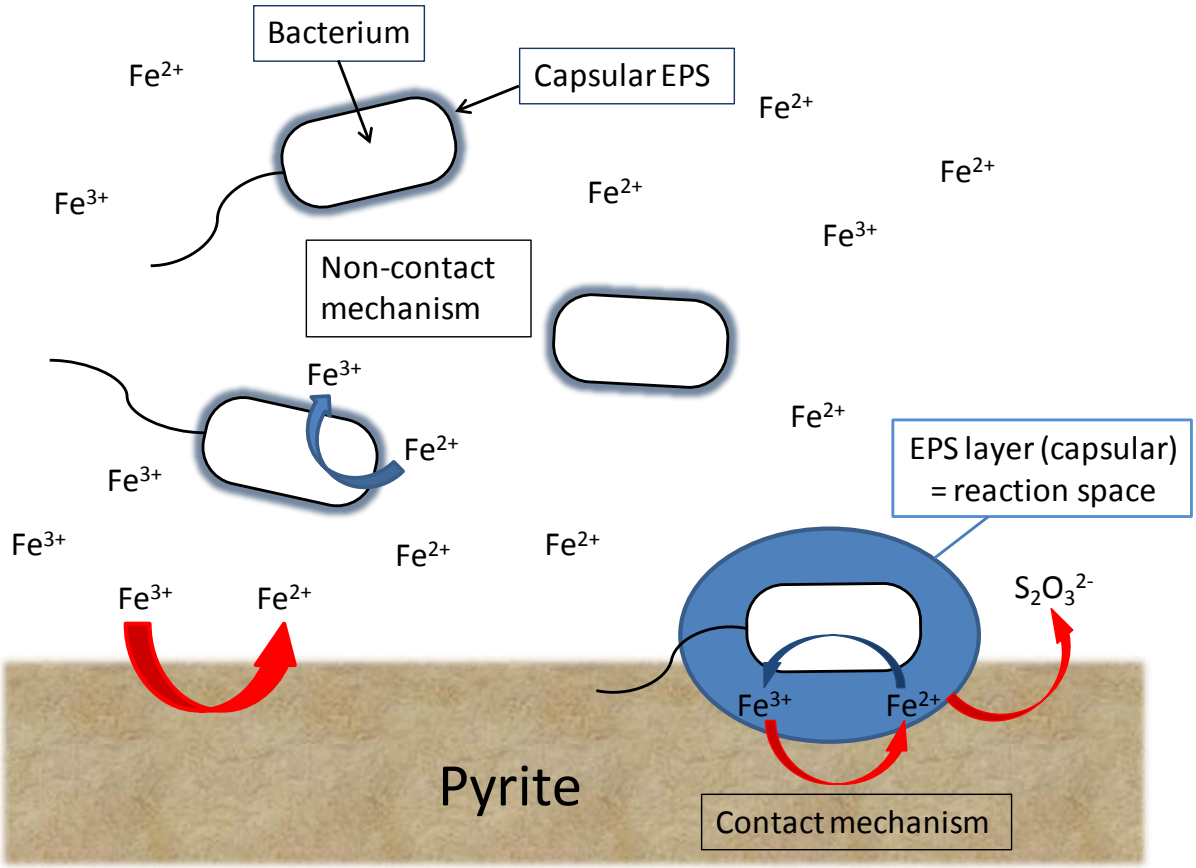

Figure 2: Schematic overview of the non-contact and the contact leaching mechanisms (Figure modified from Rohwerder et al. 2003b)
Planktonic cells oxidize iron(II) ions in the non-contact mechanism. Iron(III) ions attack the metal sulfide and are reduced to iron(II) ions.
Attached cells are embedded in EPS on the metal sulfide surface. Iron(III) ions complexed in the EPS facilitate the dissolution of metal sulfides. Produced iron(II) ions are directly re-oxidized by the attached bacteria to iron(III). Thereby, the attacking agent is regenerated.

The non-contact mechanism is based on the oxidation of iron(II) ions by planktonic cells in the bulk solution. The produced iron(III) ions are the oxidation agent for the mineral sulfides and are reduced by the mineral dissolution process to iron(II) ions.
The contact mechanism is based on the attachment of leaching organisms to the mineral sulfide surface. The electrochemical processes, resulting in dissolution of the mineral, occur at the interface between the organisms and the mineral surface. The dissolved iron(II) ions are directly oxidized to iron(III) ions and are again the oxidizing agent for the mineral sulfide (Sand et al. 2001).

1.4. Influence of leaching rate

Rodríguez and co-workers found that high mineral sulfide dissolution rates were most likely due to increased initial bacterial attachment to the mineral (Rodríguez et al. 2003). However, bacterial activity as well as the microbial biomass is an important parameter influencing leaching rates. Besides microbiological factors, several other factors can influence mineral leaching rates such as types of crystal structure, conductivity, redox potential and particle size of the mineral. But also temperature, acidity and iron ion content of the media can influence the leaching rate (Natarajan 1990). Iron(III) ions are identified as limiting factor of the oxidation rate (Singer and Stumm 1970, Moses et al. 1987).

1.5. Leaching organisms

Diverse acidophilic microorganisms are described in leaching processes. Identified are mesophilic, moderate thermophilic and thermophilic metal sulfide oxidizing bacteria as well as extremely thermophilic archaea. Most organisms grow chemolithoautotrophically and fix carbon dioxide. Bacteria like *Proteobacteria* (*Acidithiobacillus* spp.; formerly named *Thiobacillus* spp.), *Nitrospira* (*Leptospirillum* spp.), *Actinobacteria* (*Acidimicrobium ferrooxidans*) and *Firmicutes* (*Alicyclobacillus disulfidooxidans*) belong to the mesophilic and moderately thermophilic microorganisms. Mesophilic or moderately thermophilic archaea are e.g. *Euryarchaeota* (*Ferroplasma* spp.). All thermophilic metal oxidizers belong to the archaeal phylum *Crenarchaeota* within the order *Sulfolobales*; family *Sulfolobaceae*.

This study focused on three mesophilic iron- and/or sulfur-oxidizing bacteria; *Acidithiobacillus ferrooxidans* ATCC 23270, *Acidithiobacillus thiooxidans* DSM 622 and *Leptospirillum ferrooxidans* DSM 2705.

A. ferrooxidans is the most studied metal sulfide oxidizing organism and serves in many studies as reference organism (Sand et al. 1992, Leduc and Ferroni 1994, Kelly and Wood 2000, Karavaiko et al. 2003, Valdés et al. 2007, Beard et al. 2011). It was first described by Temple and Colmer (Colmer and Hinkel 1947, Temple and Colmer 1951) and later on reclassified by Kelly and Wood (Kelly and Wood 2000). Strains of *A. ferrooxidans* are detected regularly in acidic environments, e.g. in acid mine drainage, industrial tank- and more abundant in heap-leaching operations (Brierley 1997, Rawlings 2005, Schippers and Bosecker 2005, Schippers 2007, Yang et al. 2007, Kock and Schippers 2008, Schippers et al. 2010). Temple and Colmer described *A. ferrooxidans* as Gram-negative non-spore forming motile rod (Temple and Colmer 1951). Flagella and pili were observed for several strains. However, neither flagella nor the genes encoding them have been detected for the type strain ATCC 23270 (Valdés et al. 2007, Li et al. 2010).

A. ferrooxidans cells are described as rod-shaped (width: 0.4 - 0.5 µm, length: 1 - 3 µm), obligately acidophilic (pH < 4.0) chemolithoautotrophs. They grow at pH 1.3 up to 4.5 (optimum 2.5) within a temperature range of 10 to 37 °C (optimum 30 - 35 °C). The G + C content is 58 - 59 mol % (Harrison 1982, Schippers 2007). *A. ferrooxidans* is capable to oxidize iron(II) ions, sulfur compounds like elemental sulfur, thiosulfate, trithionate, tetrathionate, sulfide and hydrogen (Temple and Colmer 1951, Landesman et al. 1966, Espejo and Romer 1987, Hazeu et al. 1988, Drobner et al. 1990, Schippers et al. 1996, Valdés et al. 2007). It grows anaerobically with sulfur compounds or hydrogen as electron donor and Fe(III) ions as electron acceptor at extremely low pH values (Brock and Gustafson 1976, Sand 1989, Pronk et al. 1992, Hongyu et al. 2011). Furthermore, metal sulfides such as pyrite (FeS_2), arsenopyrite (AsFeS), chalcopyrite ($CuFeS_2$), bornite (Cu_5FeS_4), covellite (CuS), galena (PbS), millerite (NiS) as well as synthetic metal sulfides CdS, CoS, CuS, Cu_2S, FeS, MnS, MoS_2, NiS, PbS, SnS and ZnS can be oxidized by *A. ferrooxidans* (Silver and Thorma 1974, Sakaguchi et al. 1976, Torma and Sakaguchi 1978, Tributsch and Bennett 1981a, Tributsch and Bennett 1981b, Pistorio et al. 1994, Tuovinen et al. 1994, Garcia et al. 1995, Nagaoka et al. 1999, Bevilaqua et al. 2010). CO_2 is fixed by means of the Calvin-Benson Cycle (DiSpirito and Tuovinen 1982a, Valdés et al. 2007). Diazotrophic growth of

A. ferrooxidans by N_2 assimilation has been reported (Mackintosh 1978, Norris et al. 1995, Valdés et al. 2007).

Acidithiobacillus thiooxidans was first described by Waksman and Joffe in 1922 (Waksman and Joffe 1922). Strains were isolated from acidic environments such as soil, sulfur deposits or mine waste. In tank- or heap leaching operations *A. thiooxidans* occurs together with iron oxidizers like *A. ferrooxidans* or *Leptospirillum ferrooxidans* (Waksman and Joffe 1922, Gomez and Bosecker 1999, Rzhepishevska et al. 2005, Rawlings 2005, Jones et al. 2011). Strains are growing in pH-ranges of 0.5 up to 5.5 (optimum of 2.0 - 3.0) within temperature ranges of 10 to 37 °C (optimum 28 – 30 °C; Schippers 2007). It is a Gram-negative, obligatory autotrophic bacterium and can fix CO_2 via the Calvin Benson cycle (Schippers 2007, Valdés et al. 2007). The G + C content is 52 - 53 mol % (Harrison 1982, Schippers 2007). It is motile by means of a polar flagellum (Doetsch et al. 1967) and can grow using elemental sulfur, thiosulfate or tetrathionate (Waksman and Joffe 1922, Rittenberg and Grady 1950, Suzuki 1965, Barton and Shively 1968, Suzuki et al. 1992, Chan and Suzuki 1994). *A. thiooxidans* is incapable of oxidizing iron(II) ions or pyrite, but in mixed cultures with *L. ferrooxidans* growth has been shown by oxidizing sulfur which has been formed by *L. ferrooxidans* (Bacela-Nicolau and Johnson 1999, Kelly and Wood 2000). However, it can grow with acid soluble minerals like covellite, galena, and sphalerite (Lizama and Suzuki 1991, Pistorio et al. 1994, Curutchet et al. 1995, Schippers and Sand 1999a).

Leptospirillum ferrooxidans was isolated by Markosyan 1972 and validly described by Hippe 2000 (Markosyan 1972, Hippe 2000). *L. ferrooxidans* is regularly found in mixed cultures together with sulfur-oxidizing microorganisms in bioleaching operations as well as in acid mine drainage environments (Battaglia et al. 1994, Goebel and Stackebrandt 1994, Schrenk et al. 1998, Bond et al. 2000, Rawlings 2002, Okibe et al. 2003, Rawlings 2005). It is a Gram-negative, obligate aerobic, chemolithoautotrophic, non-spore forming acidophilic iron-oxidizer (Pivovarova et al. 1981, Sand et al. 1992, Hippe 2000). Its G + C content is 52 mol % (Harrison and Norris 1985). Growth was observed between pH 1.2 up to 4.0 with an optimum between 1.5 - 3.0 at temperatures of 28 - 30 °C (Sand et al. 1992). CO_2 is fixed by the Benson-Calvin cycle (Balashova et al. 1974, Tyson et al. 2004). Nitrogen fixation was described by Norris, Parro and co-workers (Norris et al. 1995, Parro and Moreno-Paz 2003, Parro and Moreno-Paz 2004). *L. ferrooxidans* cannot oxidize any sulfur compound (Balashova et al. 1974, Sand et al. 1992). But it is able to oxidize e.g. pyrite, sphalerite and

chalcopyrite in pure cultures (Norris 1983, Sand et al. 1992, Schippers et al. 1996, Florian et al. 2011). Young cultures consist of *Vibrio*-like cells, older cultures of spirilla-shaped cells with up to 3 - 5 turns (Harrison and Norris 1985, Sand et al. 1992, Hippe 2000, Rojas-Chapana and Tributsch 2004). Cells are motile with a corkscrew-like motion by a single polar flagellum (Harrison and Norris 1985, Hippe 2000). Cultures grown on ferrous iron in shake flask tend to form aggregates consisting of slime-embedded cells (Harrison and Norris 1985).
Leaching bacteria like *Acidithiobacilli* or *Leptospirilli* obtain their energy by coupling ferrous ion, sulfur and/or metal sulfide oxidation to the reduction of O_2. This process is presented by the half-reaction, whereby O_2 is reduced to H_2O (Equation 8):

Equation 8 $2e^- + ½\ O_2 + H^+ \rightarrow H_2O$

Consecutively, NADH and ATP are generated in electron and H^+ consuming processes.
Several biological pathways for degradation of sulfur compounds, iron(II) oxidation and the electron transport have been published (Ingledew 1982, Rohwerder and Sand 2003a, Rohwerder and Sand 2007b, Quatrini et al. 2009, Bird et al 2011).

A. ferrooxidans, *A. thiooxidans* and *L. ferrooxidans* were usually found in mixed cultures with several other species. The composition of communities varies spatially and seasonally, it correlates with geochemical and physical conditions like pH, temperature, conductivity and humidity (Hallmann et al. 1992, Schippers et al. 1995, Edwards et al. 1999, Bond and Banfield 2001, Barker and Banfield 2003, Kock et al. 2007, Yin et al. 2007, Kock and Schippers 2008). Laboratory leaching experiments showed higher dissolution rates of mineral sulfides in mixed cultures compared to pure cultures, especially in mixed cultures of iron- and sulfur-oxidizing microorganisms. The sulfur-oxidizing organisms increase the leaching rates by removing sulfur-rich products that accumulate on mineral surfaces (Norris and Kelly 1978, Dopson and Lindström 1999, Qui et al. 2005, Akcila et al. 2007, Fub et al. 2008, Zhang et al. 2008, Okibe and Johnson 2009).

Little is known about unique environmental niches and specific function in bioleaching communities composed of single species. Beneficiation of each other seems to play a role in biofilm formation and attachment of bacteria to mineral surfaces. *Ferroplasma* spp. has been attributed to play an important role in some leaching habitats (Edwards et al. 2000). But no genes involved in EPS production have been detected so far (Rohwerder and Sand 2007a). *Leptospirillum* spp., whose genome contains genes for EPS production, causes aggregate

formation already in bulk solution by producing high amounts of EPS. Less attaching organisms were stimulated to attach and establish themselves in a mixed biofilm on pyrite surfaces. The sulfur oxidizer *Acidithiobacillus caldus* attaches less than e.g. the sulfur oxidizer *A. thiooxidans* to pyrite in pure cultures, however, in mixed cultures with *Leptospirillum ferriphilum* the tendency to attach increases (Noël et al. 2010, Florian et al. 2011).

1.6. Bacteria on pyrite

1.6.1. Bacterial attachment and biofilm formation

According to the proposed contact mechanism, bacterial attachment and biofilm formation on mineral surfaces is significant for the whole leaching process. Especially initial attachment as first step in biofilm formation is critical. Biofilms are defined as colonies of microbial cells embedded in extracellular polymeric substances (EPS) attached to a surface. The formation of a conditioning film on surfaces prior to bacterial attachment is reported. This conditioning film is formed due to the adsorption of (macro) molecules on the surfaces (van der Aa and Dufrêne 2002, Donlan 2002).

Biofilms develop in multiple stage processes (Figure 3 a - d). The initial stage of biofilm formation includes the attachment of microorganisms to the solid surface (Figure 3a). This can be reversible or irreversible (Figure 3b). Irreversibly attached cells start to form microcolonies surrounded by EPS and develop a continuous biofilm (Figure 3c; Sauer et al. 2002). Leaching bacteria form monolayer biofilms surrounded by a mucilaginous layer of EPS (Edwards et al. 1998, Harneit et al. 2006). Hence, a continuous biofilm is developed, cell clusters slough off and the biofilm disperses (Figure 3d; Sauer et al. 2002). Rojas-Chapana and Tributsch visualized parts of a *L. ferrooxidans* biofilm, which were released into the bulk solution from a biofilm on a pyrite surface. This released material contained, besides *L. ferrooxidans* cells surrounded by capsular EPS, dispersed pyrite nanoparticles being between 5 – 50 nm (Rojas-Chapana and Tributsch 2004).

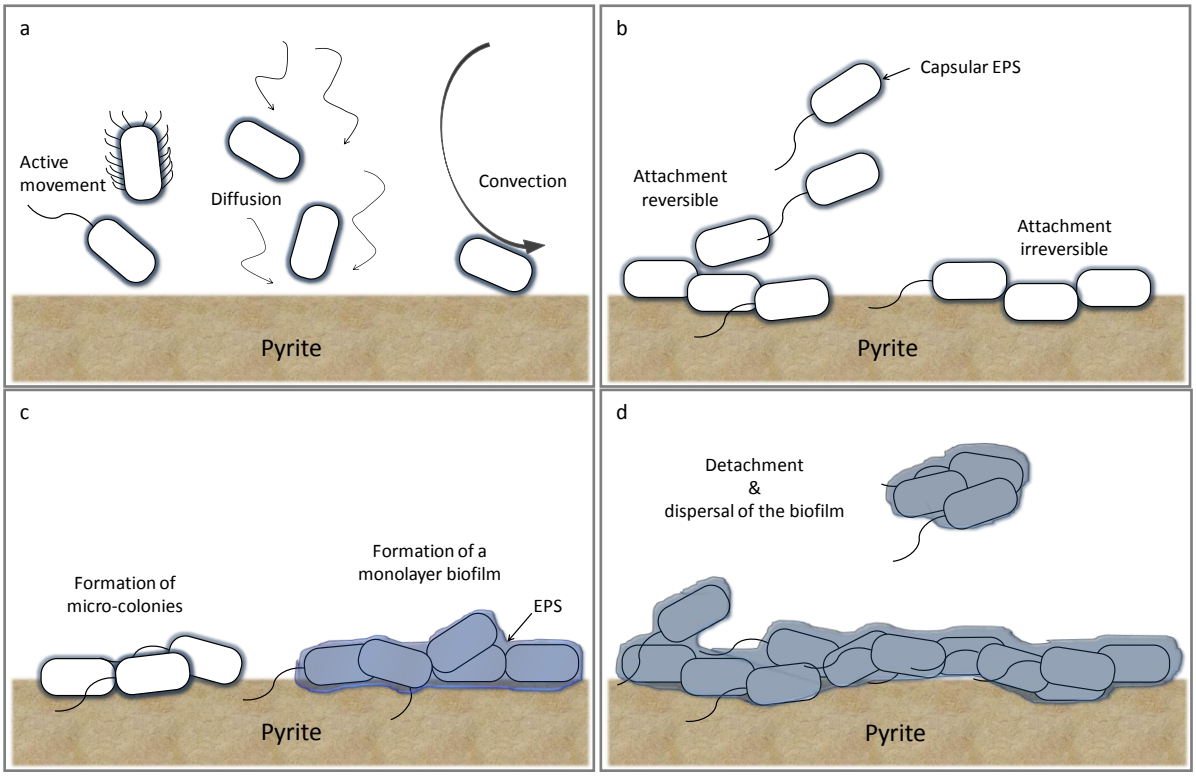

Figure 3 a - d: Steps in biofilm development
a: active or passive movement of cells to the mineral surface; b: primary attachment, reversible and irreversible; c: formation of microcolonies, formation of an initial biofilm surrounded by EPS; d: growth of a biofilm, detachment and dispersal of parts of the biofilm.

Biofilm formation starts with the transport of cells to the solid surface (Figure 3a). Different ways of transport like diffusion, convection or active movement are known. Diffusion is a slow transport, compared to convection or active movement, caused by Brownian movement. Sedimentation of bacteria to the surface may be significant under certain conditions. Several orders of magnitude faster is the transport of cells by convection as compared to diffusion.

Motile microorganisms are able to target-orientated attachment onto solid surfaces by active movement directed by chemotaxis (Loosdrecht et al. 1990). Chemotaxis is the phenomenon, where bacteria direct their movement according to certain chemicals such as iron(II) ions (acidophilic iron-oxidizers; Acuña et al. 1992). Quorum sensing (QS) is a cell-to-cell communication system with stimulus and response correlated with the microbial density (Winans and Bassler 2002). It is recognized as a regulator for biofilm formation and seems to be existent in leaching organisms. QS systems have been detected e.g. in *Acidithiobacillus ferrooxidans* (Farah et al. 2005, Ruiz et al. 2007).

The attachment of leaching bacteria to a mineral surface is highly affected by extracellular polymeric substances. Previous work showed that a removal of EPS from cells decreased the attachment tendency to mineral surfaces (Gehrke et al. 1998, Yu et al. 2010).

EPS excreted by microorganisms are biopolymers consisting of polysaccharides, proteins, lipids and nucleic acids. Accumulated within biofilms may be multivalent cations, biogenic and inorganic particles, colloidal and dissolved compounds (Wingender et al. 1999).

The chemical composition of EPS of leaching organisms was determined, e.g. for *A. ferrooxidans*, *A. thiooxidans* and *L. ferrooxidans* (Gehrke et al. 1995, Gehrke et al. 1998, Gehrke et al. 2001, Kinzler et al. 2003). Main components are sugars and lipids as well as in low concentration free fatty acids. Nitrogen and phosphorus are present only in minor amounts, proteins and hexosamines were not detected. However, the EPS composition differs by growth substrates. Iron(III) ions are embedded in the EPS, if cells are grown with substrates like pyrite or iron sulfate. They form glucuronic acid-iron ion complexes in a molar ratio of 2 mol glucuronic acid to 1 mol iron(III) ions (Sand et al. 1998, Gehrke et al. 1998).

Jiao and co-workers quantified the EPS compounds from two natural microbial pellicle biofilms, grown in acid mine drainage solution. Both samples comprised carbohydrates, metals as second major constituent, small quantities of proteins and low amounts of DNA and lipids. The metal composition, analyzed by inductively coupled plasma atomic emission spectroscopy (ICP-AES), showed that Fe was the most abundant metal in both biofilm samples (Jiao et al. 2010).

The occurrence of iron(III) ions complexed by glucuronic acid results in a net positive charge of the leaching organisms, allowing them to attach to negative charged metal sulfide surfaces such as pyrite (Gehrke et al. 1998). These electrostatic forces become significant at distances of 50 nm. Another factor that affects bacterial adhesion to solid surfaces are weak attractive van der Waals interactions, acting usually over large separation distances (>50 nm) (Busscher et al. 1990, Chen et al. 2011).

Experiments with addition of iron(III) ions resulted in increased attachment of cells to pyrite and chalcopyrite (Yu et al. 2010).

1.6.3. Attachment sides on pyrite

It has been previously reported that bacterial attachment on pyrite increases the leaching rate (Shrihari et al. 1995, Rodríguez et al. 2003). Pyrite is one of the most occurring metal sulfides on earth, and is of great interest for bioleaching and AMD/ARD studies. More than 80 different crystal forms of pyrite are known. The most common forms are hexahedron, octahedron, pentagonal dodecahedron and they combinations (Murowchick and Barnes 1987). Figure 4 shows the most common pyrite crystal forms with symmetry elements.

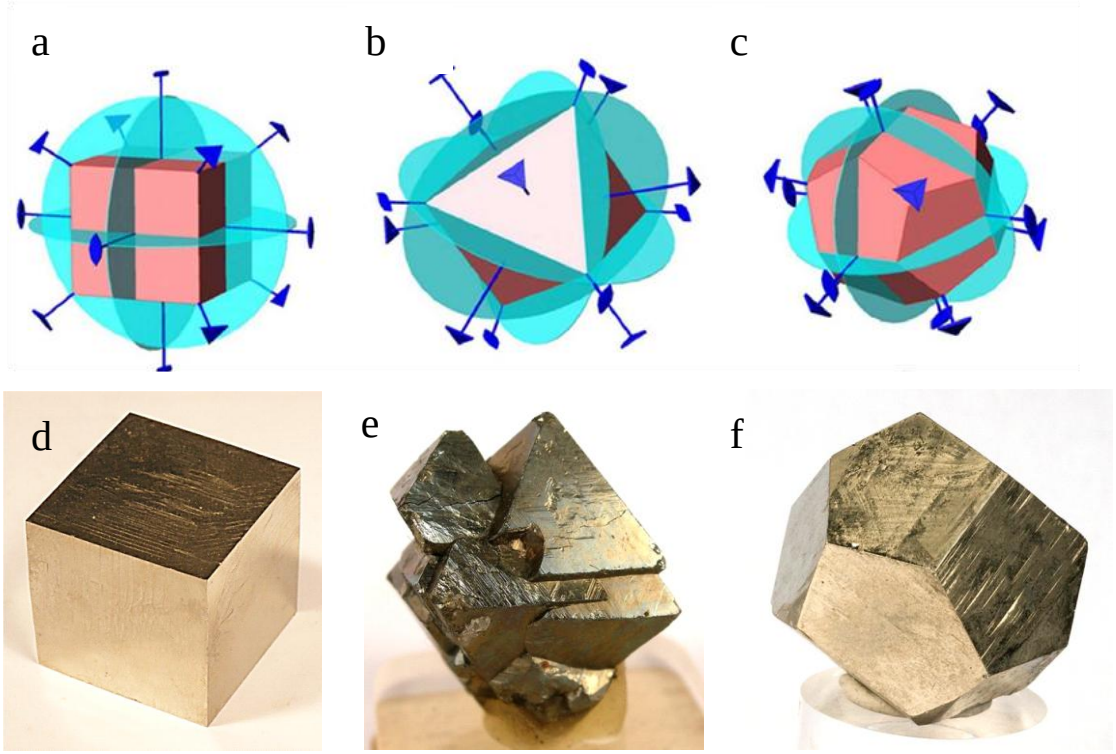

Figure 4 a - f: Crystal forms of pyrite (Etzel 2008)
a & d: hexahedron {100}; b & e: octahedron {111}; c & f: pentagonal dodecahedron {210}. Three mirror planes are perpendicular to each axis, three two-fold axes of rotation parallel to each axis and three-fold inversion axis of rotation.

The cleavages on the pyrite surface are not, as sometimes assumed, scratches. These cleavages are a product of the crystal habit and can be used for the identification of the pyrite crystal. Cleavages define how a crystal breaks and are suspected to be inherent in bacterial attachment topography (Edwards et al. 1998).

Since it is known that microbial attachment to the mineral surface plays a pivotal role in bioleaching, much work has been performed to identify bacterial attachment sides.

It is known from previous work that leaching organisms do not attach randomly onto pyrite (Andrews 1988, Gehrke et al. 1998, Gehrke et al. 2001, Kinzler et al. 2003). Andrews

proposed that selective adsorption to pyrite surfaces is associated with dislocation sides, where e.g. sulfur atoms are accumulated and thereby constitute cathodically active regions (Andrews 1988).

Gehrke and co-workers demonstrated that *A. ferrooxidans* cells attach specifically to dislocation sides on pyrite using atomic force microscopy (AFM). A statistical evaluation indicates an attachment of 76 % of cells to visible surface imperfect such as cracks and grain boundaries (Gehrke et al. 1998).

Besides visible mineral sulfide surface imperfections, the role of microtopographical surface features in aligning bacterial adhesion was studied. Experimental data show correlation between microbial cell alignment and crystallographic directions. The depth of surface features like scratches was of less importance than cross-sectional shapes of the mineral surface (Edwards et al. 1998, Edwards et al. 2000, Edwards and Rutenberg 2001).

1.6.4. Reaction space between mineral surface and bacteria

Cells attached to a mineral sulfide surface are surrounded by EPS; thus, the EPS fills the void between the outer membrane of the cell and the surface (Sand and Gehrke 2006). Dissolution processes take place in this reaction space. Taylor and Lower determined an average EPS thickness of 29 nm surrounding planktonic iron grown *A. ferrooxidans* cells. These findings serve as quantitative measure of the reaction space (Tayler and Lower 2008). Atomic force microscopy studies of single etch pits of leached pyrite imply a reaction space within 100 nm (Telegdi et al. 1998, Pace et al. 2005).

Details of the dissolution processes are not clarified until now, however. Two assumptions are needed to explain how the process might function (Sand and Gehrke 2006). The first assumption considers an electron tunneling effect. Electrons can bridge a distance of about 2 nm by tunneling from one electron hole to another (Medvedev and Stuchebrukhov 2001). Iron(III) ions complexed in the EPS (surrounding the attached cells) can take up a tunneling electron from the mineral surface and the reduction process can occur.

The second assumption is based on the fact that iron(II) ion- glucuronic acid complexes are not stable and iron(II) ions can migrate within EPS space (Harneit et al. 2006). If the mobile ions diffuse toward the outer membrane they will be oxidized by enzymatic systems of the cell and the formed iron(III) ions will enter the cycle again. Consequently, the chemical reaction occurs outside the cell within the EPS- generated microenvironment (Sand and Gehrke 2006).

1.7. Problem formulation and aim of the study

Bacterial leaching processes as applied in the mining industry or known as unwanted AMD/ARD are gaining increasing interest.

Bioleaching used in industrial applications (biomining) to win valuable metals from low grade ores is environmentally friendly and inexpensive. However, these leaching processes are not fully understood and have to be further optimized.

Furthermore, bacterial leaching causes in unwanted processes (AMD/ARD) acidification of surface- and groundwater concomitant with pollution by heavy metals. These processes have to be mitigated.

Parameters such as bacterial attachment, EPS production and strain composition are assumed to play a major role in leaching processes. However, little is known about the interactions between various species in mixed leaching communities regarding the EPS production, attachment behavior and at least leaching efficiency. With this knowledge commercial leaching processes may be optimized or unwanted natural leaching processes may become controllable.

In this study pyrite was used as model mineral, because it is one of the most frequent mineral sulfides on earth and often involved in bioleaching processes. Three different iron- and/or sulfur-oxidizing model organisms namely *A. ferrooxidans* ATCC 23070, *L. ferrooxidans* DSM 2705 and *A. thiooxidans* DSM 622 were used to evaluate attachment and leaching processes in pure and mixed cultures.

The main key questions of this study were:

- Which strain or strain composition is the most efficient in pyrite leaching?
- Which pure culture shows the highest initial attachment and in which pattern onto a pyrite surface?
- Which mixed culture shows the highest initial attachment and in which pattern onto a pyrite surface?
- Which member of a mixed culture is the first colonizer of a metal sulfide surface?
- Which member of a mixed culture needs a pre-colonization by other bacteria to be able to attach or to establish itself in a biofilm?
- Where does primary colonization occur?

2. Materials & Methods

2.1. Bacterial strains and growth media

Selected strains were obtained from the culture collection of the department Aquatic Biotechnology, Biofilm Centre, Universität Duisburg-Essen. All strains are known to be members of pyrite leaching consortia.

Table 1: Bacterial strains

Strain	Origin	Reference
Acidithiobacillus ferrooxidans ATCC 23270^T	Acid, bituminous coal mine effluent, USA	Temple and Colmer 1951, Kelly and Wood 2000
Acidithiobacillus thiooxidans DSM 622^T	Isolate from a pond in Göttingen, Germany	Waksman and Joffe 1922, Kelly and Wood 2000
Leptospirillum ferrooxidans DSM 2705^T	Copper deposits, Armenia	Markosyan 1972, Balashova et al. 1974, Hippe 2000

A. ferrooxidans ATCC 23270 and *L. ferrooxidans* DSM 2705 were grown in the autotrophic medium according to Mackintosh (Mackintosh 1978).

Table 2: Growth medium for *Acidithiobacillus ferrooxidans* ATCC 23270 and *Leptospirillum ferrooxidans* DSM 2705 (Mackintosh 1978)

Solutions	Components	Quantity per Liter	
Basal solution	$(NH_4)_2SO_4$	132	mg
	$MgCl_2 \cdot 6\ H_2O$	25	mg
	$CaCl_2 \cdot 2\ H_2O$	147	mg
	KH_2PO_4	27	mg
	H_2SO_4 conc.	0.53	mL
Trace elements	$MnCl_2 \cdot 4\ H_2O$	100	mg
	$ZnCl_2$	70	mg
	$CoCl_2$	120	mg
	H_3BO_3	31	mg
	$Na_2MoO_4 \cdot 2\ H_2O$	12.1	mg
	$CuCl_2 \cdot 2\ H_2O$	85.2	mg
Iron(II) sulfate solution	$FeSO_4 \cdot 7\ H_2O$	10	g
	H_2SO_4 conc.	8	mL

All solutions were prepared with deionized water and sterilized at 110 °C, 1.5 bar for 90 minutes separately. The basal solution was prepared as concentrate (50-fold) and diluted before use. The iron(II) ion solution was acidified (pH 1.2) with sulfuric acid to prevent iron(II) oxidation and precipitation. After autoclaving the solutions were combined, the pH of the combined medium was 1.8.

A. thiooxidans DSM 622 was grown in the autotrophic medium DSMZ 71.

Table 3: Growth medium DSMZ 71 for *Acidithiobacillus thiooxidans* DSM 622

Solutions	Components	Quantity per Liter
Basal solution	KH_2PO_4	3 g
	$MgSO_4 \cdot 7\ H_2O$	0.5 g
	$(NH_4)_2SO_4$	3 g
	$CaCl_2 \cdot 2\ H_2O$	0.25 g
Thiosulfate solution	$Na_2S_2O_3 \cdot 5\ H_2O$	5 g

Both solutions were prepared with deionized water. The pH of the basal salt solution was adjusted to 4.4 with sulfuric acid and sterilized at 110 °C, 1.5 bar for 90 minutes. Thiosulfate solution was sterile filtered (Filtopur S 0.2, 0.20 µm, Sarstedt, Nümbrecht, Germany) and both solutions were combined before use.

2.2. Purity control

The purity control was performed by light microscopy (100x magnification objective, Leica DMLS), with unique cell morphology being the main criteria. Additionally, strains were cultured in a medium for meso-acidophilic chemoorganotrophic bacteria according to Harrison (Harrison 1981), where a lack of growth indicates absence of possible contaminating acidophilic chemoorganotrophic bacteria.

Table 4: Growth medium for purity control (Harrison 1981)

Components	Quantity per Liter
K_2HPO_4	0.5 g
$MgSO_4 \cdot 7\ H_2O$	0.5 g
$(NH_4)_2SO_4$	2 g
KCl	0.1 g
Trypticase Soy Broth	0.1 g
Glucose	1 g

2.3. Culture conditions

Stock- and pre-cultures were grown in 100 mL narrow-neck Erlenmeyer flasks containing 50 mL growth medium. Cultures were shaken at 160 rpm on a rotary shaker in darkness at 28 °C. All cultures were grown until the substrate was largely consumed (approx. 3 days). The oxidation of iron(II) ions to iron(III) ions was indicated by a change in color from slightly green to rust-brown. Additionally, iron-ion concentration was determined quantitatively by the phenanthroline method (Anonymous 1984). Quantification of thiosulfate consumption by sulfate-oxidizing *A. thiooxidans* DSM 622 cells was determined by ion-exchange chromatography (Weiß 1991). After growth, stock cultures were stored for a maximum of four weeks and pre-cultures for a maximum of three days at 17 °C before transfer to fresh culture medium.

Pre- or mass cultures were grown with an inoculum of 10 % v/v in 1 L (filled with 500 mL medium) Erlenmeyer flasks or 5 L conical shoulder bottles (filled with 4.5 L medium), respectively. The growth conditions for cultures in 1 L bottles were identical to those of the stock cultures. Bacteria grown in 5 L bottles were incubated at the same temperature but with supply of sterile pressurized air under stirring (500 rpm) in darkness. Cells were grown until reaching the early stationary phase after approximately three days (determined by cell count using a Thoma hemocytometer, see chapter 2.5.

2.4. Cell harvest

For attachment- and leaching experiments, cultures were harvested by centrifugation (Gentrikon H-401, Berthold Hermle KG) at 6000 rpm (rotor A6.9) for 10 min at 10 °C. Once harvested, cells were washed three times with basal salt solution for removal of retained iron or sulfur compounds. Afterwards cells were re-suspended in basal salt solution. Cell suspensions were kept at 17 °C for 24 h to allow reconstruction of EPS before the experiments started.

2.5. Determination of planktonic cell number

The planktonic cell number was determined using a modified Thoma hemocytometer (depth = 0.1 mm, volume per small square = 0.0025 m^2) and a light microscope (Leica DMLS, Wetzlar GmbH) in phase contrast mode with 400x magnification.
The total cell number was calculated according to Equation 9 and is given in cells per mL without exception:

Equation 9 $$\boldsymbol{TCC = \frac{n_{cells}}{A_{chamber} \times D_{chamber} \times F} \times 1000}$$

TCC = Total cell number [cells/mL]
n_{cells} = Number of cells counted
$A_{chamber}$ = Area [mm^2]
$D_{chamber}$ = Depth of the chamber [mm]
F = Dilution factor

2.6. Strain composition and bacterial number for attachment- and leaching experiments

Composition of the pure and mixed cultures and corresponding cell numbers for the investigation of attachment to pyrite grains and leaching of pyrite coupons are shown in Table 5.

Table 5: Pure and mixed cultures and corresponding cell numbers for experiments on attachment to pyrite grains and leaching of pyrite coupons

Culture	Cell number [cells/mL]			
	L.f.	***A.f.***	***A.t.***	**total**
L. ferrooxidans[1]	$5 \cdot 10^8$			$5 \cdot 10^8$
A. ferrooxidans[2]		$5 \cdot 10^8$		$5 \cdot 10^8$
A. thiooxidans[3]			$5 \cdot 10^8$	$5 \cdot 10^8$
L. ferrooxidans[1] & *A. ferrooxidans*[2]	$2.5 \cdot 10^8$	$2.5 \cdot 10^8$		$5 \cdot 10^8$
L. ferrooxidans[1] & *A. thiooxidans*[3]	$2.5 \cdot 10^8$		$2.5 \cdot 10^8$	$5 \cdot 10^8$
A. ferrooxidans[2] & *A. thiooxidans*[3]		$2.5 \cdot 10^8$	$2.5 \cdot 10^8$	$5 \cdot 10^8$
A. ferrooxidans[2] & *A. thiooxidans*[3] & *L. ferrooxidans*[1]	$1.7 \cdot 10^8$	$1.7 \cdot 10^8$	$1.7 \cdot 10^8$	$5 \cdot 10^8$

[1]*Leptospirillum ferrooxidans* DSM 2705, [2]*Acidithiobacillus ferrooxidans* ATCC 23270,
[3]*Acidithiobacillus thiooxidans* DSM 622

For the investigation of bacterial attachment to pyrite coupons and leaching of pyrite grains Table 6 summarizes the composition of the pure and mixed cultures and the corresponding cell number.

Table 6: Pure and mixed cultures and corresponding cell numbers for attachment experiments to pyrite coupons and leaching of pyrite grains

Culture	Cell number [cells/mL]			
	L.f.	***A.f.***	***A.t.***	**total**
L. ferrooxidans[1]	$1 \cdot 10^8$			$1 \cdot 10^8$
A. ferrooxidans[2]		$1 \cdot 10^8$		$1 \cdot 10^8$
A. thiooxidans[3]			$1 \cdot 10^8$	$1 \cdot 10^8$
L. ferrooxidans[1] *& A. ferrooxidans*[2]	$5 \cdot 10^7$	$5 \cdot 10^7$		$1 \cdot 10^8$
L. ferrooxidans[1] *& A. thiooxidans*[3]	$5 \cdot 10^7$		$5 \cdot 10^7$	$1 \cdot 10^8$
A. ferrooxidans[2] *& A. thiooxidans*[3]		$5 \cdot 10^7$	$5 \cdot 10^7$	$1 \cdot 10^8$
A. ferrooxidans[2] *& A. thiooxidans*[3] *& L. ferrooxidans*[1]	$3.3 \cdot 10^7$	$3.3 \cdot 10^7$	$3.3 \cdot 10^7$	$1 \cdot 10^8$

[1]*Leptospirillum ferrooxidans* DSM 2705, [2]*Acidithiobacillus ferrooxidans* ATCC 23270,
[3]*Acidithiobacillus thiooxidans* DSM 622

2.7. Pyrite for the leaching- and attachment experiments

Pyrite (FeS_2) was used as substrate for leaching experiments and/or as substratum for bacterial attachment assays.

2.7.1. Pyrite grains

Pyrite grains were obtained from the Suior mine in Maramures, Cavnic, Romania. This pyrite is a waste product originating from the separation of gold from the whole ore body by flotation processing (Mangold 2006).

Table 7 shows the detailed composition of the flotation pyrite. It was analyzed by X-ray fluorescence spectroscopy at the Geology department, Faculty for Biology and Geography, Universität Duisburg – Essen.

Table 7: Chemical composition of pyrite from the Suior mine

Symbol	Concentration		Error	
Na_2O	< 0,27	%	(0,0)	%
MgO	0,716	%	0,067	%
Al_2O_3	< 0,026	%	(0,0)	%
SiO_2	0,432	%	0,013	%
P_2O_5	< 0,013	%	(0,0)	%
S	17,47	%	0,02	%
K_2O	< 0,012	%	(0,0099)	%
CaO	< 0,014	%	(0,0052)	%
TiO_2	0,03121	%	0,00045	%
V	< 15	µg/g	(6,2)	µg/g
Cr	< 5,0	µg/g	(0,0)	µg/g
MnO	< 0,00039	%	(0,0)	%
Fe_2O_3	35,32	%	0,04	%
Co	< 18	µg/g	(0,0)	µg/g
Ni	30,2	µg/g	2,6	µg/g
Cu	380,2	µg/g	5,1	µg/g
Zn	52,5	µg/g	1,7	µg/g
Ga	< 1,1	µg/g	(0,0)	µg/g
Ge	< 0,9	µg/g	(0,0)	µg/g
As	1083	µg/g	5	µg/g
Se	1,6	µg/g	0,2	µg/g
Rb	< 0,8	µg/g	(0,0)	µg/g
Sr	2,4	µg/g	0,4	µg/g
Y	2,1	µg/g	0,5	µg/g
Zr	4,5	µg/g	0,5	µg/g
Nb	1,9	µg/g	0,5	µg/g
Mo	< 0,7	µg/g	(0,0)	µg/g
Ag	12,8	µg/g	1,1	µg/g
Cd	4,6	µg/g	0,7	µg/g
In	< 0,2	µg/g	(0,0)	µg/g
Sn	3,7	µg/g	0,4	µg/g
Sb	22,5	µg/g	0,6	µg/g
Te	< 1,3	µg/g	(0,0)	µg/g
Cs	< 1,3	µg/g	(0,0)	µg/g
Ba	< 1,8	µg/g	(0,0)	µg/g
La	< 2,4	µg/g	(0,9)	µg/g
Hf	< 0,1	µg/g	(0,0)	µg/g
Ta	< 21	µg/g	(0,0)	µg/g
Hg	< 1,8	µg/g	(0,0)	µg/g
Tl	4,6	µg/g	1,4	µg/g
Pb	97,5	µg/g	2,9	µg/g
Bi	< 3,1	µg/g	(0,0)	µg/g
Th	< 3,0	µg/g	(1,1)	µg/g
U	< 1,9	µg/g	(0,0)	µg/g

Based on the method not all components (e.g. C, N, O, SO_4^{2-}, $FeCO_3$) of pyrite were determined (Ehrhardt et al. 1968).

The specific surface area of the flotation pyrite was determined by the BET method (Brunauer et al. 1938). The surface of the fraction 45 - 200 µm was 0.1111 ± 0.0027 m^2/g (Mangold 2006).

Prior to experiments, the pyrite was sieved using a sieve shaker (Co. Retsch) to a final grain size of 50 to 100 µm. The sieved pyrite was boiled in 6 M HCl for 30 minutes, rinsed to neutrality with deionized water and washed twice with acetone (p.a.) to remove oxidation products and to obtain high-grade purity. The washed pyrite was dried at 60 °C and 10 g each were filled in bottles sealed with air-tight rubber caps. The bottles were extensively flushed with nitrogen to avoid oxidation processes, dry-sterilized at 115 °C for 48 h and stored under nitrogen atmosphere until use.

2.7.2. Pyrite coupons

Slices of 1 - 2 mm thickness were cut from museum grade pyrite crystals (about 3.5 cm^3, Figure 5a) using a Logitech Model 15 saw with a diamond cut-off wheel (B 127, ø 127, thickness 0.48, ATM GMBH). The obtained slices were broken to smaller pieces with a total area of about 0.5 - 1 cm^2 (Figure 5b). These coupons were cleaned and stored as described in chapter 2.7.1.

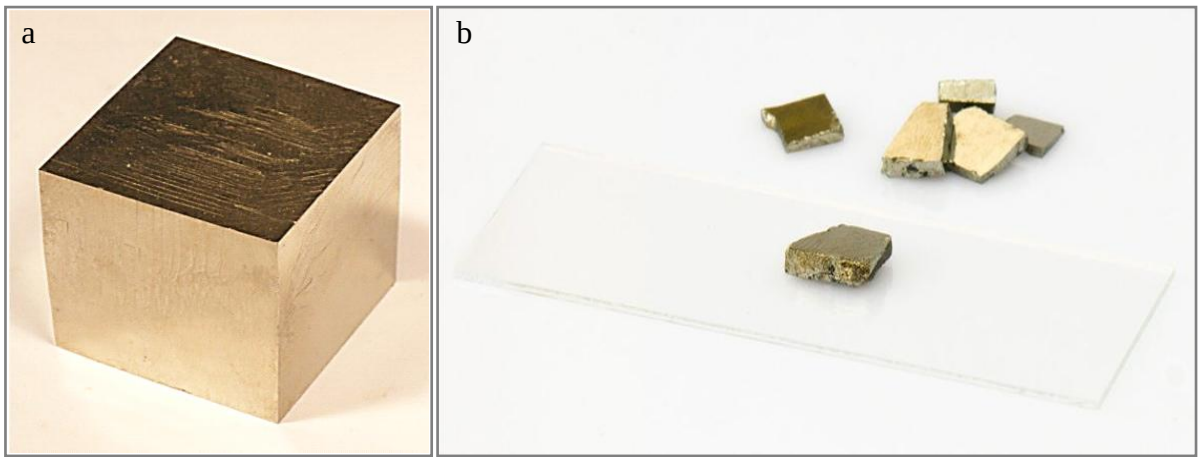

Figure 5 a & b: Pyrite
a: Museum grade pyrite crystal from dump Victoria, Navajun/district Rioja in Spain, b: pyrite coupons, cut off the 6 outside faces of pyrite cubes, size about 0.5 - 1 cm

2.8. Quantification of bacterial attachment to pyrite grains

Bacterial attachment experiments to pyrite grains were performed in 100 mL Erlenmeyer flasks filled with 50 mL Mackintosh basal salt solution (Mackintosh 1978) and 10 g pyrite grains (50 – 100 µm). Pure and mixed cultures of *A. ferrooxidans* ATCC 23270, *L. ferrooxidans* DSM 2705 and *A. thiooxidans* DSM 622 were used with an initial total cell number of $5 \cdot 10^8$ cells/mL (refer to Table 5). In order to determine unspecific attachment to the glass wall of the Erlenmeyer flask, control experiments were performed without addition

of pyrite for each of the assays. The cultures were shaken at 160 rpm on a rotary shaker in darkness at 28 °C. Samples of 1 mL were taken over a time period of 7 h after 0, 5, 10, 20, 30, 60, 90, 120, 240, 300, 360 and 420 minutes. Remaining pyrite was removed from the samples by centrifugation at 100 g for 30 sec. Planktonic cell number was determined using a hemocytometer (see chapter 2.5.). The total amount of attached cells was calculated by subtracting the planktonic cell number from the initial cell number.

2.8.1. Statistical evaluation

All attachment experiments to pyrite grains were performed in 6 independent biological replicates and mean values are presented with respective percental standard deviations.

2.9. Quantification of bacterial leaching of pyrite grains

Leaching experiments were performed with *A. ferrooxidans* ATCC 23270, *L. ferrooxidans* DSM 2705 and *A. thiooxidans* DSM 622 in pure and mixed cultures as shown in Table 6.
300 mL Erlenmeyer flasks were filled with 150 mL Mackintosh basal salt solution (Mackintosh 1978) and 10 g pyrite (50 – 100 µm). Initial total cell number was adjusted to $1 \cdot 10^8$ cells/mL (Table 6). Cultures were shaken at 160 rpm on a rotary shaker in darkness at 28 °C. Samples of 2 mL were taken three times a week for a period of 31 days. After determination of pH and total cell number, samples were frozen at -20 °C for quantification of iron ion-, sulfate- and sulfur concentration (see chapter 2.13.).

2.9.1. Statistical evaluation

All leaching experiments with pyrite grains were performed in biologically independent quadruplicates (n = 4) and mean values with respective percental standard deviations are presented.

2.10. Quantification of bacterial attachment to pyrite coupons

Attachment experiments to pyrite coupons were performed in conical reaction vessels (50 mL centrifuge tubes, Corning) with vertically inserted coupons. Figure 6 shows the final experimental set up.

Figure 6: Experimental set-up for analysis of bacterial attachment to pyrite surfaces
Pyrite coupons were fixed with their naturally grown surface side up on microscope glass slides and placed vertically into the reaction vessel. Tubes for aeration with outlet at the bottom of the vessel ensured continuous and homogenous mixing of the cell suspension.

Pyrite coupons were fixed with their naturally grown surface up with instant adhesive (2-component epoxy resin, UHU) on microscope glass slides (Roth) and stored under nitrogen atmosphere until use. For the attachment experiments they were placed vertically into the reaction vessels and 50 mL of the respective bacterial culture was added. For continuous mixing of the cell suspension a gentle flow of air (sterile by filtration) was applied via tubes ending at the bottom of the vessel. After 1 or 8 h incubation, the pyrite coupons were removed. For the unspecific enumeration of attached cells the DNA fluorochrome 4',6-diamino-2-phenylindole (DAPI) was used (Porter and Feig 1980). For the specific enumeration and identification of attached cells from mixed cultures, fluorescence *in situ* hybridization was employed (DeLong et al. 1989).

2.10.1. Bacterial attachment to precolonized pyrite coupons

The secondary attachment behavior of pure cultures of *A. ferrooxidans* ATCC 23270, *L. ferrooxidans* DSM 2705 and *A. thiooxidans* DSM 622 to precolonized pyrite coupons was studied in the following way. Table 8 summarizes the strains used for precolonization as well as for secondary attachment (see below chapter 2.10.2.). The initial total cell number for the secondary attachment was adjusted to $1 \cdot 10^8$ cells/mL (refers to Table 6). Samples were taken after 1 and 8 h. Secondary attached cells were visualized by fluorescence *in situ* hybridization (FISH) using specific probes for *A. ferrooxidans*, *L. ferrooxidans* or *A. thiooxidans.*

Table 8: Strains for pre-colonization and for secondary attachment experiments to pyrite coupons

Pre-colonizer:	**Secondary attachment to precolonized pyrite coupons by:**
L. ferrooxidans[1]	*L. ferrooxidans*[1]
	A. ferrooxidans[2]
	A. thiooxidans[3]
A. ferrooxidans[2]	*L. ferrooxidans*[1]
	A. ferrooxidans[2]
	A. thiooxidans[3]
A. thiooxidans[3]	*L. ferrooxidans*[1]
	A. ferrooxidans[2]
	A. thiooxidans[3]

[1]*Leptospirillum ferrooxidans* DSM 2705, [2]*Acidithiobacillus ferrooxidans* ATCC 23270, [3]*Acidithiobacillus thiooxidans* DSM 622

2.10.2. Precolonization of pyrite coupons: formation of biofilms

Pyrite coupons were incubated in pure cultures of *A. ferrooxidans* ATCC 23270, *L. ferrooxidans* DSM 2705 and *A. thiooxidans* DSM 622 with initial cell numbers of $5 \cdot 10^8$ cells/mL. Coupons were placed horizontally with the naturally grown side up at the bottom of 100 mL Erlenmeyer flasks filled with 50 mL bacterial culture at 28 °C, aerated, in darkness. After 3 days, the coupons were removed from the bacterial solution, rinsed with sterile-filtered deionized water and dried at 55 °C for 24 h in order to inactivate all bacterial cells. Afterwards, the coupons were stored in a desiccator until use.

Viability of cells was tested on one hand by incubation (on the coupon) in fresh media with iron(II) ions or thiosulfate, respectively, as substrate. On the other hand, live/dead staining (Live/Dead®Baclight™Bacterial Viability kit Invitrogen™) of the cells was performed on the mineral surface. EPS residues were visualized by the use of the fluorescence labeled lectin Concanavalin A (ConA). Coupons, which were used for testing cell viability and visualization of EPS residues, were not used for further attachment experiments.

2.10.3. Statistical evaluation

All attachment experiments to pyrite coupons were performed with 10 independent biological replicates (10 coupons). Cells on 10 randomly chosen areas on each coupon were counted using an ocular counting grid (125 µm x 125 µm) installed in the epifluorescence microscope. DAPI- and FISH-stained cells were quantified within the same areas. Because of the high variation of cell numbers per counting grid, results were statistically evaluated using frequency distribution histograms. The frequency distribution describes the abundance of certain values (cell numbers) within defined classes (Table 9). The results are presented in frequency tables, where each entry contains the relative frequency of the abundance in percentage of the classes. Classes are given as cell numbers per counting grid (125 µm x 125 µm). The actual selected classes of cell numbers are summarized in Table 9.

Table 9: Classes of cell numbers

Class
0 cells
1 - 50 cells
51 - 100 cells
101 – 150 cells
151 – 200 cells
201 – 250 cells
251 – 300 cells
301 – 350 cells
351 – 400 cells
401 – 450 cells
451- 500 cells
> 500 cells

Figure 7 shows an example of a frequency distribution histogram from bacterial attachment to pyrite coupons together with detailed explanations.

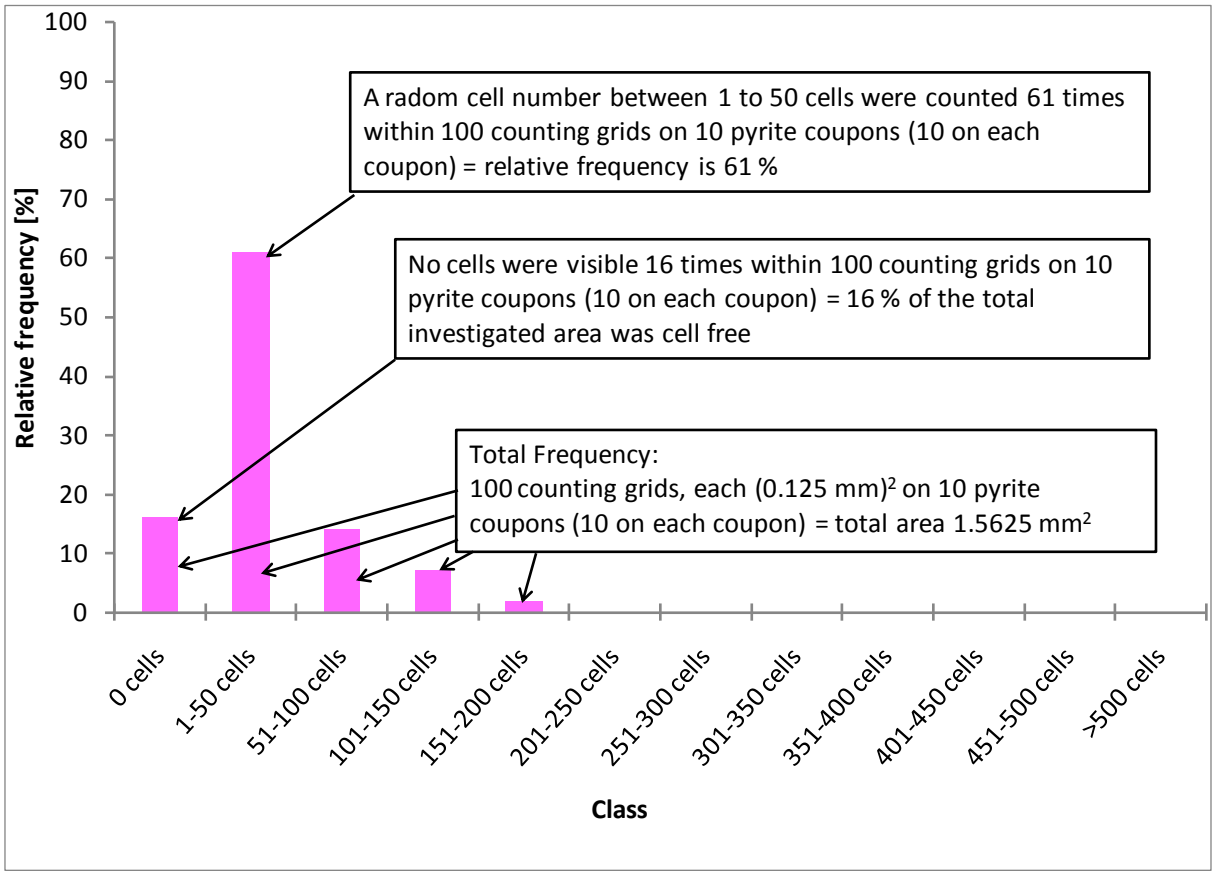

Figure 7: Example of frequency distribution histogram to describe bacterial attachment to pyrite coupons
The 12 classes represent the x- axis and are classified in cell numbers. On the y-axis the respective abundance in relative frequency [%] is plotted. n = 100 counting grids (equipment of the epifluorescence microscope, 125 µm x 125 µm). Cells of a total area of 1.5625 mm^2 were enumerated for each pure or mixed culture.

Calculation of standard deviation (s)

Standard deviations (s) are calculated based on the absolute frequency. In the following Equation 10 to Equation 16 all intermediate steps necessary for this calculation are described.

First the relative frequency p_j is calculated by division of the absolute observed value within a class n_j by the sum of all classes n.

Equation 10 $$p_j = \frac{n_j}{n}$$

The class width d_j is then calculated by subtracting the lower class limit xl_j from the upper class limit xu_j:

Equation 11 $$d_j = xu_j - xl_j$$

The class midpoint x'j is determined by adding the upper and lower class limits xu_j and xl_j respectively, followed by division by two:

Equation 12 $$x'j = \frac{(xu_j + xl_j)}{2}$$

In the next step, the sum of all class midpoints x'j multiplied by the value within the classes n_j is calculated:

Equation 13 $$\sum xn_j = x'j \times n_j$$

The mean x is calculated by dividing the sum of all class midpoints xn_j by the total number of classes n:

Equation 14 $$x = \frac{\sum xn_j}{n}$$

Afterwards, the sample variance is calculated as described in Equation 15:

Equation 15 $$s^2 = \frac{\sum(x'j - x)^2 \times n_j}{n}$$

Finally the standard deviation is calculated by taking the square root of the variance:

Equation 16 $$s = \sqrt{s^2}$$

2.11. Quantification of bacterial leaching of pyrite coupons

Leaching experiments with pyrite coupons were performed using pure cultures of *A. ferrooxidans* ATCC 23270 and *L. ferrooxidans* DSM 2705. Pyrite coupons were precolonized by *A. ferrooxidans* ATCC 23270, *L. ferrooxidans* DSM 2705 and *A. thiooxidans* DSM 622 cells. Experiments without precolonization and/or leaching bacteria served as controls. Table 10 shows the combinations of precolonizers and leaching organisms.

Table 10: Combination of precolonizing and leaching bacteria on pyrite coupons

Precolonizing strains:	Leaching strains:
L. ferrooxidans[1]	*A. ferrooxidans*[2]
L. ferrooxidans[1]	*L. ferrooxidans*[1]
L. ferrooxidans[1]	None
A. ferrooxidans[2]	*A. ferrooxidans*[2]
A. ferrooxidans[2]	*L. ferrooxidans*[1]
A. ferrooxidans[2]	None
A. thiooxidans[3]	*A. ferrooxidans*[2]
A. thiooxidans[3]	*L. ferrooxidans*[1]
A. thiooxidans[3]	None
None	*A. ferrooxidans*[2]
None	*L. ferrooxidans*[1]
None	None

[1]*Leptospirillum ferrooxidans* DSM 2705, [2]*Acidithiobacillus ferrooxidans* ATCC 23270, [3]*Acidithiobacillus thiooxidans* DSM 622

The detailed procedure for precolonization of pyrite coupons is described in chapter 2.10.2. The leaching experiments were performed in reaction tubes filled with 10 mL Mackintosh basal salt solution (Mackintosh 1978). Initial total cell number was adjusted to $5 \cdot 10^8$ cells/mL. Cultures were shaken at 40 rpm on a rotary shaker at 28 °C in darkness. Samples of 200 µL were taken once a week for a period of 8 weeks. Iron ions were quantified using the phenanthroline method (see chapter 2.13.1.). Planktonic growth was monitored by phase contrast microscopy with 400x magnification (Leica DMLS, Wetzlar GmbH).

Pyrite coupons were weighed before and after incubation with bacteria in order to determine the weight loss in percent of the mineral sulfide by bacterial leaching activity.
After 8 weeks incubation, coupons were removed from the solution and cells and their EPS were stained by DAPI and fluorescently labeled lectin ConA. Cells and mineral surfaces were visualized by combined epifluorescence microscopy (EFM) and atomic force microscopy (AFM).

2.11.1. Statistical evaluation

The leaching experiments with pyrite coupons were performed in biological independent duplicates (n = 2) and the results are presented as mean values with their respective percental standard deviations.

2.12. Visualization of cells and EPS on pyrite surfaces

In order to visualize bacteria and their EPS on pyrite surfaces, various staining methods were applied. Visualization was performed by the use of epifluorescence microscopy partly in combination with atomic force microscopy. DAPI was used to stain the entirety of cells; FISH gave the possibility to distinguish different strains in a mixed culture. EPS was visualized by the use a lectin (ConA). The viability of cells on mineral surfaces was controlled by the use of a live/dead-kit.

2.12.1. Whole-cell staining by DAPI (4’,6-diamino-2-phenylindole)

DAPI (Sigma Aldrich) was used for enumeration of cells as well as counterstaining in combination with FISH on pyrite coupons.
DAPI binds non-intercalative to DNA with great affinity (Porter and Feig 1980) and is fully compatible with FISH (Amann et al. 1995, Amann et al. 2001). A DAPI working solution (0.01 % w/v) was prepared by dissolving 10 mg DAPI in 94.6 mL deionized water adding 5.4 mL formaldehyde (36 %). The solution was sterile-filtered and stored at 4 °C in darkness. For whole cell staining alone, pyrite coupons were washed twice with Mackintosh basal salt solution (Mackintosh 1978). Then, the mineral surface was completely covered with DAPI working solution for 15 minutes. Afterwards, remaining DAPI solution was removed by carefully rinsing with sterile-filtered deionized water and coupons were air-dried subsequently. The detailed protocol for DAPI counter-staining in combination with FISH is described in the following chapter.

2.12.2. Fluorescence *in situ* Hybridization (FISH)

Fluorescence *in situ* hybridization (FISH) is a fast and cheap method to detect single species of a leaching community in their habitat on the mineral surface. This technique allows simultaneous visualization, identification, enumeration and localization of microbial cells without ex-situ cultivation (DeLong et al. 1989, Moter and Göbel 2000, Amann et al. 2001). 16S rRNA represents the most commonly targeted molecule for FISH. It is present in all living organisms, occurs in a high copy number, includes highly conserved sequence domains and is relatively genetically stable (Woese 1987, Amann et al. 1990, Amann et al. 1995). Oligonucleotide probes hybridize specifically to its complementary target sequence. Probes have between 15 to 30 base pairs in length and are covalently linked to a single fluorochrome dye molecule at the 5´-end (Amann et al. 2001). Long probes are more specific and might carry more labels than short probes. However, long probes have less access to their target than shorter probes. The simultaneous microscopic detection of two or three species is possible using fluorochromes with different excitation and emission maxima.

The hybridization procedure is based on Amman's original protocols and was adapted to the special conditions of acidic environments by González-Toril (Amann et al. 1995, González-Toril et al. 2006). For this work the FISH-protocol was further modified to match the requirements of the visualization of cells on pyrite surfaces.

Fluorescently-labeled rRNA-targeted oligonucleotide probes specific for the detection of *A. ferrooxidans, A. thiooxidans* and *L. ferrooxidans* (Schrenk et al. 1998, Bond and Banfield 2001, Kimura et al. 2003, Amann et al. 2001) were used. FISH probes were labeled by the fluorochromes fluorescein-isothiocyanate (FITC) and the cyanine dye Cy3. For counterstaining DAPI was used. For mixed cultures composed of two different organisms DAPI and one Cy3-labeled oligonucleotide probe were used. For three organisms, DAPI and two different FISH-probes labeled with FITC and Cy3 were used.

With these combinations, the simultaneous visualization and identification of two or three different organisms with little spectral overlap between the fluorochromes of the probes was possible.

Controls for all FISH-probes were performed with pure cultures and the respective probe as well as with the non-targeting strains. Counterstaining with DAPI showed that probes hybridize only to the target strain, respectively (data not shown).

Table 11: Spectral characteristics of fluorochromes for detection of microorganisms

Fluorochrome	Wavelength		Color
	Excitation (nm)	Emission (nm)	
Fluorescein-isothiocyanate (FITC)	492	528	green
Cy3™	550	570	orange/red
4',6-diamidino-2-phenylidoledihydrochloride (DAPI)	358	461	blue

Wavelengths may vary depending on the respective manufacturer. Emission spectra might change in different solvents or sample conditions (Cullander 1999).

Fixation and permeabilization of cells

The fixation of cells is crucial for satisfying FISH results. It must be performed immediately after sampling to protect the bacterial rRNA from degeneration by endogenous ribonucleases (RNAses) (Moter and Göbel 2000). Additionally, it ensures sufficient probe penetration and maintains the cell integrity (Moter and Göbel 2000).

Cells were fixed and permeabilized directly on pyrite surfaces. According to a protocol from González-Toril, samples were placed in an acidic solution of deionized water and H_2SO_4 (pH 2) with a final concentration of 4 % formaldehyde (v/v) at 4 °C for 30 minutes (González-Toril et al. 2006). Afterwards, samples were washed twice with phosphate buffer (PBS: NaCl 4 g; KCl 0.1 g; $Na_2HPO{\cdot}2\ H_2O$ 0.72g; KH_2PO_4 0.1 g filled up to 1000 mL with deionized water) to neutralize the sample and to remove precipitates. Then samples were dehydrated with ethanol in increasing concentration (50 %, 70 %, 100 %) for 1 minute each. After subsequent air drying, samples were stored at -20 °C until hybridization.

Hybridization

The hybridization was performed with varying the formamide concentration (Table 12) depending on the oligonucleotide probe used. Formamide is required to lower the melting temperature of the nucleic acids by weakening the hydrogen bonds.

For hybridization, samples were covered with 10 µL hybridization buffer mixed with 2 µL solution of a specific oligonucleotide probe (Table 13). Samples were incubated in sealed light impermeable reaction tubes (50 mL). Filter paper soaked with 1 mL of the hybridization buffer (without probe) was placed into the tube to saturate the gaseous phase. Afterwards, samples were hybridized at 46 °C for 2 h in darkness.

Table 12: Hybridization buffer

Components	Concentrations
Sodium chloride	0.9 M
Sodium dodecyl sulfate	0.01 %
Tris-HCL	20 mM
Formamide	20 % * 35 % ** 40 % ***

* probe (TF539), ** probe (ATT223), *** probe (LEP665)

Table 13: Fluorescent-labeled oligonucleotide probes (25 nM)

Probe	Target	Sequence (5' to 3')	Specificity	labeled with	Formamide (%)	Reference
TF 539	16S	CAGACCTAACGTACCGCC	*Acidithiobacillus ferrooxidans*	CY3	20 or (35)*	Schrenk et al. 1998
ATT 223	16S	AGACGTAGGCTCCTCTTC	*Acidithiobacillus thiooxidans*	CY3	40	Kimura et al. 2003
LEP 665	16S	CGCTTCCCTCTCCCAGCCT	*Leptospirillum ferrooxidans*	CY3, FITC	35	Bond and Banfield 2001

Cy3= Indocarbocyanine dye, FITC= Fluorescein-isothiocyanate, *if probe TF539 was used together with probe LEP665

Washing step

After 2 h hybridization, samples were transferred into preheated washing buffer (Table 14) and incubated for 20 minutes at 48 °C to remove unbound probes. Afterwards, samples were rinsed with sterile-filtered deionized water to remove salts and air-dried. After DAPI staining (chapter 2.12.1), coupons were carefully washed with sterile-filtered deionized water, dehydrated with 80 % ethanol and air-dried. Samples were stored at -20 °C in darkness for microscopic documentation.

Table 14: Washing buffer

Components	Concentrations
Sodium chloride	0.9 M
Sodium dodecyl sulfate	0.01 %
Tris-HCL	20 mM

2.12.3. Lectin staining (Concanavalin A)

Florescence-labeled Concanavalin A (ConA) allows the visualization of specific polysaccharide residues in EPS (Strathmann et al. 2002). ConA is a lectin protein, which binds to certain sugars and has a high affinity to α-D-mannosyl, α-D-glucosyl, α-D-glucosyl residues, branched α-mannosidic structures, high α-mannose type, hybrid types and complex type biantennary N-Glycans. ConA has already been used successfully to visualize whole EPS of monolayer biofilms of acidophilic bacteria on metal sulfides (Fife et al. 2000, Mangold et al. 2008b, Florian et al. 2010, Holuscha 2010).

In this study, ConA conjugated with tetramethylrhodamine-5-isothiocyanate (TRITC) was used. Stock solutions were prepared to a final concentration of 1 mg/mL in 10 mM PBS (pH 7.5). Aliquots were stored at -20 °C in darkness until use. Working solutions of 50 µg/mL were prepared by dilution of stocks with sterile, particle-free deionized water and stored in darkness at 4 °C no longer than two weeks.
Samples were fully covered by lectin working solution and incubated for 15 minutes in darkness. Afterwards, coupons were rinsed carefully with sterile-filtered deionized water to remove unbound lectin and air-dried. Stained samples were visualized by fluorescence microscopy (chapter 2.12.5.).

2.12.4. Live/Dead staining

The Live/Dead® BacLight™ Bacterial Viability kit (Invitrogen), a mixture of SYTO9 and propidium iodide stains, was used to distinguish intact cells from membrane-damaged cells of precolonized pyrite coupons.

All cells were stained by SYTO 9 (green), a dye which marks nucleic acids and is able to penetrate intact as well as damaged cells. However, propidium iodide (red) cannot pass intact cell membranes, thus it only stains cells with damaged membranes.
Stock- and working solutions were prepared according to the manufacturers manual; working solutions were stored at 4 °C in darkness no longer than 2 weeks.
Pyrite samples were stained according to the manufacturer's manual by fully covering them with working solution for 15 minutes. Residual stains were removed by rinsing with sterile-filtered deionized water. After air-drying, samples were examined by fluorescence microscopy (chapter 2.12.5.).

2.12.5. Visualization of fluorescently labeled cells by epifluorescence microscopy (EFM)

Fluorescently stained cells and EPS were visualized using a Zeiss Axio Imager A1m equipped with a HBO 100 mercury vapor lamp for fluorescence microscopy and a HAL 100 halogen lamp for light microscopy. 50x air- (Zeiss EC Epiplan-NEOFLUAR 50x/0.8 HD) and 100x air- (Zeiss EC Epiplan-NEOFLUAR 100x/0.9 Pol) objectives were used. Different fluorochromes were selectively visualized using Zeiss filter sets 49 for DAPI (blue), 10 for FITC (green) and 20 for Cy3 (red). Images were taken using a digital microscope camera (AxioCam M Rc5) and processed using the software AxioVision4.

2.12.6. Visualisation of pyrite coupon surfaces, cells and their EPS by combined atomic force- and epifluorescence microscopy

Atomic force microscopy (Binning et al. 1986) is an established technique for imaging the surfaces of biological systems in their native environment with high spatial resolution (Shao et al. 1996, Engel et al. 1997). Bacterial cells and the associated biofilms on opaque mineral surfaces such as pyrite can be investigated (Beech et al. 2002).
The AFM measures the forces between the cantilever tip and the sample. The tip is located at the free end of the cantilever and is brought very close to the sample surface. A piezo element is used to move the cantilever across the sample, line by line. The forces between tip and sample result in a positive or negative deflection of the cantilever. This deflection is measured using a laser beam, focused on and reflected from the back side of the cantilever onto a four-quadrant photo detector (Figure 8) and converted into an image.

Several modes of operations such as contact mode, non-contact mode or tapping mode (intermittent contact mode) are commonly used. In this work, only contact mode has been used with the tip being in mechanical contact to the sample surface (Figure 8).

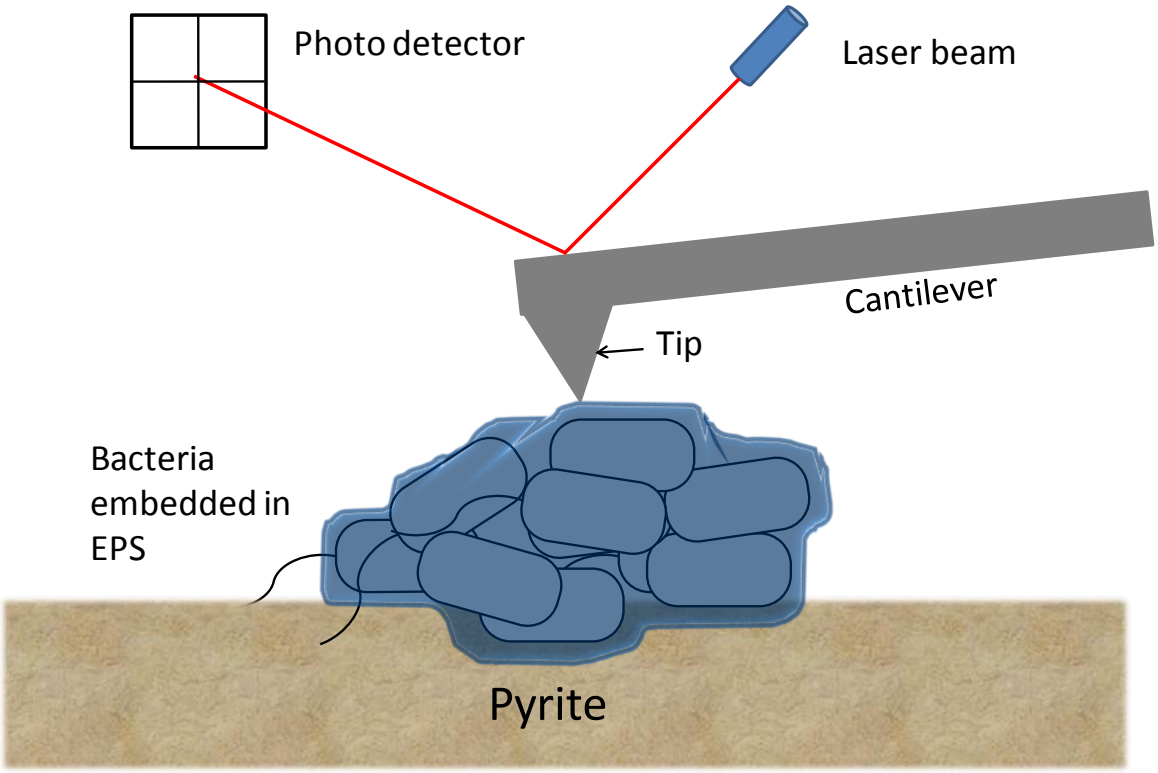

Figure 8: Schematic drawing of an AFM apparatus in contact mode

To properly distinguish biofilms, single cells and surrounding EPS from topographic features, techniques such as fluorescence staining by DAPI (cells) or labeled lectins (polysaccharides, i.e. EPS) with subsequent visualization by EFM are needed. The combination of both techniques allows visualization of the surface in high resolution as well as reliable identification of biofilm constituents at the same side of a certain sample. In a BioMAT Workstation™, AFM and EFM are fully independent instruments connected by a shuttle stage. By the use of the shuttle stage, a sample can be transferred between both instruments and examination of the same spot on a surface with a spatial deviation of less than 5 µm with both microscopes is possible (Mangold et al. 2008a, Mangold et al. 2008b).

The workstation consists of an epifluorescence microscope in combination with an atomic force microscope (JPK instrument, Nano Wizard II with JPK SPM Image processing (v.3.x) software). Samples were visualized in contact mode with a line rate of 0.5 Hz and a setpoint of 1 V using cantilevers CSC37a (Mikromasch, Estonia).

2.13. Analytical experiments

2.13.1. Quantification of iron ions

Iron ions were quantified according to the German standard methods for the examination of water, waste water and sludge; cations; determination of iron (DIN 38406-1) (Anonymous 1984). The so called phenanthrolinium test is based on the spectrophotometric determination of a red colored complex under acidic conditions, formed by ferrous iron and 1.10 - phenanthroline.

In a second step, iron(III) ions are reduced to iron(II) ions by the addition of hydroxylamine. Thus, the total iron ion concentration can be determined. The concentration of iron(III) ions can be calculated by subtracting iron(II) ion concentration from total iron ion concentration. A 5 point standard curve (0.8 - 4 mg/L Fe) was used.

Standards and samples were measured at 492 nm using a UV-VIS spectrophotometer (Cary 50, Varian INC.) equipped with software ADL Shell (modified by F. Leon-Morales).

Table 15: Reagents for phenanthrolinium test

Solutions	Components	Quantity per Liter
Ammonium acetate solution*	ammonium acetate	400 g
	glacial acetic acid (100%) heated	500 mL
Phenanthrolinium solution	1.10-phenanthrolinium chloride	100 mg
Hydroxylamine solution	$NH_2OH \cdot HCl$	2 g
Iron(II) sulfate solution	$FeSO_4 \cdot 7\ H_2O$	80 mg
	1 M HCl	10 mL

* Deionized water has to be added before solution is cooled down

2.13.1.1. Statistical evaluation

All samples were measured in triplicate and mean values with percental standard deviations are presented.

2.13.2. Quantification of sulfate

Sulfate was quantified using an ion exchange chromatograph (DX 500, Dionex). The instrument was equipped as specified in Table 16. Technical set ups are described in Table 17.

Table 16: Equipment for the ion exchange chromatograph

Autosampler	AS 3500
Pre-column	AG17C 2·50 mm
Separation column	AS17C 2·250 mm
Supressor	ASRS 300 2 mm Exchanger self-generating
Gradient generator in combination with EluGen cartridge	EG 50 EGC II KOH
Gradient pump	GP 40
Conductivity detector	CD 20
Software	Chromeleon Dionex 6.70 Build 1820

Table 17: Technical settings for ion exchange chromatography

Injection-volume	10 µL
Eluent flow-rate:	0.36 mL/min
Eluent system:	0 – 2.5 min, 10 mM KOH; 2.5 – 3.5 min, 20 mM KOH; 3.5 – 4.5 min, 30 mM KOH; 4.5 – 5.5 min, 40 mM KOH; 5.5 – 6.5 min, 50 mM KOH; 6.5 – 8.5 min, 10 mM KOH.

Samples were diluted 1:10 with 5 mM phosphate buffer (40 % 50 mM KH_2PO_4, 60 % 50 mM K_2HPO_4, pH 7). After 30 min incubation, samples were centrifuged (Biofuge, Heraeus Sepatech) for 10 min at 6600 g. The supernatants were further diluted 1:10 with bidistilled water and then measured. The peak area generated by the conductivity signal is quantified by an integrator and the amount of sulfate is calculated by comparison with external calibration standards.

2.13.2.1. Statistical evaluation

All samples were measured in duplicate. Results are presented as mean values with percental standard deviations.

2.13.3. Quantification of elemental sulfur

Elemental sulfur was determined using a high-performance liquid chromatography (HPLC) system (Kontron/Bio-Tek Instruments). The system is composed of a type 465 autosampler, gradient generator 425, pump 422, diode array detector 440 and separation column (EC 125/4 NUCLEODUR 100-5 C18 ec, Macherey-Nagel, Germany). Methanol (p.a.) was used as mobile phase with a flow rate of 1.2 mL/min. Data was processed by integrated software DS 450 - MT1-EMS V.1.32. For each measurement a chromatogram at 254 nm was logged, each for a period of 10 min. The sample preparation in detail is presented in Figure 9.

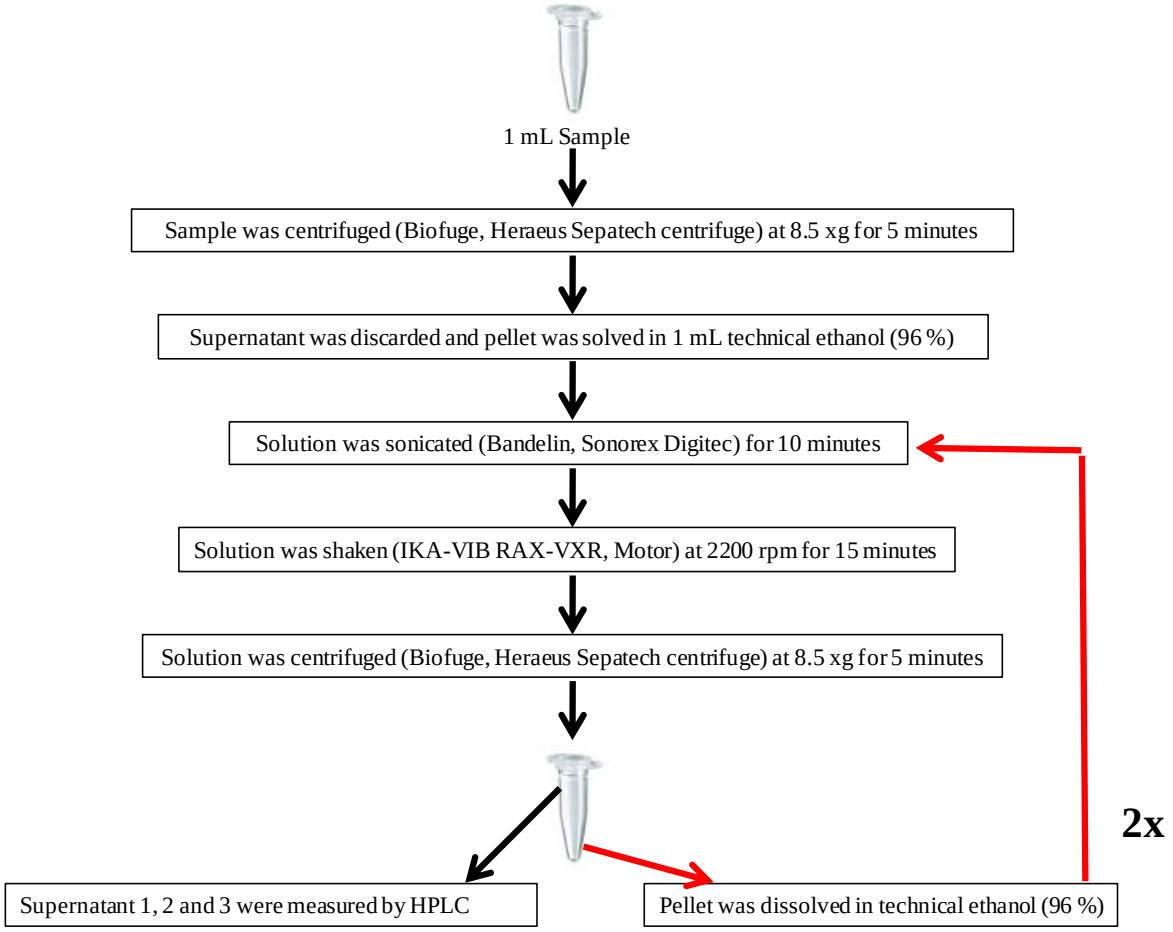

Figure 9: Scheme of sample preparation for elemental sulfur determination using HPLC

2.13.3.1. Statistical evaluation

All samples were measured in duplicate. Results are presented as mean values with percental standard deviations.

3. Results

The bacterial attachment of pure and mixed cultures to pyrite, their interaction and leaching efficiency was tested in various experiments.
Initial attachment of pure and mixed cultures and leaching of pyrite grains was quantified in standardized shake-flask experiments.
Details of attachment of pure and mixed cultures were investigated with pyrite coupons. To study the initial attachment and biofilms on mineral surfaces several fluorochromes such as DAPI, FISH and lectin were applied followed by visualization with a combination of EFM and AFM.
Furthermore, the initial attachment of leaching bacteria to pyrite coupons already covered by biofilms (inactivated cells) was investigated. Consecutively, leaching experiments with precolonized and virgin pyrite coupons were performed to study the influence of these biofilms on bacterial leaching.

3.1. Bacterial attachment to pyrite grains

A simple method -the shake flask experiment- has been standardized in previous studies to investigate bacterial attachment to mineral grains (Kock 2003, Stein 2004, Florian 2007, Mafanya 2007, Noël 2008). The direct cell counting of the planktonic population allows the quantification of attached cells to the mineral surface.
This technique was used to determine the attachment of cells of *A. ferrooxidans* ATCC 23270, *L. ferrooxidans* DSM 2705 or *A. thiooxidans* DSM 622 to pyrite grains in pure and mixed cultures. Attachment after 7 h incubation is shown in Figure 10.

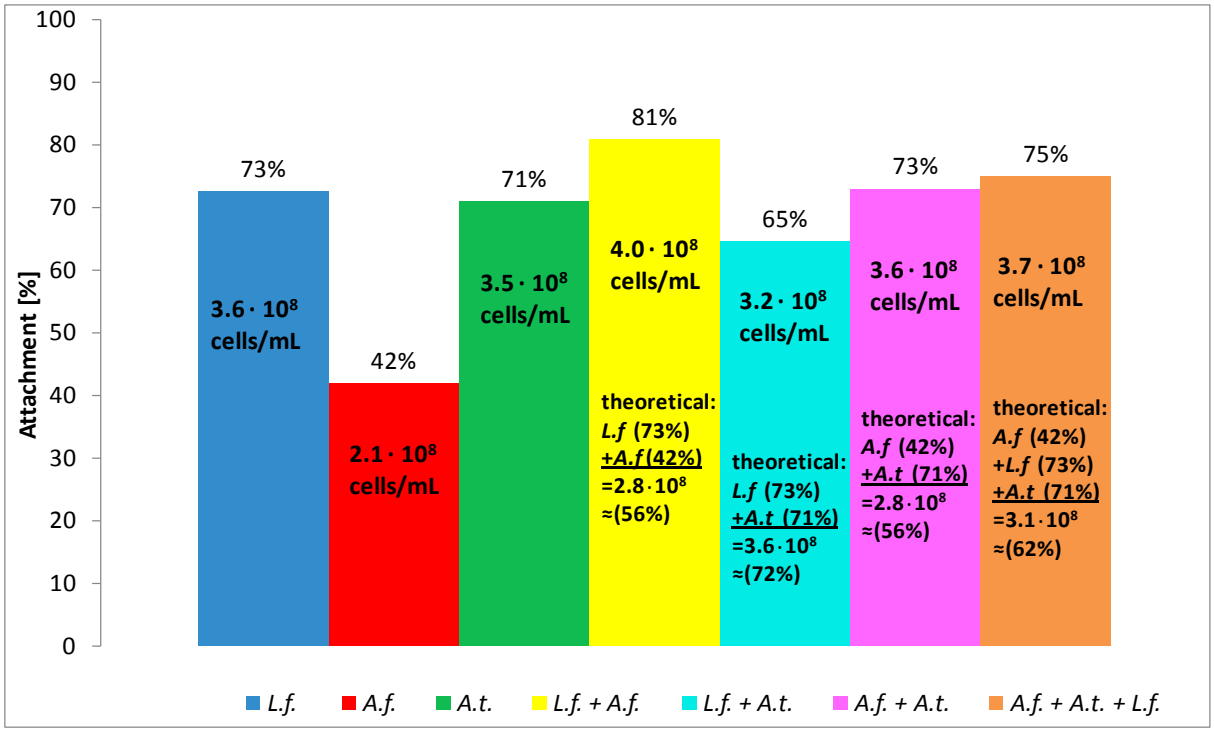

Figure 10: Bacterial attachment to pyrite grains after 7 h incubation
Attachment of *L. ferrooxidans* DSM 2705 (*L.f.*), *A. ferrooxidans* ATCC 23270 (*A.f.*), *A. thiooxidans* DSM 622 (*A.t.*) in pure and mixed cultures to pyrite grains. Initial total cell number $5 \cdot 10^8$ cells/mL (two strains: 50 % each strain respectively; three strains: 33 % each strain respectively), 50 mL basal salt solution, 10 g pyrite grains (50 - 100 µm), 28 °C, shaken (120 rpm).
Bars represent percental bacterial attachment; the corresponding absolute cell number as cells/mL is indicated on the bar. The theoretical value of the attached cells of the mixed culture was calculated by the addition of the percental attachment of each member (calculated for the respective cell number) of the mixed culture.
Standard error (n = 6): *L.f.* 17 %, *A.f.* 13 %, *A.t.* 12 %, *L.f.* + *A.f.* 10 %, *L.f.* + *A.t.* 14 %, *A.f.* + *A.t.* 10 %, *A.f.* + *A.t.* + *L.f.* 14 %.

Cells of *A. ferrooxidans* showed the lowest attachment with 42 % to pyrite grains after 7 h incubation. Pure cultures of *L. ferrooxidans* and *A. thiooxidans* showed comparable results with 73 % and 71 % attached cells to pyrite grains, respectively.

Results obtained for the mixed cultures exhibited that the attachment of the individual strains in a mixed culture was different from the attachment of each strain in pure culture. This was indicated by comparing the calculated theoretical attachment with experimental attachment values.

The largest difference between calculated and determined values was found for mixed cultures of *L.f* + *A.f.* Considerably more attached cells to pyrite grains were detected than theoretically anticipated. If 73 % of $2.5 \cdot 10^8$ cells/mL of *L.f.* cells and 42 % of $2.5 \cdot 10^8$

cells/mL of *A.f.* (as indicated from the pure culture experiments) would attach to pyrite the expected total cell number of attached cells should be $2.8 \cdot 10^8$ cells/mL. Thus, 56 % of the mixed culture would theoretically attach to pyrite grains. De facto, 81 % of the cells were found to attach to pyrite.

Mixed cultures of *L.f.* + *A.t.* showed 7 % lower attachment to pyrite grains than theoretically anticipated. 65 % of the cells of this mixed culture attached to pyrite grains. However, 72 % would theoretically attach if cells of *L.f.* and *A.t.* would attach like shown for the pure cultures.

Mixed cultures of *A.f.* + *A.t.* and *L.f.* + *A.f.* + *A.t.* showed comparably high attachment of 73 % and 75 %, respectively. However, the attachment of both mixed cultures was 17 % and 13 % higher than theoretically anticipated.

The main attachment of cells to pyrite grains of cells from both pure and mixed cultures occurred within the first 30 minutes, with the equilibrium being established within 120 minutes (6. Appendix; Figure 47). Controls performed without the addition of pyrite showed unspecific attachment to glass to account for less than 5 % for all pure and mixed cultures (data not shown).

3.2. Bacterial leaching of pyrite grains

Bacterial leaching of pyrite grains (50 – 100 µm) by pure and mixed cultures of *L. ferrooxidans* DSM 2705, *A. ferrooxidans* ATCC 23270 and *A. thiooxidans* DSM 622 was performed in shake flask experiments at 28 °C for 31 d. The parameters pH, planktonic cell number and concentrations of iron ions, sulfate and elemental sulfur were determined.

3.2.1. Decrease of the pH in bulk solutions during leaching of pyrite grains

Bacterial leaching of pyrite causes a decrease of pH in the bulk solution by the release of protons. Table 18 shows the decrease of the pH for each culture after 31 days. The pH had been adjusted to 2.0 at the beginning of the experiment.

Table 18: Decrease of the pH in bulk solutions after 31 d
ΔpH for pure and mixed cultures of *L. ferrooxidans* DSM 2705 (*L.f.*), *A. ferrooxidans* ATCC 23270 (*A.f.*), *A. thiooxidans* DSM 622 (*A.t.*) and control in the bulk solutions after 31 days. Initial total cell number $1 \cdot 10^8$ cells/mL (two strains: 50 % each strain respectively; three strains: 33 % each strain respectively), 150 mL basal salt solution, 10 g pyrite grains (50 - 100 µm), 28 °C, shaken (120 rpm). Standard error (n = 4) equal or less than 0.08.

Strains	ΔpH
L.f.	0.6
A.f.	0.4
A.t.	0.0
L.f. + *A.f.*	0.8
L.f. + *A.t.*	0.7
A.f. + *A.t.*	0.4
A.f. + *A.t.* + *L.f.*	0.7
Control	0.0

Neither for the bulk solution of the abiotic controls nor for solutions containing pure cultures of *A. thiooxidans* were a change in pH observed within 31 days. Pure cultures of *L. ferrooxidans* and *A. ferrooxidans* as well as all mixed cultures caused a comparable decrease of the pH after 31 days. The lowest drop of pH (0.4) was found for pure cultures of *A. ferrooxidans* and mixed cultures of *A.f.* + *A.t.*, while the highest drop of pH (0.8) was found for the mixed cultures composed of *L.f.* + *A.f.*

3.2.2. Planktonic cell numbers during leaching of pyrite grains

Cells occur attached to the mineral surface as well as in the planktonic phase during the leaching process. However, if the planktonic cell number decreases significantly in the shake flask experiments over weeks (death phase), inability of using pyrite as substrate is indicated. The total number of planktonic cells in this experiment was determined by the use of a hemocytometer (chapter 2.5.).

Progress of total cell numbers of planktonic cells of pure and mixed cultures of *L. ferrooxidans* DSM 2705, *A. ferrooxidans* ATCC 23270 and *A. thiooxidans* DSM 622 in leaching experiment over a period of 31 days is presented in Figure 11.

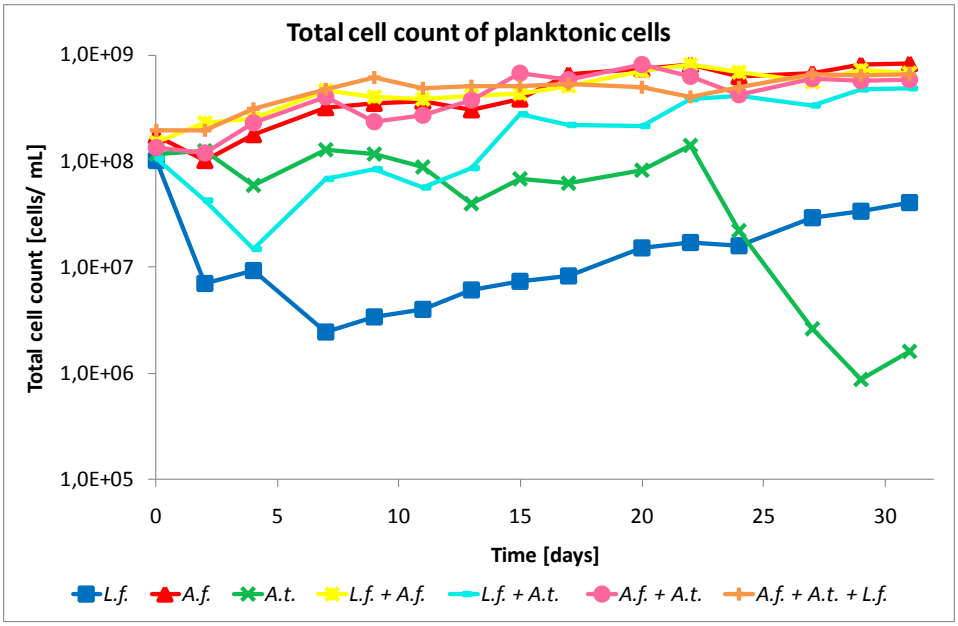

Figure 11: Planktonic cell numbers during leaching of pyrite grains
Total cell number of planktonic cells in pure and mixed cultures of *L. ferrooxidans* DSM 2705 (*L.f.*), *A. ferrooxidans* ATCC 23270 (*A.f.*) and *A. thiooxidans* DSM 622 (*A.t.*). Initial total cell number $1 \cdot 10^8$ cells/mL (two strains: 50 % each strain respectively; three strains: 33 % each strain respectively), 150 mL basal salt solution, 10 g pyrite grains (50 - 100 µm), 28 °C, shaken (120 rpm). Standard error (n = 4) less or equal than 20 %.

Numbers of the planktonic cells of *L. ferrooxidans* decreased until the 7th day from initially $1 \cdot 10^8$ to $2 \cdot 10^6$ cells/mL, afterwards the cell number increased to $4 \cdot 10^7$ cells/mL at the end of the leaching experiment. Cell numbers of *A. thiooxidans* remained between $1 \cdot 10^8$ to $4 \cdot 10^7$ cells/mL from the 2nd day till the 22nd day. From the 22nd day the cell number decreased rapidly until the end of the leaching experiment to $8 \cdot 10^5$ cells/mL. Cell numbers of mixed cultures of *L.f. + A.t.* decreased to $1 \cdot 10^7$ cells/mL till the 4th day. Afterwards, a continuous increase in cell numbers was found with $5 \cdot 10^8$ cells/mL at the end of the experiment. Pure cultures of *A. ferrooxidans* and mixed cultures of *L.f. + A.f.*, *A.f. + A.t.* and *A.f + A.t. + L.f.* showed an increase in cell numbers between $3 \cdot 10^8$ to $8 \cdot 10^8$ cells/mL till the end of the experiment after 31 days. Abiotic control remained cell-free (data not shown).

3.2.3. Iron(III) ion concentrations in the bulk solutions during leaching of pyrite grains

Due to the dissolution of pyrite grains, iron(III) ions accumulate as an oxidation product in the bulk solution. Consequently, bacterial leaching can be quantified by an increase in iron(III) ion concentration. Results for the leaching of pyrite grains by pure and mixed cultures of

L. ferrooxidans DSM 2705, *A. ferrooxidans* ATCC 23270 and *A. thiooxidans* DSM 622 are presented in Figure 12.

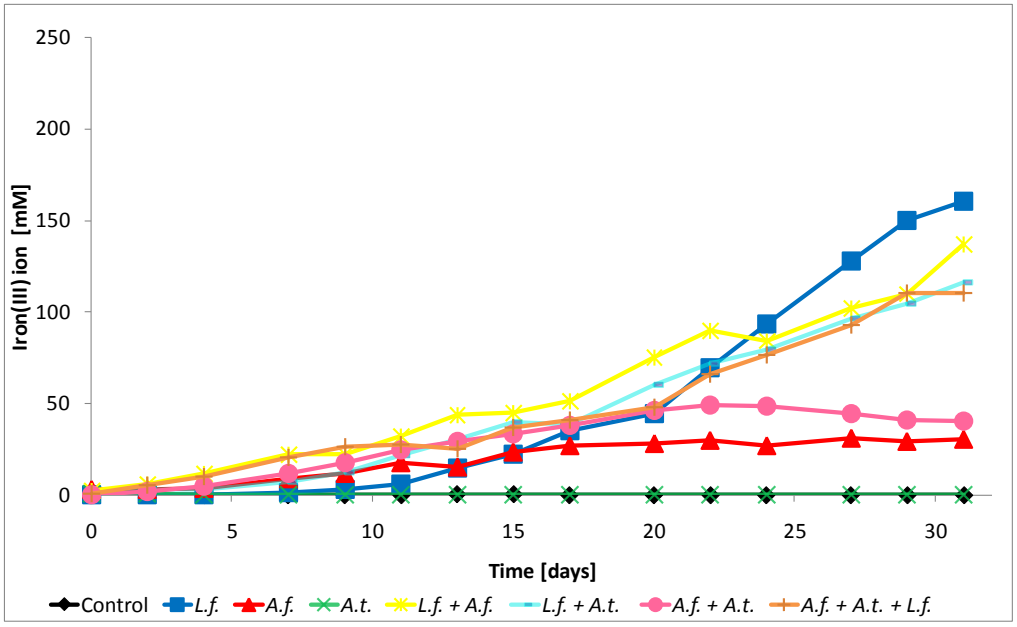

Figure 12: Iron(III) ion concentrations during leaching of pyrite grains
Iron(III) ion concentrations in bulk solutions of pure and mixed cultures of *L. ferrooxidans* DSM 2705 (*L.f.*), *A. ferrooxidans* ATCC 23270 (*A.f.*), *A. thiooxidans* DSM 622 (*A.t.*) and abiotic control. Initial total cell number $1 \cdot 10^8$ cells/mL (two strains: 50 % each strain respectively; three strains: 33 % each strain respectively), 150 mL basal salt solution, 10 g pyrite grains (50 - 100 µm), 28 °C, shaken (120 rpm). Standard error (n = 4) less or equal 9 %.

Iron(III) ion concentrations in the bulk solutions of the abiotic controls and inoculated with *A. thiooxidans* were always below the detection limit (0.3 mM). Pure cultures of *A. ferrooxidans* and the mixed cultures of *A.f. + A.t.* produced iron(III) ion concentrations of 30 and 40 mM after 31 days, respectively.

Mixed cultures containing *L.f. + A.f.*, *L.f. + A.t.* or *A.f. + A.t. + L.f.* cells exhibited a continuous increase in iron(III) ion concentrations with a maximum of 140, 120 and 110 mM respectively at the end of the leaching experiments.

The highest iron(III) ion concentration at the end of the leaching experiment (160 mM) was detected in the bulk solution of the pure culture of *L. ferrooxidans*.

3.2.4. Iron(II) ion concentrations in the bulk solutions during leaching of pyrite grains

Dissolved iron(II) ions are oxidized by iron-oxidizing bacteria to iron(III) ions. Consequently, the iron(II) ion concentration remains low during leaching processes. However, if leaching bacteria (e.g. *A. thiooxidans*) are not able to dissolve pyrite nor to oxidize iron(II) ions and no chemical dissolution takes place, the iron(II) ion concentration remains low. Figure 13 shows the iron(II) ion concentrations in pure and mixed cultures of *L. ferrooxidans* DSM 2705, *A. ferrooxidans* ATCC 23270 and *A. thiooxidans* DSM 622 growing with pyrite grains.

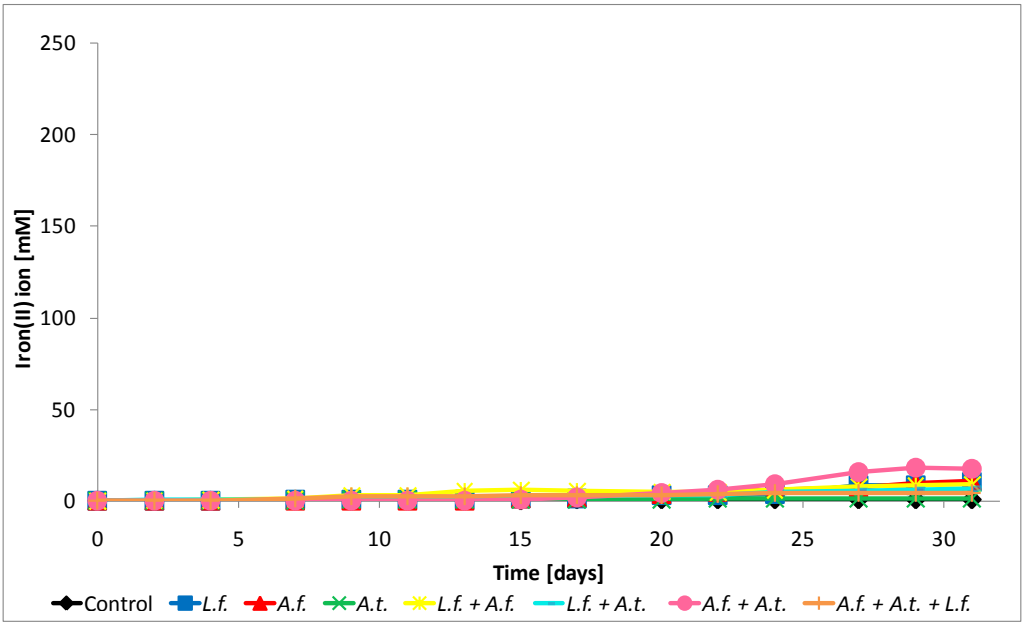

Figure 13: Iron(II) ion concentrations during leaching of pyrite grains
Iron(II) ion concentrations in bulk solutions of pure and mixed cultures of *L. ferrooxidans* DSM 2705 (*L.f.*), *A. ferrooxidans* ATCC 23270 (*A.f.*), *A. thiooxidans* DSM 622 (*A.t.*) and abiotic control. Initial total cell number $1 \cdot 10^8$ cells/mL (two strains: 50 % each strain respectively; three strains: 33 % each strain respectively), 150 mL basal salt solution, 10 g pyrite grains (50 - 100 µm), 28 °C, shaken (120 rpm).Standard error (n = 4) less or equal 9 %.

Iron(II) ion concentrations in bulk solutions of pure cultures of *A. thiooxidans* and the controls remained throughout the whole leaching experiment below the detection limit (0.3 mM). Concentrations for pure cultures of *L. ferrooxidans*, *A. ferrooxidans* and all mixed cultures were low and did not exceed a maximum of 17 mM till the end of the leaching experiment.

3.2.5. Sulfate concentrations in bulk solutions during leaching of pyrite grains

Sulfate is the final product of the oxidation of the sulfur moiety from pyrite. The courses of sulfate production are shown in Figure 14.

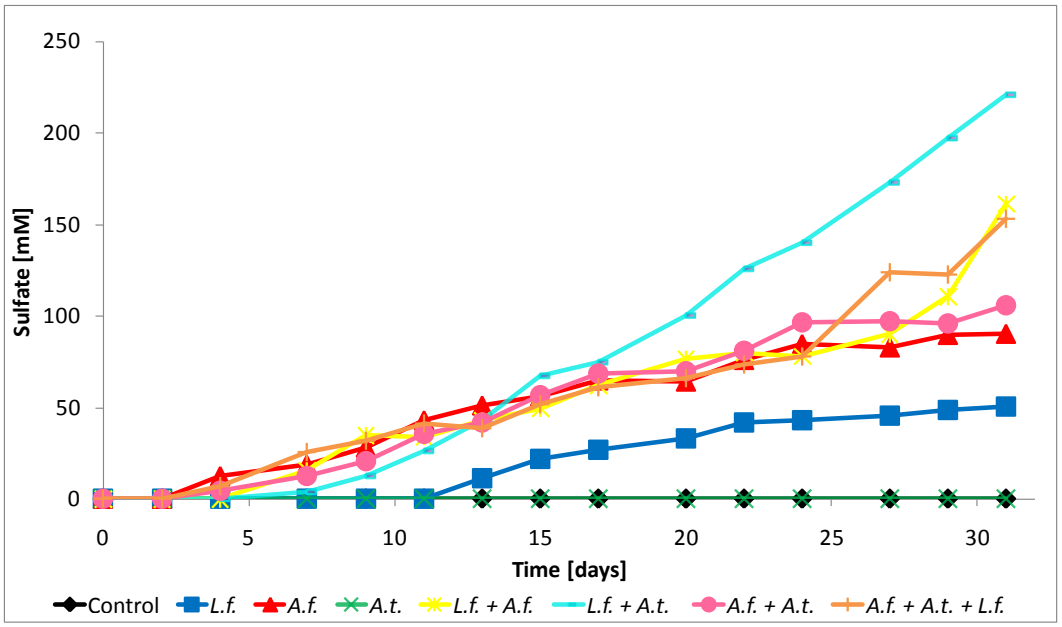

Figure 14: Sulfate concentrations during leaching of pyrite grains
Sulfate concentrations in bulk solutions of pure and mixed cultures of *L. ferrooxidans* DSM 2705 (*L.f.*), *A. ferrooxidans* ATCC 23270 (*A.f.*), *A. thiooxidans* DSM 622 (*A.t.*) and abiotic control. Initial total cell number $1 \cdot 10^8$ cells/mL (two strains: 50 % each strain respectively; three strains: 33 % each strain respectively), 150 mL basal salt solution, 10 g pyrite grains (50 - 100 µm), 28 °C, shaken (120 rpm).Standard error (n = 4) less or equal 11 %.

Sulfate concentrations in leaching cultures of *A. thiooxidans* and in abiotic controls remained below detection limit (10 µM). For pure cultures of *L. ferrooxidans* low sulfate concentrations (50 mM) after 31 days were measured.

The increase of sulfate concentrations in pure cultures of *A. ferrooxidans* and mixed cultures of *L.f* + *A.f.*, *A.f.* + *A.t.* and *A.f.* + *A.t.* + *L.f.* were comparable and ranged between 100 to 118 mM till the 24th day of the experiment. Afterwards, sulfate concentrations of the mixed cultures of *L.f.* + *A.f.* and *A.f.* + *A.t.* + *L.f.* increased slower compared to *A.f.* and *A.f.* + *A.t.*

The highest sulfate concentrations were determined for mixed cultures of *L.f.* + *A.t.* with 221 mM at the end of the leaching experiment.

3.2.6. Elemental sulfur concentrations in bulk solutions during leaching of pyrite grains

Elemental sulfur may occur as intermediate product in the pyrite leaching process.

No elemental sulfur was detected in the bulk solutions of pure and mixed cultures, except of those of *L. ferrooxidans*. Here, 4.1 mM elemental sulfur (n = 4, standard deviation= ± 0.07 mM) was found at the end of the leaching experiment due to the missing sulfur oxidation ability of this bacterium.

3.3. Bacterial attachment to pyrite coupons

Bacterial attachment of pure and mixed cultures of *L. ferrooxidans* DSM 2705, *A. ferrooxidans* ATCC 23270 and *A. thiooxidans* DSM 622 to pyrite coupons was investigated. Comparable results were obtained in attachment experiments to both the sawn and the grown side of pyrite coupons. No differences in cell number as well as cell distribution on the mineral surface were found (data not shown). However, the grown side is better to visualize by EFM and AFM than the sawn side of a coupon. Accordingly, only results for an enumeration of cells as well as images of cells, biofilms and mineral surfaces from the grown side of the pyrite coupons are presented in the following.

The enumeration of cells for pure and mixed cultures as well as the investigations of the cell distribution on mineral surfaces was done by cell staining with DAPI. By the use of FISH the attachment of single strains within a mixed culture on the mineral surface was investigated.

Cells of *L. ferrooxidans* DSM 2705, *A. ferrooxidans* ATCC 23270 and *A. thiooxidans* DSM 622 mainly attach to pyrite grains within 20 min. In contrast, attachment of the same strains to pyrite coupons was not evaluable until at least 1 h after start. Below 1 h the number of attached cells on the mineral surface was insufficient for counting (data not shown). Thus, experiments with incubation times of 1, 2, 3, 4, 5, 6, 7 and 8 h were performed. No linear increase of cell attachment was observed. Total numbers of attached cells varied strongly. However, on average the number of attached cells increased during the maximum experimental time of 8 h. The generation time of *L. ferrooxidans* DSM 2705, *A. ferrooxidans* ATCC 23270 and *A. thiooxidans* DSM 622 ranges between 7 - 8 h under optimal conditions in liquid media (see chapter 2.1.). Therefore, incubation was terminated after 8 h to avoid an increase in cell numbers on the mineral surface by cell growth. The following figures show results for the initial cell attachment to pyrite coupons for 1 and 8 h incubation time.

Results for cell counts are shown as frequency distribution histograms. Fluorescence microscopic images demonstrate the bacterial distribution on the mineral surface.

3.3.1. Attachment of pure cultures of *L. ferrooxidans* DSM 2705, *A. ferrooxidans* ATCC 23270 or *A. thiooxidans* DSM 622 to pyrite coupons

The results of the attachment experiments of pure cultures of *L. ferrooxidans*, *A. ferrooxidans* or *A. thiooxidans* to pyrite coupons after 1 and 8 h are presented in Figure 15 a and b.

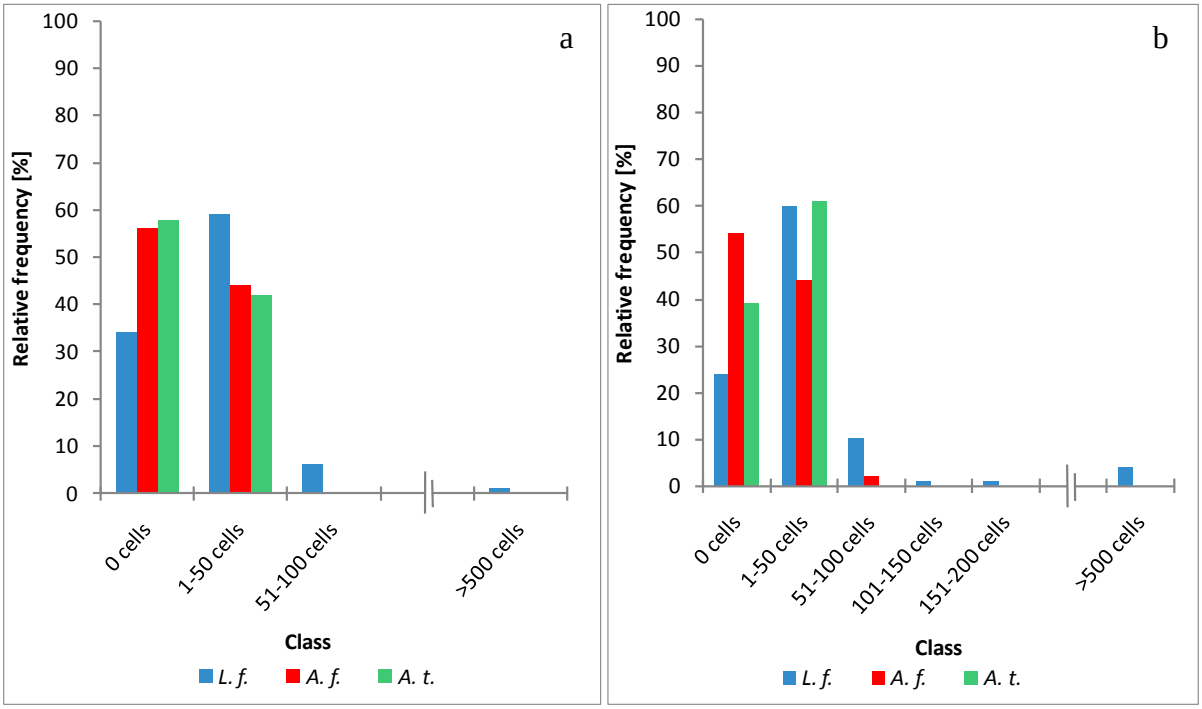

Figure 15 a & b: Attachment of cells from pure cultures of *L. ferrooxidans* DSM 2705 (*L.f.*), *A. ferrooxidans* ATCC 23270 (*A.f.*) and *A. thiooxidans* DSM 622 (*A.t.*) to pyrite coupons after 1 h (a) and 8 h (b)
Initial total cell number $1 \cdot 10^8$ cells/mL, 50 mL basal salt solution, 28 °C, aerated. DAPI stained cells were analyzed of 100 ocular counting grids (125 µm x 125 µm) from 10 coupons, total area 1.5625 mm^2 for each strain.
Standard error (n = 100) for 1h: *L.f.* = 18.51, *A.f.* = 12.66, *A.t.* = 12.58.
Standard error (n = 100) for 8h: *L.f.* = 27.5, *A.f.* = 15.43, *A.t.* = 12.44.

After 1 h incubation, the highest attachment to pyrite coupons was found for pure cultures of *L. ferrooxidans*. This strain exhibited with 34 % the lowest amount of cell-free areas, whereas, for *A. ferrooxidans* and *A. thiooxidans* 56 % and 58 % of the areas remained cell-free. For *L. ferrooxidans* the highest percentage (59 %) of attached cells in the class of 1 to 50 cells was found. Some areas exhibited cell numbers between 51 – 100 cells. Only in 1 out of overall 100 counted areas (1 %) more than 500 cells of *L. ferrooxidans* were determined.
For pure cultures of *A. ferrooxidans* and *A. thiooxidans* attachment was only detected within the class of 1 - 50 cells.

After 8 h, attachment of *L. ferrooxidans* and *A. thiooxidans* increased as compared to the attachment after 1 h incubation. In contrast, the attachment of *A. ferrooxidans* did not increase significantly. Attachment of all cultures was found again mainly within the class 1 - 50 cells. Cells of the pure cultures of *L. ferrooxidans* and *A. thiooxidans* showed comparable relative frequencies of 60 % and 61 %, respectively, within this class.

Cells of the pure cultures of *A. ferrooxidans* showed the lowest attachment of all pure cultures. Cell attachment occurred with a relative frequency of 44 % within the class of 1 – 50 cells and 54 % of the areas remained cell-free.

The lowest number (24 %) of cell-free areas as well as the highest cell number of attached cells was detected for *L. ferrooxidans.* Thus, the highest attachment of pure cultures to pyrite coupons was determined for *L. ferrooxidans*.

3.3.1.1. Images of the attachment of cells of pure cultures of *L. ferrooxidans* DSM 2705, *A. ferrooxidans* ATCC 23270 or *A. thiooxidans* DSM 622 to pyrite coupons after 1 h

Figure 16 a – c illustrates the distribution of attached cells of pure cultures of *L. ferrooxidans* (a), *A. ferrooxidans* (b) or *A. thiooxidans* (c) on pyrite coupons after 1 h incubation.

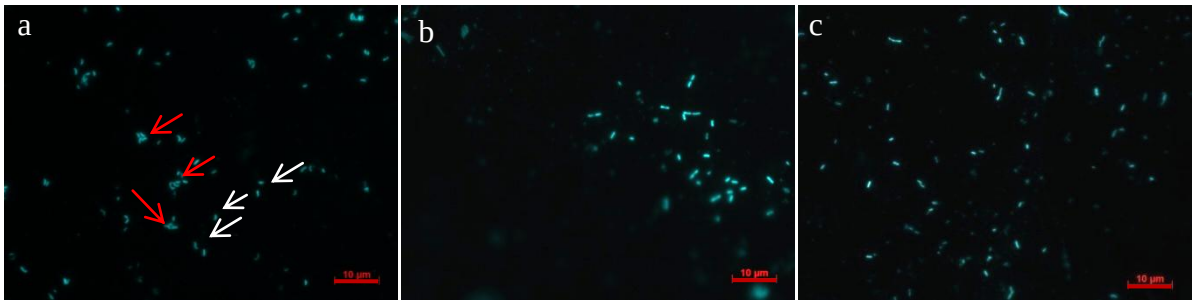

Figure 16 a - c: Pyrite surfaces with attached, DAPI stained cells of *L. ferrooxidans* DSM 2705 (a), *A. ferrooxidans* ATCC 23270 (b) or *A. thiooxidans* DSM 622 (c) from pure cultures after 1 h
Fig. a: DAPI stained *L. ferrooxidans* DSM 2705 cells on pyrite coupon; red arrows: cell clusters; white arrows: single cells.
Fig. b: DAPI stained *A. ferrooxidans* ATCC 23270 cells on pyrite coupon.
Fig. c: DAPI stained *A. thiooxidans* DSM 622 cells on pyrite coupon.
Initial total cell number $1 \cdot 10^8$ cells/mL, 50 mL basal salt solution, 28 °C, aerated.
Each image represents 90 x 70 µm, scale bar 10 µm.

Cells of *L. ferrooxidans*, *A. ferrooxidans* and *A. thiooxidans* attached unevenly to the pyrite coupons. Large areas as well as in some instances whole pyrite coupons remained free of attached bacteria (data not shown). Only in case of *L. ferrooxidans* single cells (white arrows) as well as small clusters (red arrows) were found after 1 h incubation (Figure 16a).

The typical cell distribution of *A. ferrooxidans* on pyrite coupons after 1 h incubation is illustrated in Figure 16b. Cells were attached as single cells.

Single cells of *A. thiooxidans* were found to be more regularly dispersed over the mineral surface than the ones of *L. ferrooxidans* and *A. ferrooxidans*.

3.3.1.2. Images of the attachment of cells from a pure culture of *L. ferrooxidans* DSM 2705 to pyrite coupons after 8 h

DAPI stained pyrite-attached cells of pure cultures of *L. ferrooxidans* after 8 h incubation are presented in Figure 17 a - c.

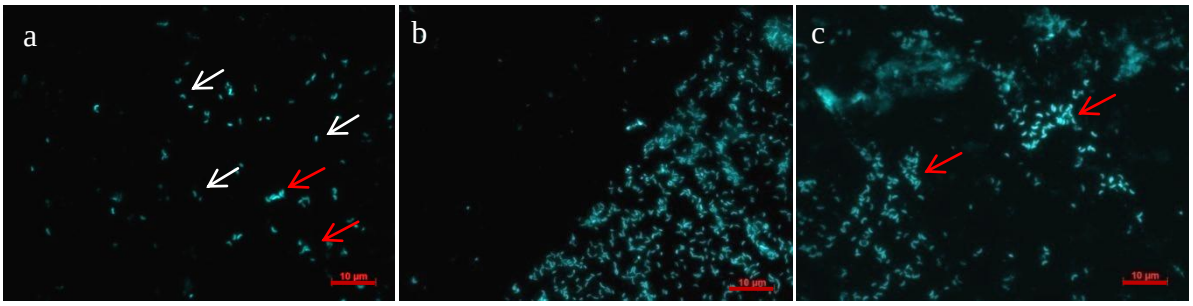

Figure 17 a - c: Typical images of pyrite surfaces with attached, DAPI stained cells of *L. ferrooxidans* DSM 2705 from pure culture after 8 h
White arrow: single cell; red arrow: cell cluster. Initial total cell number $1 \cdot 10^8$ cells/mL, 50 mL basal salt solution, 28 °C, aerated.
Each image represents 90 x 70 µm, scale bar 10 µm.

A sparsely colonized surface area is visible in Figure 17a. Single cells (white arrows) as well as small cell-clusters (red arrows) appear.

In Figure 17b a part of the surface is covered densely by cells of *L. ferrooxidans*, whereas the remaining area was found to be free of cells. This attachment pattern was frequently observed for *L. ferrooxidans* after 8 h incubation (see also Figure 17c).

3.3.1.3. Images of the attachment of cells from a pure culture of *A. ferrooxidans* ATCC 23270 to pyrite coupons after 8 h

DAPI stained cells of pure cultures of *A. ferrooxidans* attached to pyrite surfaces after 8 h incubation are presented in Figure 18 a - c.

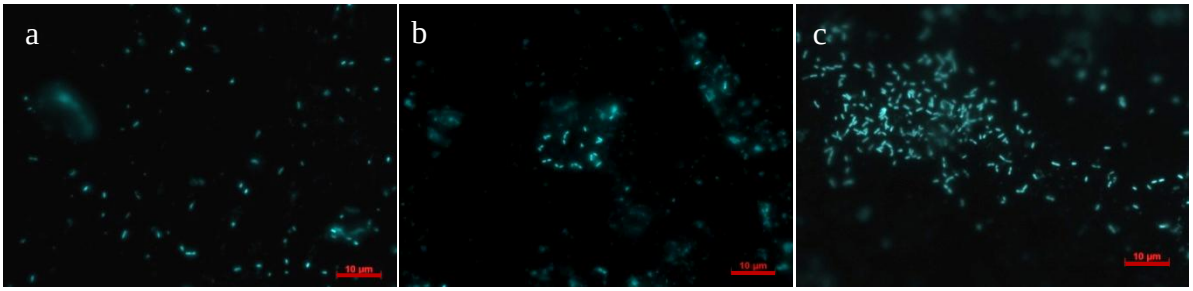

Figure 18 a - c: Typical images of pyrite surfaces with attached, DAPI stained cells of *A. ferrooxidans* ATCC 23270 after 8 h
Initial total cell number $1 \cdot 10^8$ cells/mL, 50 mL basal salt solution, 28 °C, aerated. Each image represents 90 x 70 µm, scale bar 10 µm.

Cells of *A. ferrooxidans* occurred mainly as single cells in low cell numbers (Figure 18 a & b). Cell numbers above 50 cells per counting grid (125 µm x 125 µm) were rarely found (Figure 18c).

3.3.1.4. Images of the attachment of cells from a pure culture of *A. thiooxidans* DSM 622 to pyrite coupons after 8 h

DAPI stained pyrite-attached cells of pure cultures of *A. thiooxidans* after 8 h incubation are presented in Figure 19 a - c. Representative images with low (Figure 19a), middle (Figure 19b) and high (Figure 19c) cell numbers of *A. thiooxidans* are shown.

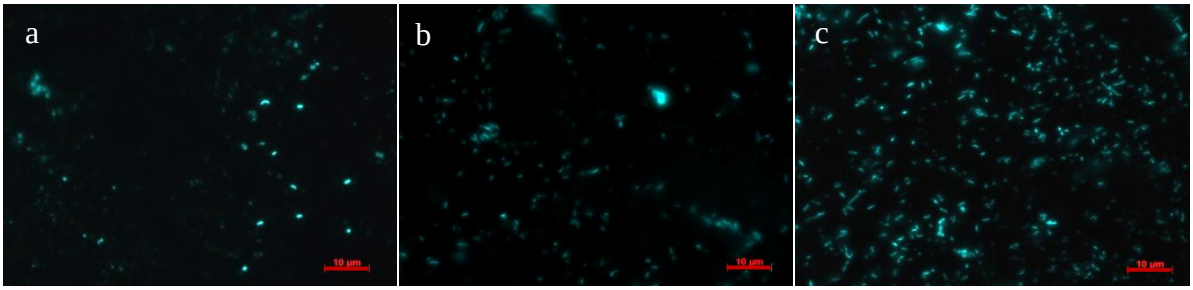

Figure 19 a - c: Typical images of pyrite surfaces with attached, DAPI stained cells of *A. thiooxidans* DSM 622 after 8 h
Initial total cell number $1 \cdot 10^8$ cells/mL, 50 mL basal salt solution, 28 °C, aerated. Each image represents 90 x 70 µm, scale bar 10 µm.

Cells of *A. thiooxidans* were found, compared to cells of *A. ferrooxidans* or *L. ferrooxidans*, more evenly distributed. However, also with this bacterium large areas of the pyrite surface remained uncolonized. Cells were mainly separated (no physical cell-to-cell contact).

3.3.2. Attachment of mixed cultures to pyrite coupons

Cells of mixed cultures on pyrite surfaces were visualized and enumerated by combining DAPI staining with FISH. The total cell number of mixed cultures was determined by the use

of DAPI, whereas FISH allowed the enumeration of the cells of individual strains within the mixed cultures. Results of the total cell number of the mixed culture as well as the corresponding cell number of the individual strains within the mixed culture are given in frequency distribution histograms. Additionally, representative fluorescence microscopic images of colonized areas demonstrate the bacterial distribution on the mineral surface after 8 h incubation.

3.3.2.1. Attachment of a mixed culture composed of *L. ferrooxidans* DSM 2705 and *A. ferrooxidans* ATCC 23270 to pyrite coupons after 1 and 8 h

The frequency distribution histogram of bacterial attachment to pyrite of a mixed culture of *L. ferrooxidans* and *A. ferrooxidans* coupons is presented in Figure 20 a and b.

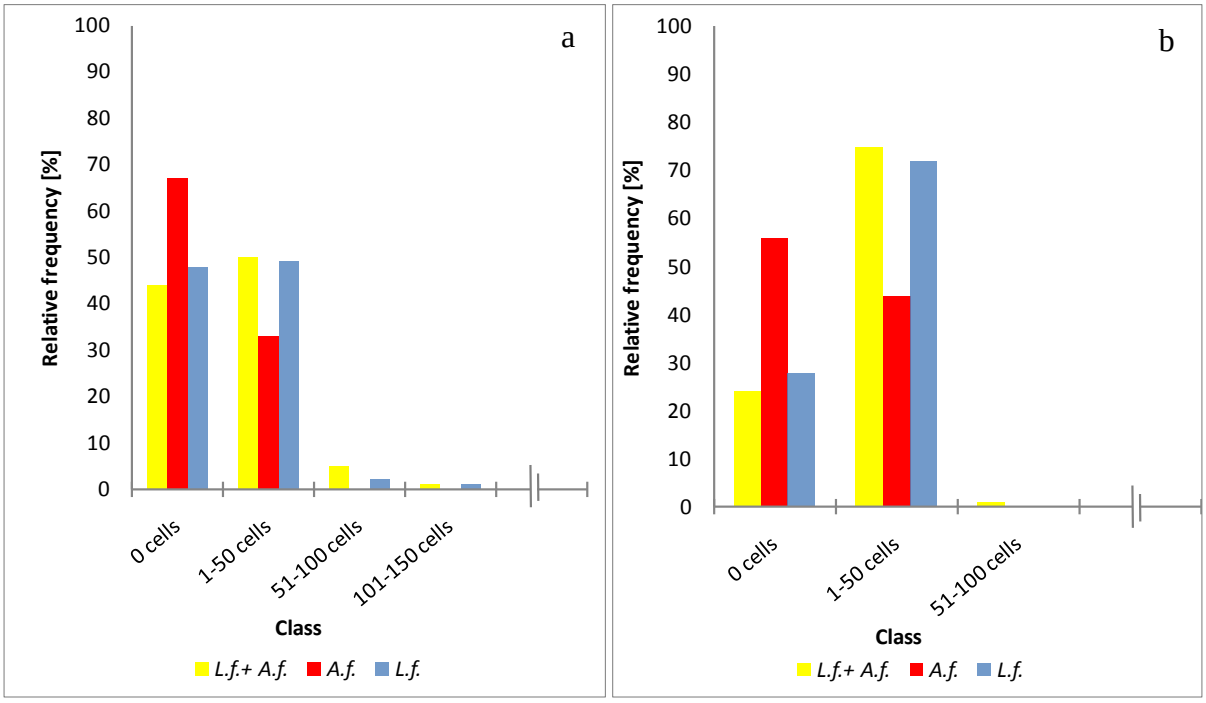

Figure 20 a & b: Attachment of a mixed culture of *L. ferrooxidans* DSM 2705 (*L.f.*) and *A. ferrooxidans* ATCC 23270 (*A.f.*) to pyrite coupons after 1 h (a) and 8 h (b) Initial total cell number $1 \cdot 10^8$ cells/mL (each strain 50 % respectively), 50 mL basal salt solution, 28 °C, aerated. DAPI staining: cells of *L.f.* and *A.f.*; FISH (probe TF539): cells of *A.f.* Determination of DAPI- and FISH stained cells was performed within the same counting grid. Cells of *L. ferrooxidans* were calculated by subtracting *A. ferrooxidans* cells from total cell number. ■ *L.f.* + *A.f.*: frequency of total number of DAPI stained cells. ■ *A.f.*: frequency of fluorescence *in situ* hybridized *A. ferrooxidans* cells within the mixed culture. ■ *L.f.*: calculated frequency of *L. ferrooxidans* cells within the mixed culture. Cells were analyzed of 100 ocular counting grids (125 µm x 125 µm) from 10 coupons, total area 1.5625 mm^2. Standard error (n = 100) for 1 h: *L.f.* + *A.f.* = 21.25, *A.f.* = 23.22, *L.f.* = 17.6.Standard error (n = 100) for 8 h: *L.f.* + *A.f.* = 12.22, *A.f.* = 12.65, *L.f.* = 11.45.

In Figure 20a attachment frequencies of cells of a mixed culture of *L. ferrooxidans* and *A. ferrooxidans* indicate higher numbers for cells of *L. ferrooxidans* attached to a pyrite surface than the numbers of cells of *A. ferrooxidans* after 1 h. Cells of *A. ferrooxidans* were not found on 67 % of the investigated area, whereas only 48 % of the areas were free of *L. ferrooxidans* cells. The attachment occurred mainly within the class 1 - 50 cells. Increased attachment was rarely observed.

In comparison to the results after 1 h incubation, attachment of the mixed culture of *A.f.* + *L.f.* was increased after 8 h incubation. Less cell-free areas were found (24 %) than after 1 h. However, the relation of attached cells of *A. ferrooxidans* and *L. ferrooxidans* after 8 h is comparable to the one after 1 h. Again, higher cell numbers of *L. ferrooxidans* than of *A. ferrooxidans* were detected. More areas without cells of *A. ferrooxidans* were found than those without *L. ferrooxidans* cells. Furthermore, attachment frequency mainly ranged in the class of 1 – 50 cells.

Images of cells of a mixed culture composed of *L. ferrooxidans* DSM 2705 and *A. ferrooxidans* ATCC 23270 attached to a pyrite coupon after 8 h

DAPI stained (Figure 21a) and fluorescence *in situ* hybridized (Figure 21b) pyrite-attached cells of a mixed culture containing *L. ferrooxidans* and *A. ferrooxidans* after 8 h incubation are presented in the following fluorescence microscope images.

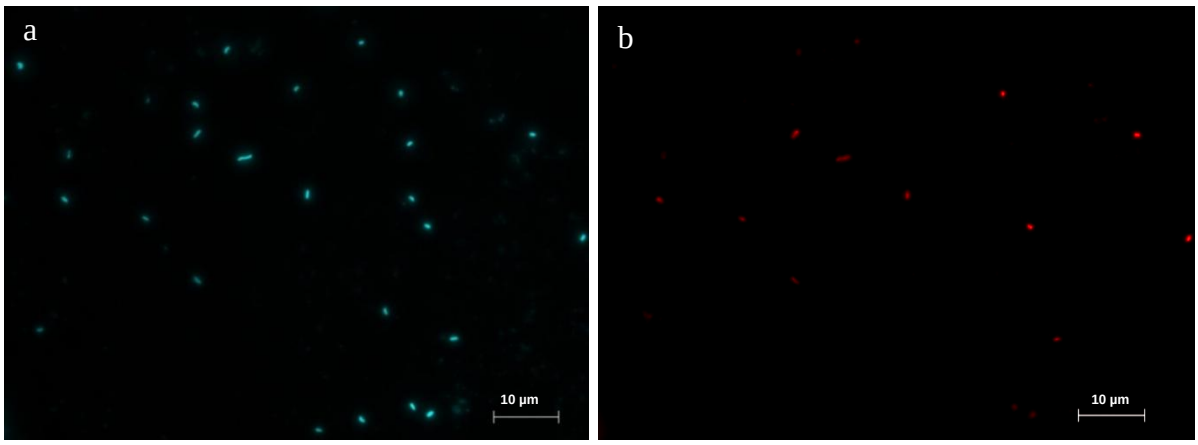

Figure 21 a & b: Representative images of a pyrite surface with attached cells from a mixed culture containing *L. ferrooxidans* DSM 2705 and *A. ferrooxidans* ATCC 23270 after 8 h

Fig. a: DAPI stained cells of *L. ferrooxidans* and *A. ferrooxidans*; Fig. b: fluorescence *in situ* hybridized *A. ferrooxidans* cells (probe TF539). Both images originate from the same side on the coupon surface. Initial total cell number $1 \cdot 10^8$ cells/mL (each strain 50 % respectively), 50 mL basal salt solution, 28 °C, aerated. Each image represents 90 x 70 µm, scale bar 10 µm.

The cells of the mixed culture of *L. ferrooxidans* and *A. ferrooxidans* were found to be heterogeneously distributed on the pyrite surface, except for a few clusters. Figure 21a gives a typical attachment pattern. *A. ferrooxidans* and *L. ferrooxidans* occurred mainly as single cells on the mineral surface. In Figure 21b only *A. ferrooxidans* cells are visible by the use of a specific FISH probe (TF539). Physical interspecies cell-to-cell contact was not observed in mixed cultures of *L. ferrooxidans* and *A. ferrooxidans* on mineral surfaces.

3.3.2.2. Attachment of cells of a mixed culture composed of *L. ferrooxidans* DSM 2705 and *A. thiooxidans* DSM 622 to pyrite coupons after 1 and 8 h

Frequency distributions of cell attachment of *L. ferrooxidans* and *A. thiooxidans* to pyrite coupons in a mixed culture after 1 h (Figure 22a) and 8 h (Figure 22b) incubation is presented in the following histograms.

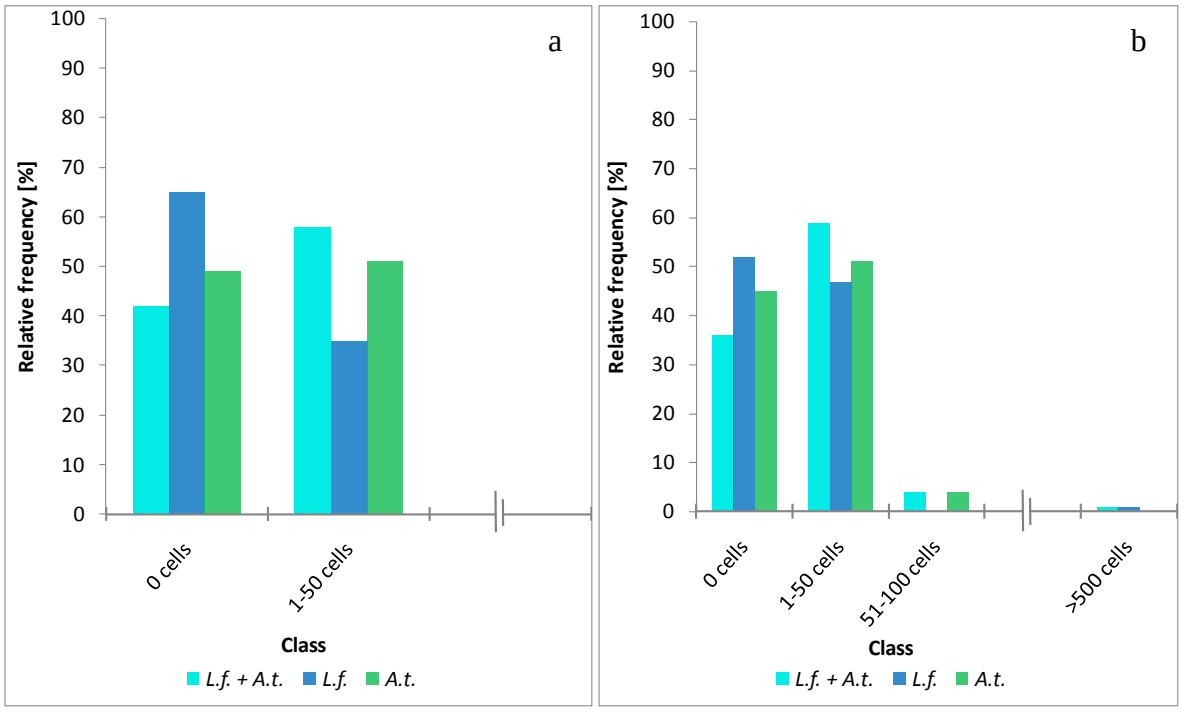

Figure 22 a & b: Attachment of a mixed culture of *L. ferrooxidans* DSM 2705 (*L.f.*) and *A. thiooxidans* DSM 622 (*A.t.*) to pyrite coupons after 1 h (a) and 8 h (b)
Initial total cell number $1 \cdot 10^8$ cells/mL (each strain 50 % respectively), 50 mL basal salt solution, 28 °C, aerated. DAPI staining: cells of *L.f.* and *A.t.*; FISH (probe LEP665): cells of *L.f.* Determination of DAPI- and FISH stained cells was performed within the same counting grid. Cells of *A. thiooxidans* were calculated by subtracting *L. ferrooxidans* cells from total cell number. *L.f.* + *A.t.*: frequency of total number of DAPI stained cells. *L.f.*: frequency of fluorescence *in situ* hybridized *L. ferrooxidans* cells within the mixed culture. *A.t.*: calculated frequency of *A. thiooxidans* cells within the mixed culture. Cells were analyzed from 100 ocular counting grids (125 µm x 125 µm) from 10 coupons, total area 1.5625 mm^2. Standard error for (n = 100) 1 h: *L.f.* + *A.t.* = 12.58, *L.f.* = 13.8, *A.t.* = 12.83. Standard error for (n = 100) 8 h: *L.f.* + *A.t.* = 16.89, *L.f.* = 12.73, *A.t.* = 17.4.

After 1 h, the mixed cultures containing cells of *L. ferrooxidans* and *A. thiooxidans* showed attachment with cell numbers only in the class of 1 to 50 cells. In total 42 % of the areas were found to be cell-free. The attachment of *A. thiooxidans* is more dominant than the attachment of *L. ferrooxidans* after 1 h incubation. Cells of *L. ferrooxidans* were not found in 65 out of 100 (65 %) investigated areas, whereas only 49 % of the areas remained free of *A. thiooxidans* cells.

After 8 h incubation, the attachment of *A. thiooxidans* cells was still higher than the attachment of *L. ferrooxidans* cells. Numbers of attached cells of the mixed cultures as well as of both individual strains ranged mainly in the class of 1 – 50 cells. Cells of *A. thiooxidans* were found within the class 51 – 100 cells with a relative frequency of 4 %. In one counting grid (125 µm x 125 µm) more than 500 cells of *L. ferrooxidans* cells were counted.

In comparison with the other mixed cultures such as *L.f. + A.f.*, *A.f. + A.t.* and *A.f. + A.t. + L.f.* within the same experimental set up, the lowest attachment after 8 h incubation was found for the mixed cultures of *L. ferrooxidans* with *A. thiooxidans*.

Images of cells of a mixed culture composed of *L. ferrooxidans* DSM 2705 and *A. thiooxidans* DSM 622 attached to a pyrite coupon after 8 h

DAPI stained (Figure 23a) and fluorescence *in situ* hybridized (Figure 23b) pyrite-attached cells of a mixed culture containing *L. ferrooxidans* and *A. thiooxidans* after 8 h incubation are presented in the following fluorescence microscope images.

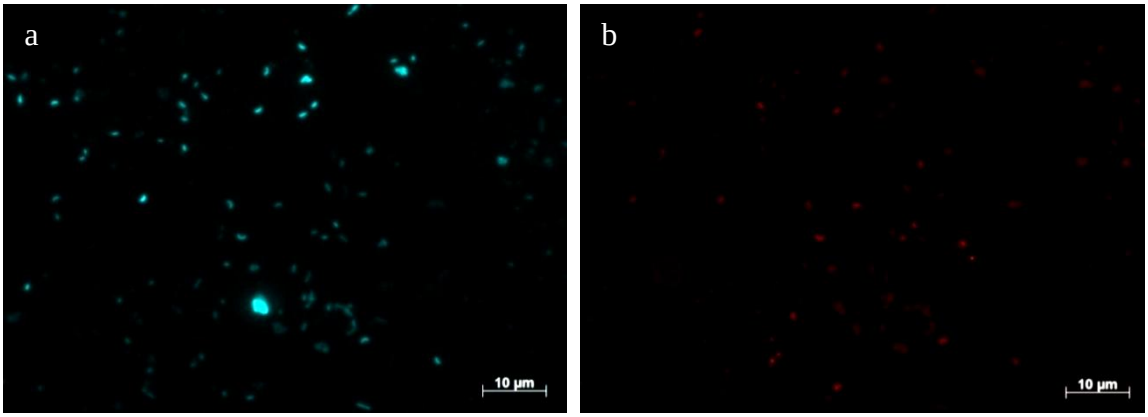

Figure 23 a & b: Representative images of a pyrite surface with attached cells from a mixed culture containing *L. ferrooxidans* DSM 2705 and *A. thiooxidans* DSM 622 after 8 h

Fig. a: DAPI stained cells of *L. ferrooxidans* and *A. thiooxidans*; Fig. b: fluorescence *in situ* hybridized *L. ferrooxidans* cells (probe LEP665). Both images originate from the same side on the coupon surface. Initial total cell number $1 \cdot 10^8$ cells/mL (each strain 50 % respectively), 50 mL basal salt solution, 28 °C, aerated. Each image represents 90 x 70 µm, scale bar 10 µm.

DAPI stained cells of the mixed culture of *L. ferrooxidans* and *A. thiooxidans* are shown in Figure 23a. Cells are heterogeneously distributed over the mineral surface. Sparsely cluster formation was observed. A lower cell number as shown in Figure 23a of *L. ferrooxidans* fluorescence *in situ* hybridized cells is shown in Figure 23b.

3.3.2.3. Attachment of a mixed culture composed of *A. ferrooxidans* ATCC 23270 and *A. thiooxidans* DSM 622 to pyrite coupons after 1 and 8 h

Frequency distribution of cell attachment of *A. ferrooxidans* and *A. thiooxidans* to pyrite coupons in a mixed culture after 1 h (Figure 24a) and 8 h (Figure 24b) incubation is presented in the following histograms.

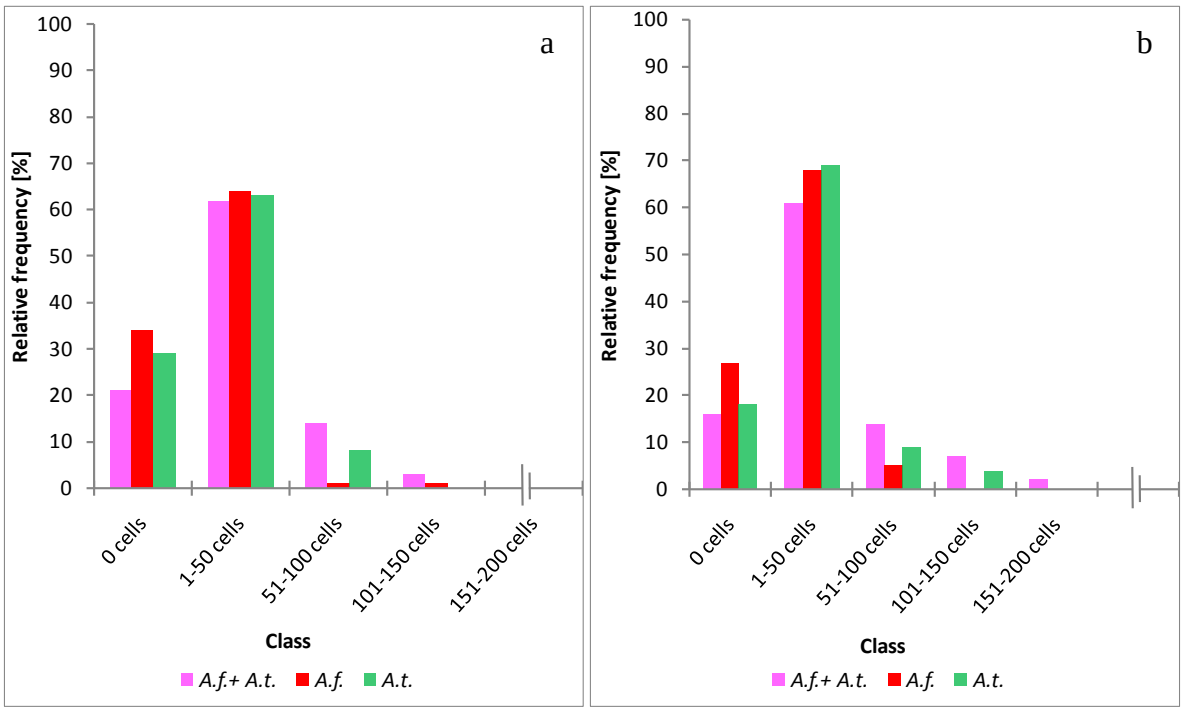

Figure 24 a & b: Attachment of a mixed culture of *A. ferrooxidans* ATCC 23270 (*A.f.*) and *A. thiooxidans* DSM 622 (*A.t.*) to pyrite coupons after 1 h (a) and 8 h (b)

Initial total cell number $1 \cdot 10^8$ cells/mL (each strain 50 % respectively), 50 mL basal salt solution, 28 °C, aerated. DAPI staining: cells of *A.f.* and *A.t.* FISH (probe TF539): cells of *A.f.* Determination of DAPI- and FISH stained cells was performed within counting grid. Cells of *A. thiooxidans* were calculated by subtracting *A. ferrooxidans* cells from total cell number. ■ *A.f.* + *A.t.*: frequency of total number of DAPI stained cells. ■ *A.f.*: frequency of fluorescence *in situ* hybridized *A. ferrooxidans* cells within the mixed culture. ■ *A.t.*: calculated frequency of *A. thiooxidans* cells within the mixed culture. Cells were analyzed from 100 ocular counting grids (125 µm x 125 µm) from 10 coupons, total area 1.5625 mm^2.
Standard error (n = 100) for 1 h: *A.f.* + *A.t.* = 27.66, *A.f.* = 30.08, *A.t.* = 17.58.
Standard error (n = 100) for 8 h: *A.f.* + *A.t.* = 37.91, *A.f.* = 16.77, *A.t.* = 26.96.

In comparison with results from the mixed cultures of *L.f.* + *A.f.* and *L.f.* + *A.t.* within the same experimental set up after 1 h incubation, increased attachment was found for the mixed cultures consisting of *A.f.* + *A.t.* Only 21 % of the investigated areas remained cell-free.

Cell numbers of attached cells ranged mainly in the class of 1 - 50 cells. Both strains showed nearly the same attachment frequency. However, cells of *A. ferrooxidans* were found only with a relative frequency of 2 % within higher classes, whereas *A. thiooxidans* with a relative frequency of 8 % in the class of 51 – 100 cells and less cell-free areas was the main attaching bacterium.

Attachment of the mixed cultures of *A. ferrooxidans* and *A. thiooxidans* was found mainly within 1 h. No significant increased attachment was observed for 8 h.

The cell number of attached cells was again highly related to the class 1 – 50 cells and cell numbers regarding to other classes were rarely found after 8 h incubation.

Images of cells of a mixed culture composed of *A. ferrooxidans* ATCC 23270 and *A. thiooxidans* DSM 622 attached to a pyrite coupon after 8 h

DAPI stained (Figure 25a) and fluorescence *in situ* hybridized (Figure 25b) pyrite-attached cells of a mixed culture containing *A. ferrooxidans* and *A. thiooxidans* after 8 h incubation are presented in the following fluorescence microscope images.

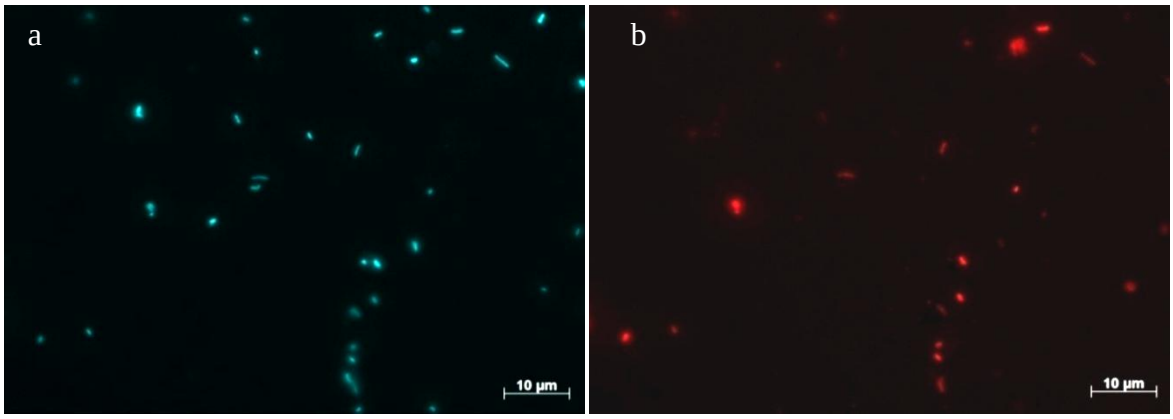

Figure 25 a & b: Representative images of a pyrite surface with attached cells from a mixed culture containing *A. ferrooxidans* ATCC 23270 and *A. thiooxidans* DSM 622 after 8 h

Fig. a: DAPI stained cells of *A. ferrooxidans* and *A. thiooxidans*; Fig. b: fluorescence *in situ* hybridized *A. ferrooxidans* cells (probe TF539). Both images originate from the same side on the coupon surface. Initial total cell number $1 \cdot 10^8$ cells/mL (each strain 50 % respectively), 50 mL basal salt solution, 28 °C, aerated. Each image represents 90 x 70 µm, scale bar 10 µm.

Cells of the mixed cultures composed of *A. ferrooxidans* and *A. thiooxidans* showed no cluster formation on the mineral surface. Attached cells were found heterogeneously

distributed on the mineral surface (Figure 25 a and b). No interspecies physical contact between *A. ferrooxidans* and *A. thiooxidans* cells was observed.

3.3.2.4. Attachment of a mixed culture composed of *L. ferrooxidans* DSM 2705, *A. ferrooxidans* ATCC 23270 and *A. thiooxidans* DSM 622 to pyrite coupons after 1 and 8 h

The highest amount of attached cells to pyrite coupons with mixed cultures was determined for the assay composed of cells of *A. ferrooxidans*, *A. thiooxidans* and *L. ferrooxidans*, as shown in Figure 26 a and b.

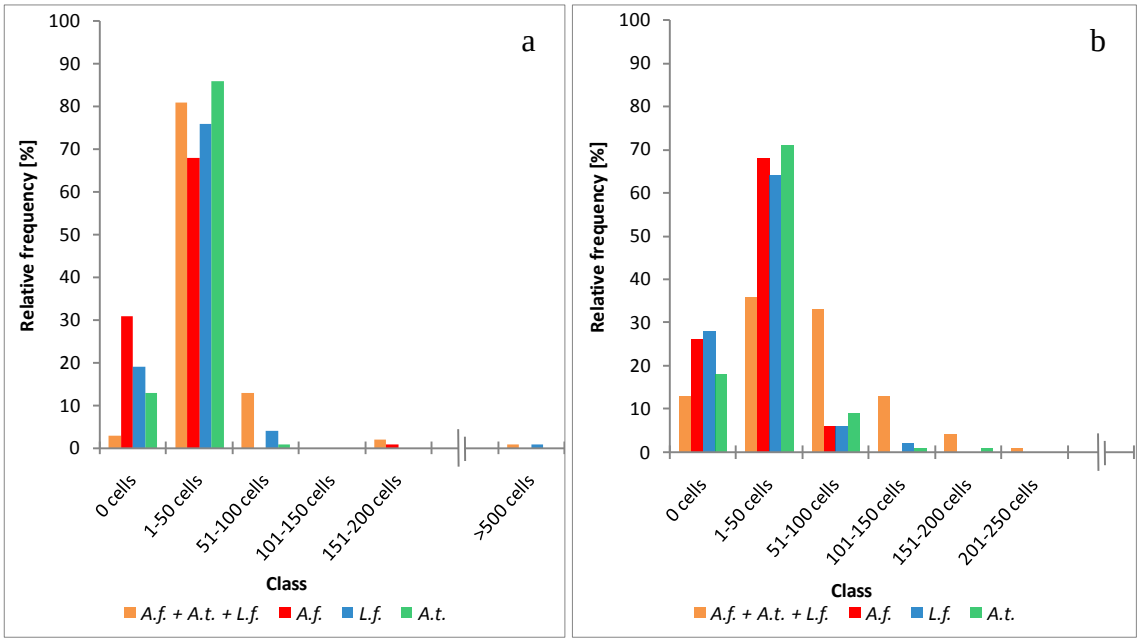

Figure 26 a & b: Attachment of a mixed culture of *A. ferrooxidans* ATCC 23270 (*A.f.*), *A. thiooxidans* DSM 622 (*A.t.*) and *L. ferrooxidans* DSM 2705 (*L.f.*) to pyrite coupons after 1 h (a) and 8 h (b)

Initial total cell number $1 \cdot 10^8$ cells/mL (each strain 33 % respectively), 50 mL basal salt solution, 28 °C, aerated. DAPI staining: cells of *A.f.*, *A.t.* and *L.f.* FISH (probes TF539 and LEP665): cells of *A.f.* and *L.f.* respectively. Determination of DAPI- and FISH stained cells was performed within the same counting grid. Cells of *A. thiooxidans* were calculated by subtracting *A. ferrooxidans* and *L. ferrooxidans* cells from total cell number. *A.f.* + *A.t.* + *L.f.*: frequency of total number of DAPI stained cells. *A.f.*: frequency of fluorescence *in situ* hybridized (TF539) *A. ferrooxidans* cells within the mixed culture. *L.f.*: frequency of fluorescence *in situ* hybridized (LEP665) *L. ferrooxidans* cells within the mixed culture. *A.t.*: calculated frequency of *A. thiooxidans* cells within the mixed culture. Cells were analyzed from 100 ocular counting grids (125 µm x 125 µm) from 10 coupons, total area 1.5625 mm^2.

Standard error (n = 100) for 1 h: *A.f.* + *A.t.* + *L.f.* = 27.0, *A.f.* = 19.63, *L.f.* = 14.85, *A.t.* = 10.1. Standard error for (n = 100) 8 h: *A.f.* + *A.t.* + *L.f.* = 48.38, *A.f.* = 17.49, *L.f.* = 22.97, *A.t.* = 25.71.

A low number of cell-free areas (3 %) was found for the mixed culture of *A.f.* + *A.t.* + *L.f.* after 1 h incubation. The total cell number of attached cells of the mixed culture as well as the cell number of attached cells of the individual strains within the mixed culture ranged mainly in the class of 1 - 50 cells. Even in this mixed culture the cells of *A. ferrooxidans* showed the lowest attachment to pyrite coupons after 1 h. In 31 % of the investigated area *A. ferrooxidans* cells were not detectable. In contrast only 19 % of the area remained free of *L. ferrooxidans* cells and 13 % free of *A. thiooxidans* cells.

A slightly decreased attachment for the mixed culture of *A.f.* + *A.t.* + *L.f.* was determined after 8 h (Figure 26b), whereas a relative frequency of 13 % cell-free areas were detected. The main attachment again was detected within the class 1 – 50 cells. Attachment was also found in higher cell numbers within the classes of 51 – 100 cells and 101 – 150 cells after 8 h. The attachment of *L. ferrooxidans* and *A. thiooxidans* after 8 h was decreased compared to the attachment after 1 h. A higher number of cell-free areas was evident for both strains.

Images of cells of a mixed culture composed of *A. ferrooxidans* ATCC 23270, *L. ferrooxidans* DSM 2705 and *A. thiooxidans* DSM 622 attached to pyrite coupons after 8 h

DAPI stained (Figure 27a) and fluorescence *in situ* hybridized *L. ferrooxidans* (Figure 27b) and *A. ferrooxidans* (Figure 27c) pyrite-attached cells of a mixed culture containing the former two strains and *A. thiooxidans* after 8 h incubation are presented in the following fluorescence microscope images.

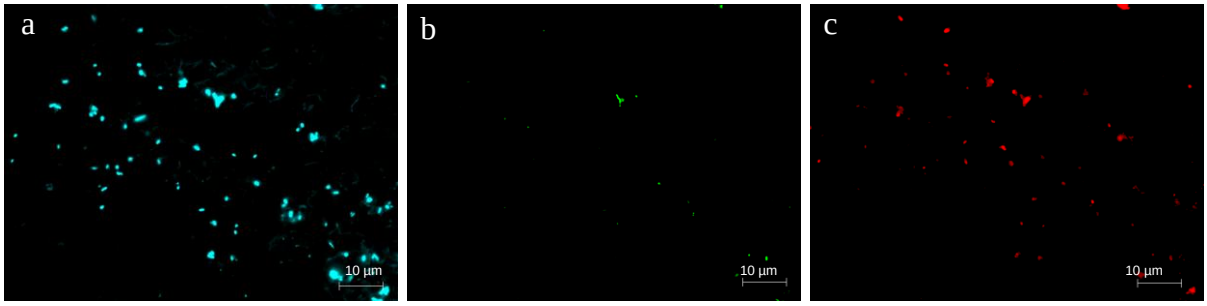

Figure 27 a - c: Representative images of a pyrite surface with attached cells from a mixed culture containing *A. ferrooxidans* ATCC 23270, *A. thiooxidans* DSM 622 and *L. ferrooxidans* DSM 2705 after 8 h

Fig. a: DAPI stained cells of *A. ferrooxidans, L. ferrooxidans*, and *A. thiooxidans*;
Fig. b: fluorescence *in situ* hybridized *L. ferrooxidans* cells (probe LEP665);
Fig. c: fluorescence *in situ* hybridized *A. ferrooxidans* cells (probe TF539).
Images a, b and c originate from the same side on the coupon surface. Initial total cell number $1 \cdot 10^8$ cells/mL (each strain 33 % respectively), 50 mL basal salt solution, 28 °C, aerated. Each image represents 90 x 70 µm, scale bar 10 µm.

In Figure 27a all DAPI stained cells of the 3 members of the mixed culture are visualized. Cells are heterogeneously distributed over the pyrite surface. However, a tendency for small cluster formation was observed. Specific FISH probes were used to identify cells of *L. ferrooxidans* (probe LEP665) and cells of *A. ferrooxidans* (probe TF539). Only a few cells were identified as *L. ferrooxidans* shown in Figure 27b and an increased cell number was identified as *A. ferrooxidans* cells shown in Figure 27c. Cells not hybridized with probes LEP665 or TF539, were considered to be mainly *A. thiooxidans* cells.

Cells of *L. ferrooxidans* were often found in clusters, which did not include cells of other species (Figure 28 a - b).

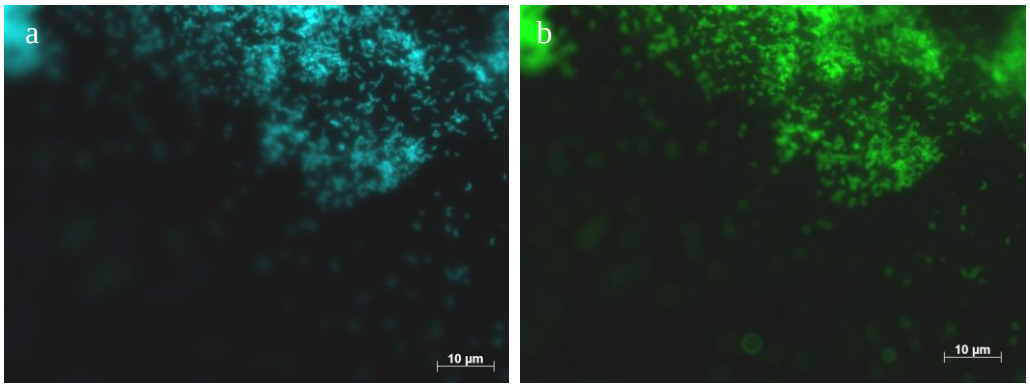

Figure 28 a & b: Image of a pyrite surface with attached cells from a mixed culture containing *A. ferrooxidans* ATCC 23270, *A. thiooxidans* DSM 622 and *L. ferrooxidans* DSM 2705 after 8 h
Fig. a: DAPI stained cells of *A. ferrooxidans*, *L. ferrooxidans*, and *A. thiooxidans*; b: fluorescence *in situ* hybridized *L. ferrooxidans* cells (probe LEP665). Both images originate from the same side on the coupon surface. Initial total cell number $1 \cdot 10^8$ cells/mL (each strain 33 % respectively), 50 mL basal salt solution, 28 °C, aerated. Each image represents 90 x 70 µm, scale bar 10 µm.

3.3.3. Comparison of the attachment of cells of *L. ferrooxidans* DSM 2705, *A. thiooxidans* ATCC 23270 and *A. thiooxidans* DSM 622 in pure or mixed cultures to pyrite coupons

A comparison of the attachment of pure cultures of *L. ferrooxidans* DSM 2705, *A. ferrooxidans* ATCC 23270 and *A. thiooxidans* DSM 622 with the attachment of the same strains in mixed cultures is presented in the following tables. Results are given in relative frequencies within defined classes. The initial cell number of strains in pure cultures is $1 \cdot 10^8$ cells/mL, whereas in mixed cultures composed of 2 or 3 strains the initial cell number of each single strain is only $5 \cdot 10^7$ cells/mL or $3 \cdot 10^7$ cells/mL (depending of mixtures composed of two or three strains). However, the different cell number is negligible, because cells were present in excess to the coverable surface of the pyrite coupon.

3.3.3.1. Comparison of the attachment of cells of *L. ferrooxidans* DSM 2705 in pure or in mixed culture to pyrite coupons

The data for attachment of *L. ferrooxidans* DSM 2705 in pure cultures as well as in mixed cultures is shown in Table 19. The data indicate the behavior of *L. ferrooxidans* attachment to pyrite coupons in pure as well as in mixed cultures with cells of *A. ferrooxidans* ATCC 23270 and/or *A. thiooxidans* DSM 622.

Table 19: Attachment of cells of *L. ferrooxidans* DSM 2705 (*L.f.*) in pure or in mixed culture to pyrite coupons after 1 and 8 h
Initial total cell number $1 \cdot 10^8$ cells/mL, mixed culture composed of 2 strains each strain 50 % respectively, mixed culture composed of 3 strains each strain 33 % respectively, 50 mL basal salt solution, 28 °C, aerated.
Quantification of *L.f.* was performed either by DAPI or by FISH. Pure culture = DAPI; *L.f.* + *A.f.* =DAPI (differentiation of *A.f.* by specific FISH probe TF539); *L.f.* + *A.t.* = FISH (probe LEP665); *A.f.* + *A.t.* + *L.f.* = FISH (probe LEP665). Cells were analyzed from 100 ocular counting grids (125 µm x 125 µm) from 10 coupons, total area 1.5625 mm^2.

	Frequency							
Class	***L.f.***		***L.f.* + *A.f.***		***L.f.* + *A.t.***		***A.f.* + *A.t.* + *L.f.***	
	1 h	**8 h**	**1 h**	**8 h**	**1 h**	**8 h**	**1 h**	**8 h**
0	34	24	48	28	65	52	19	28
1 - 50	59	60	49	72	35	47	76	64
51 - 100	6	10	2	n.d.	n.d.	n.d.	4	6
101 - 150	n.d.	1	1	n.d.	n.d.	n.d.	1	2
150 - 200	n.d.	1	n.d.	n.d.	n.d.	n.d.	n.d.	n.d.
n.d.								
> 500	1	4	n.d.	n.d.	n.d.	1	n.d.	n.d.

n.d. = not detected

Attachment of cells of *L. ferrooxidans* in pure or in mixed culture occurred mainly in the class 1 - 50 cells after 1 and 8 h. Higher cell numbers of *L. ferrooxidans* were rarely determined. More than 500 cells per counting grid (125 µm x 125 µm) were detected in a few cases. The highest attachment of *L. ferrooxidans* was found in mixed cultures of *A.f.* + *A.t.* + *L.f.* after 1 h. Only 19 % of the areas remained free of *L. ferrooxidans* cells. However, the number of attached cell was decreased after 8 h. In contrast, the attachment of pure cultures of *L. ferrooxidans* increased between 1h and 8 h.

The lowest attachment of *L. ferrooxidans* was detected for mixed cultures of *L.f.* + *A.t.* after 1 h as well as after 8 h incubation.

3.3.3.2. Comparison of the attachment of cells of *A. ferrooxidans* ATCC 23270 in pure or in mixed culture to pyrite coupons

The data for attachment of *A. ferrooxidans* ATCC 23270 in pure as well as in mixed cultures are presented in Table 20. Only slight differences in *A. ferrooxidans* ATCC 23270 attachment to pyrite coupons in pure as well as in mixed culture with cells of *L. ferrooxidans* DSM 2705 and/or *A. thiooxidans* DSM 622 were noted.

Table 20: Attachment of cells of *A. ferrooxidans* ATCC 23270 (*A.f.*) in pure or in mixed culture to pyrite coupons after 1 and 8 h
Attachment experiment: Initial total cell number $1 \cdot 10^8$ cells/mL (mixed culture composed of 2 strains each strain 50 % respectively, mixed culture composed of 3 strains each strain 33 % respectively), 50 mL basal salt solution, 28 °C, aerated. Quantification of *A.f.* was performed either by DAPI or by FISH. Pure culture = DAPI; *L.f.* + *A.f.* = FISH (probe TF539); *A.f.* + *A.t.* = FISH (probe TF539); *A.f.* + *A.t.* + *L.f.* = FISH (probe TF539). Cells were analyzed from 100 ocular counting grids (125 µm x 125 µm) from 10 coupons, total area 1.5625 mm^2.

	Frequency							
Class	***A.f.***		***L.f.* + *A.f.***		***A.f.* + *A.t.***		***A.f.* + *A.t.* + *L.f.***	
	1 h	**8 h**	**1 h**	**8 h**	**1 h**	**8 h**	**1 h**	**8 h**
0	56	54	67	56	34	27	31	26
1 - 50	44	44	33	44	64	68	68	68
51 - 100	n.d.	2	n.d.	n.d.	1	5	n.d.	6
101 - 150	n.d.	n.d.	n.d.	n.d.	1	n.d.	n.d.	n.d.
150 - 200	n.d.	n.d.	n.d.	n.d.	n.d.	n.d.	1	n.d.
n.d.								

n.d. = not detected

Attachment of cells of *A. ferrooxidans* in pure or in mixed culture occurred mainly within the class 1 - 50 cells. Higher cell numbers than these were rarely determined.

The highest attachment of *A. ferrooxidans* was determined in mixed cultures containing cells of *A. thiooxidans*. Only 26 % or 27 % of the areas remained free of *A. ferrooxidans* cells in mixed cultures of *A.f.* + *A.t.* + *L.f.* and *A.f.* + *A.t.* after 8 h experimental time. The lowest attachment of *A. ferrooxidans* was determined for the mixed culture *L.f.* + *A.f.* with 67 % uncolonized areas after 1h.

3.3.3.3. Comparison of the attachment of cells of *A. thiooxidans* DSM 622 in pure or in mixed culture to pyrite coupons

The data for attachment of *A. thiooxidans* DSM 622 in pure culture as well as in mixed cultures are given in Table 21. The data indicate differences in *A. thiooxidans* attachment to pyrite coupons in pure as well as in mixed cultures in the presence of cells of *A. ferrooxidans* ATCC 23270 and/or *L. ferrooxidans* DSM 2705.

Table 21: Attachment of *A. thiooxidans* DSM 622 (*A.t.*) as pure or in mixed cultures to pyrite coupons after 1 and 8 h
Initial total cell number $1 \cdot 10^8$ cells/mL (mixed culture composed of 2 strains each strain 50 % respectively, mixed culture composed of 3 strains each strain 33 % respectively), 50 mL basal salt solution, 28 °C, aerated. Quantification of *A.f.* was performed only by DAPI. Pure culture = DAPI; *L.f.* + *A.t.* = DAPI (differentiation of *L.f.* by specific FISH probe LEP665); *A.f.* + *A.t.* = DAPI (differentiation of *A.f.* by specific FISH probe TF539); *A.f.* + *A.t.* + *L.f.* = DAPI (differentiation of *A.f.* and *L.f.* by specific FISH probe TF539 and LEP665). Cells were analyzed from 100 ocular counting grids (125 µm x 125 µm) from 10 coupons, total area 1.5625 mm^2.

	Frequency							
Class	***A.t.***		***L.f.* + *A.t.***		***A.f.* + *A.t.***		***A.f.* + *A.t.* + *L.f.***	
	1 h	**8 h**	**1 h**	**8 h**	**1 h**	**8 h**	**1 h**	**8 h**
0	58	39	49	45	29	18	13	18
1 - 50	42	61	51	51	63	69	86	71
51 - 100	n.d.	n.d.	n.d.	4	8	9	1	9
101 - 150	n.d.	n.d.	n.d.	n.d.	n.d.	4	n.d.	1
150 - 200	n.d.	n.d.	n.d.	n.d.	n.d.	n.d.	n.d.	1
n.d.								

n.d. = not detected

Main attachment occurred in the class 1 - 50 cells. Attachment of *A. thiooxidans* in higher cell classes were only measured for mixed cultures.

The highest attachment of *A. thiooxidans* cells was found for mixed cultures whenever cells of *A. ferrooxidans* were present (*A.f.* + *A.t.* or *A.f.* + *A.t.* + *L.f.*).

The lowest attachment of *A. thiooxidans* was found in pure cultures after 1 h incubation, 58 % of the investigated areas remained *A. thiooxidans* cell-free.

3.5. Attachment of pure cultures of *L. ferrooxidans* DSM 2705, *A. ferrooxidans* ATCC 23270 or *A. thiooxidans* DSM 622 to precolonized pyrite coupons

Attachment of pure cultures of *L. ferrooxidans* DSM 2705, *A. ferrooxidans* ATCC 23270 or *A. thiooxidans* DSM 622 to precolonized (inactivated cells) pyrite surfaces was investigated. The cells attaching to the precolonized pyrite coupons were fluorescence in situ hybridized and visualized by epifluorescence microscopy. Control experiments showed that the inactivated cells of the biofilm were not visible under the epifluorescence microscope (data not shown).

Data for attached cells to precolonized pyrite coupons are presented in frequency distribution histograms.

3.5.1. Development of a biofilm on the surface of pyrite coupons

Preliminary experiments had indicated that the deposition of *L. ferrooxidans* DSM 2705, *A. thiooxidans* ATCC 23270 or *A. thiooxidans* DSM 622 isolated EPS was not possible. Even after multiple dip-coating or deposition by pipette nearly the complete pyrite coupons remained EPS-free (data not shown).

Covering pyrite coupons with biofilms by bacterial growth yielded better results. Pyrite coupons were incubated for 3 days with pure cultures of *L. ferrooxidans* DSM 2705, *A. thiooxidans* ATCC 23270 or *A. thiooxidans* DSM 622. Afterwards, the biofilm including cells were inactivated by heat-drying. The inactivation was controlled by growth experiments as well as by live/dead staining. If no regrowth could be detected in ferrous iron or thiosulfate containing medium the biofilms were considered to be heat-inactivated (data not shown). Visualization with live/dead stain showed cells on the mineral surface to be without exception red fluorescent (data not shown).

3.5.2. Visualization of 3 day-old biofilms of *L. ferrooxidans* DSM 2705, *A. ferrooxidans* ATCC 23270 or *A. thiooxidans* DSM 622 on pyrite coupons

Visualization of heat inactivated biofilms on pyrite coupons from pure cultures of *L. ferrooxidans* DSM 2705, *A. thiooxidans* DSM 622 or *A. thiooxidans* ATCC 23270 indicated that nearly the complete surface areas were covered with cells (images with DAPI stained cells are not shown) and EPS. Images of lectin-stained EPS are presented in Figure 29 a - c.

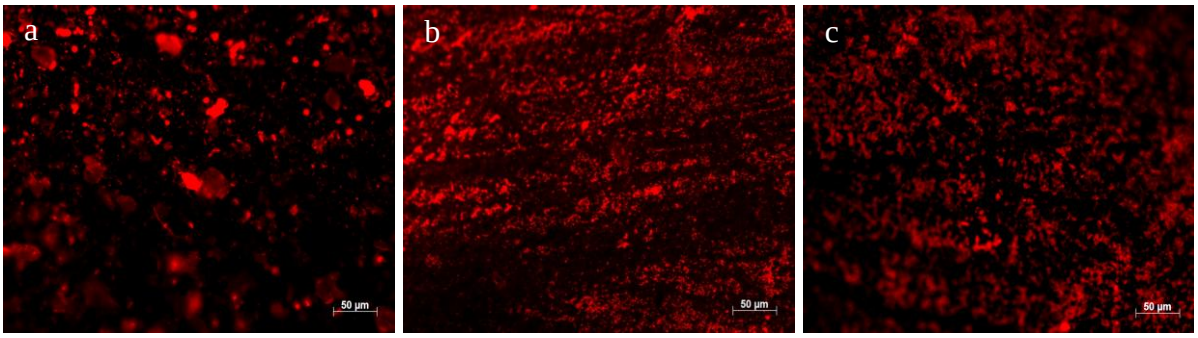

Figure 29 a - c: Visualization of heat inactivated biofilms of pure cultures of *L. ferrooxidans* DSM 2705, *A. ferrooxidans* ATCC 23270 or *A. thiooxidans* DSM 622 on pyrite coupons
Pyrite coupons were incubated horizontally with the naturally grown side up in 100 mL Erlenmeyer flasks in pure cultures of *A. ferrooxidans*, *A. thiooxidans* or *L. ferrooxidans* for 3 days. Initial total cell number $5 \cdot 10^8$ cells/mL, 150 mL basal salt solution, 28 °C, aerated. Afterwards, the biofilms were inactivated by heat-drying at 55 °C for 24 h. Biofilms were stained with lectin (ConA).
Fig. a: EFM image; pyrite coupon with biofilm of *L. ferrooxidans*;
Fig. b: EFM image; pyrite coupon with biofilm of *A. ferrooxidans*;
Fig. c: EFM image; pyrite coupon with biofilm of *A. thiooxidans*.
Each image represents 90 x 70 µm, scale bar 50 µm.

It is obvious from Figure 29 a, b and c that all three bacteria produced inhomogeneous biofilms on the pyrite surfaces.

3.5.3. Attachment of *L. ferrooxidans* DSM 2705 cells to precolonized pyrite coupons

Data for the attachment of *L. ferrooxidans* DSM 2705 to precolonized pyrite coupons after 1 and 8 h are presented in Figure 30 a and b. For comparison the data for attachment of *L. ferrooxidans* DSM 2705 to virgin pyrite coupons are shown again in the same histogram.

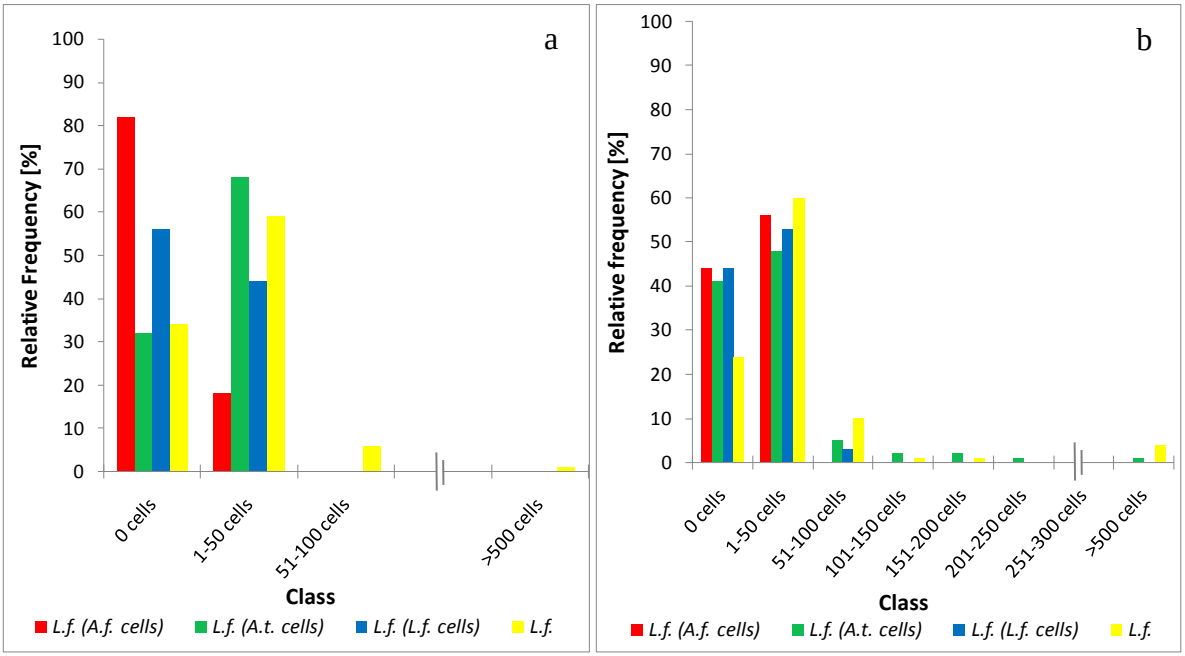

Figure 30 a & b: Attachment of cells of *L. ferrooxidans* DSM 2705 to precolonized and virgin pyrite coupons after 1 h (a) and 8 h (b)
Pyrite coupons were at first incubated horizontally, naturally grown side up, in 100 mL Erlenmeyer flasks in pure cultures of *A. ferrooxidans* ATCC 23270 (*A.f.* cells), *A. thiooxidans* DSM 622 (*A.t.* cells) or *L. ferrooxidans* DSM 2705 (*L.f.* cells) for 3 d for biofilm production. Initial total cell number $5 \cdot 10^8$ cells/mL, 150 mL basal salt solution, 28 °C, aerated. Afterwards, the biofilm was inactivated by heat-drying at 55 °C for 24 h.
Attachment experiment: initial total cell number of *L. ferrooxidans* $1 \cdot 10^8$ cells/mL, 50 mL basal salt solution, 28 °C, aerated. Determination of attached *L. ferrooxidans* cells on precolonized pyrite coupons: specific FISH probe LEP665. Cells from each set up were analyzed from 100 ocular counting grids (125 µm x 125 µm) from 10 coupons, total area 1.5625 mm^2.
Standard error (n = 100) for 1 h: *L.f.* (*A.f.* cells) = 9.8, *L.f.* (*A.t.* cells) = 11.89, *L.f.* (*L.f.* cells) = 12.66, *L.f.* = 18.51.
Standard error (n = 100) for 8 h: *L.f.* (*A.f.* cells) = 12.66, *L.f.* (*A.t.* cells) = 38.03, *L.f.* (*L.f.* cells) = 13.33, *L.f.* = 27.5.

After 1 h incubation the lowest attachment of cells of *L. ferrooxidans* was found for pyrite coupons precolonized with *A. ferrooxidans* cells. Cells were found only in 18 % of the investigated areas with cell numbers within the class 1 - 50 cells. The highest attachment of *L. ferrooxidans* was determined for pyrite coupons precolonized with cells of *A. thiooxidans*. Attachment of *L. ferrooxidans* to pyrite coupons precolonized by cells of its own strain exhibited a medium value. Attachment to virgin pyrite coupons was almost as high as the attachment to *A. thiooxidans*-precolonized.

After 8 h incubation the highest attachment of cells of *L. ferrooxidans* was determined for virgin pyrite coupons (lowest number of cell-free areas). The number of cell-free areas for inactivated biofilm-attached cells was quite similar for all assays.

The cell numbers of secondary attached *L. ferrooxidans* cells were mainly counted in the class 1 – 50 cells on virgin as well as on precolonized pyrite coupons. Numbers in higher cell classes than the previous one were rarely detectable.

3.5.4. Attachment of *A. ferrooxidans* ATCC 23270 cells to precolonized pyrite coupons

Data for the attachment of cells of *A. ferrooxidans* ATCC 23270 to precolonized and virgin pyrite coupons after 1 and 8 h are presented in Figure 31 a and b.

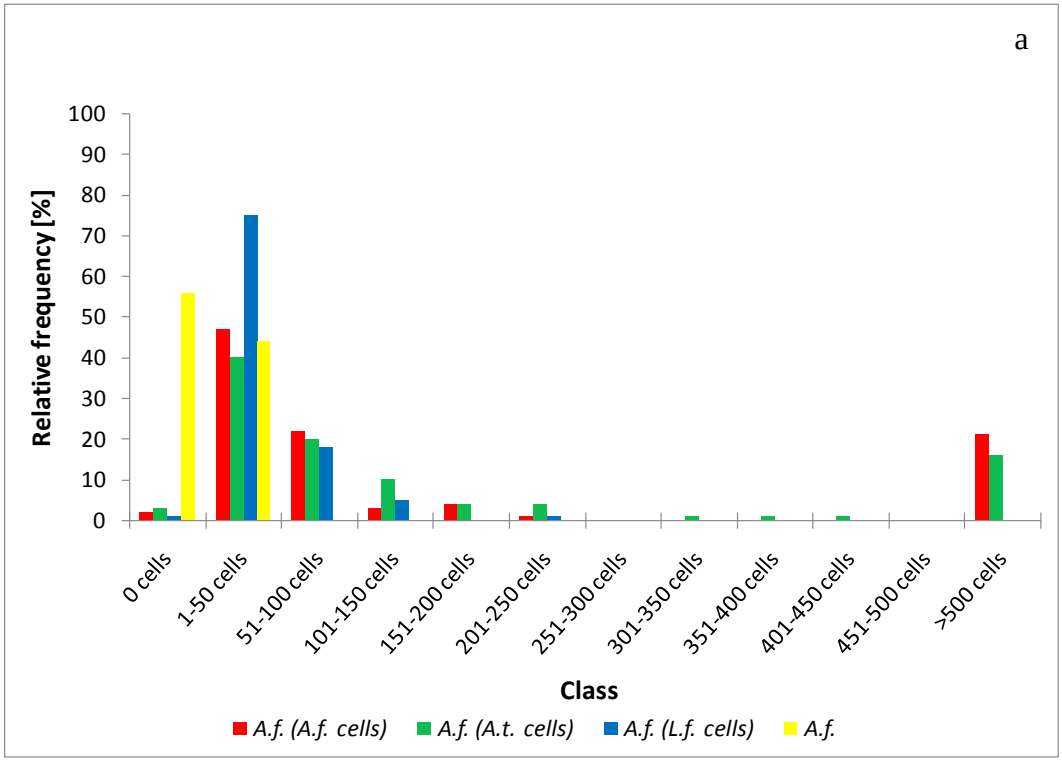

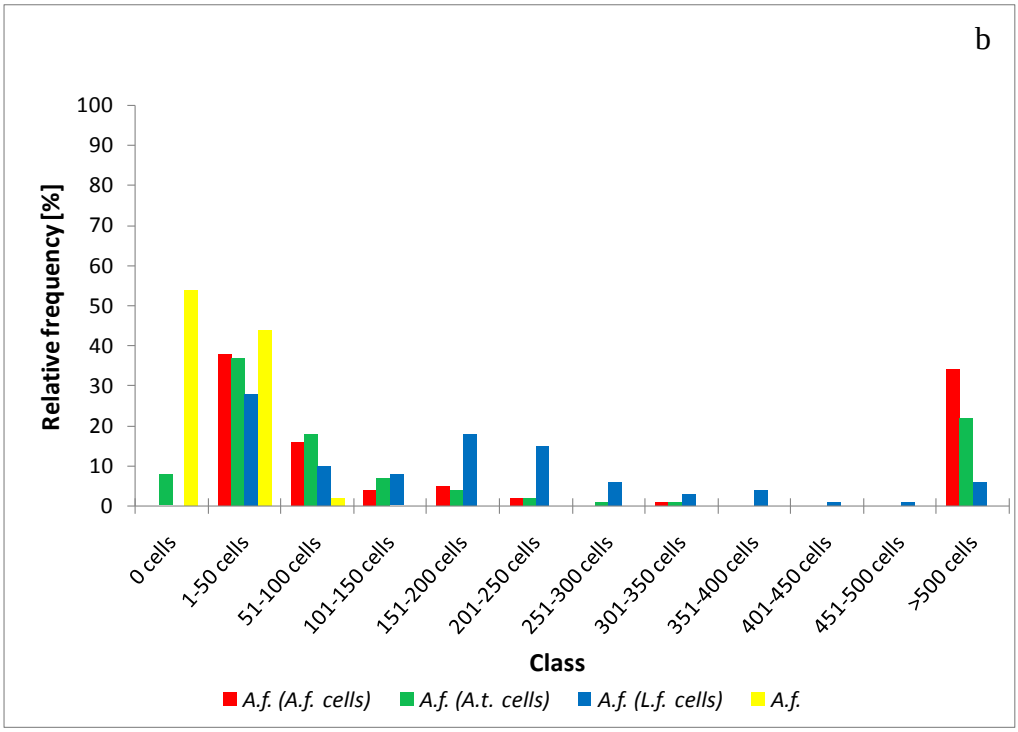

Figure 31 a & b: Attachment of cells of *A. ferrooxidans* ATCC 23270 to precolonized and virgin pyrite coupons after 1 h (a) and 8 h (b)
Pyrite coupons were at first incubated horizontally, naturally grown side up, in 100 mL Erlenmeyer flasks in pure cultures of *A. ferrooxidans* ATCC 23270 (*A.f.* cells), *A. thiooxidans* DSM 622 (*A.t.* cells) or *L. ferrooxidans* DSM 2705 (*L.f.* cells) for 3 d for biofilm production. Initial total cell number $5 \cdot 10^8$ cells/mL, 150 mL basal salt solution, 28 °C, aerated. Afterwards, the biofilm was inactivated by heat-drying at 55 °C for 24 h. Attachment experiment: initial total cell number of *A. ferrooxidans* $1 \cdot 10^8$ cells/mL, 50 mL basal salt solution, 28 °C, aerated. Determination of attached *A. ferrooxidans* cells on precolonized pyrite coupons: specific FISH probe TF539. Cells from each set up were analyzed from 100 ocular counting grids (125 µm x 125 µm) from 10 coupons, total area 1.5625 mm^2. Standard error (n = 100) from 1 h: *A.f.* (*A.f.* cells) = 45.15, *A.f.* (*A.t.* cells) = 79.22, *A.f.* (*L.f.* cells) = 33.29, *A.f.* = 12.66.Standard error (n = 100) from 8 h: *A.f.* (*A.f.* cells) = 59.4, *A.f.* (*A.t.* cells) = 63.25, *A.f.* (*L.f.* cells) = 113.56, *A.f.* = 15.43.

After 1 h attachment of *A. ferrooxidans* to precolonized pyrite surfaces was significantly increased. In all assays with precolonized pyrite surfaces the relative frequency of cell-free areas was extremely low (1 – 3 %). However, 56 % of the investigated areas of virgin pyrite coupons remained free of *A. ferrooxidans* cells. Again, most cell numbers were found within the class of 1 – 50 cells for the virgin as well as for the precolonized pyrite coupons after 1 h incubation. Attachment of *A. ferrooxidans* in higher classes with higher cell numbers above 50 cells was only determined for precolonized pyrite coupons. The highest class (> 500 cells) was determined with precolonized pyrite coupons with either *A. ferrooxidans* or *A. thiooxidans* cells.

After 8 h incubation the attachment of cells of *A. ferrooxidans* to precolonized pyrite coupons increased. Again only a few cell free areas were detected for the precolonized pyrite coupons, whereas the relative frequency for virgin pyrite coupons was again high (56 %). Attachment of *A. ferrooxidans* to precolonized pyrite coupons was again detected in high cell numbers within all higher cell classes.

3.5.5. Attachment of *A. thiooxidans* DSM 622 cells to precolonized pyrite coupons

Data for the attachment of cells of *A. thiooxidans* DSM 622 to precolonized and virgin pyrite coupons after 1 and 8 h are presented in Figure 32 a and b.

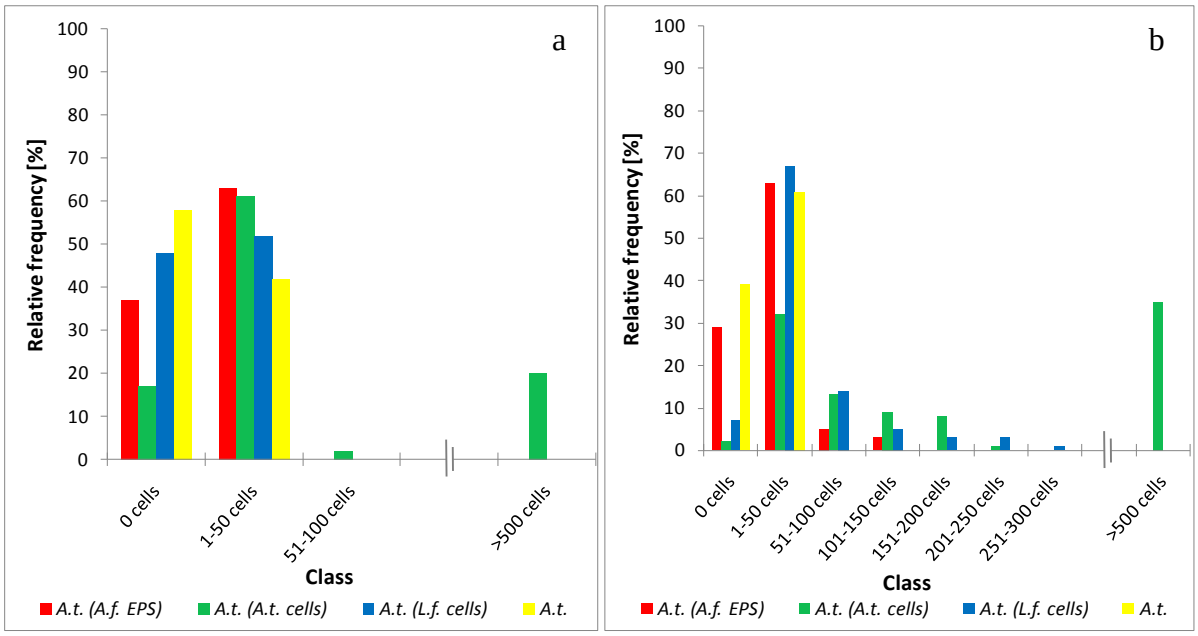

Figure 32 a & b: Attachment of cells of *A. thiooxidans* DSM 622 to precolonized and virgin pyrite coupons after 1 h (a) and 8 h (b)
Pyrite coupons were at first incubated horizontally, naturally grown side up, in 100 mL Erlenmeyer flasks in pure cultures of *A. ferrooxidans* ATCC 23270 (*A.f.* cells), *A. thiooxidans* DSM 622 (*A.t.* cells) or *L. ferrooxidans* DSM 2705 (*L.f.* cells) for 3 d for biofilm production. Initial total cell number $5 \cdot 10^8$ cells/mL, 150 mL basal salt solution, 28 °C, aerated. Afterwards, the biofilm was inactivated by heat-drying at 55 °C for 24 h. Attachment experiment: initial total cell number of *A. thiooxidans* $1 \cdot 10^8$ cells/mL, 50 mL basal salt solution, 28 °C, aerated. Determination of attached *A. thiooxidans* cells on precolonized pyrite coupons: specific FISH probe ATT223. Cells from each set up were analyzed from 100 ocular counting grids (125 µm x 125 µm) from 10 coupons, total area 1.5625 mm^2.Standard error (n = 100) for 1 h: *A.t.* (*A.f.* cells) = 12.31, *A.t.* (*A.t.* cells) = 14.81, *A.t.* (*L.f.* cells) = 12.58, *A.t.* =12.58.Standard error (n = 100) for 8 h: *A.t.* (*A.f.* cells) = 24.7, *A.t.* (*A.t.* cells) = 57.12, *A.t.* (*L.f.* cells) = 53.45, *A.t.* = 12.44.

After 1 h attachment of cells of *A. thiooxidans* to precolonized pyrite coupons was higher compared to the attachment to virgin pyrite coupons. The highest attachment of cells of

A. thiooxidans was determined for coupons precolonized by the same strain with a high relative frequency within the class > 500 cells. Only a relative frequency of 18 % cell-free areas was detected.

Again the most frequent cell class was 1 - 50 cells for precolonized and virgin pyrite coupons. After 8 h incubation attachment of *A. thiooxidans* increased in general. However, with precolonized coupons by *A. thiooxidans* the largest increase was detected. A high number of areas were colonized with more than 500 cells of *A. thiooxidans*. Also the attachment of *A. thiooxidans* to *A. ferrooxidans* or *L. ferrooxidans* precolonized pyrite coupons was found within higher classes.

3.6. Bacterial leaching of pyrite coupons

Leaching of virgin pyrite coupons and pyrite coupons with heat-inactivated biofilm by pure cultures of *L. ferrooxidans* DSM 2705 and *A. ferrooxidans* ATCC 23270 was investigated.

Controls were performed with precolonized pyrite coupons to clarify whether the precolonization might an effect on the dissolution. Additionally, purely abiotic controls were done.

Dissolution of pyrite coupons was estimated by determination of the concentration of iron(III) ions in solution and the weight loss.

Bacterial cells, biofilms and pyrite surfaces were visualized by combined epifluorescence- and atomic force microscopy. Selected visualized areas are shown in Figure 35 to Figure 46.

3.6.1. Weight loss of pyrite coupons by bacterial leaching

Data for the weight loss of virgin and of pyrite coupons with a biofilm of heat-inactivated cells of *A. ferrooxidans* ATCC 23270, *L. ferrooxidans* DSM 2705 or *A. thiooxidans* DSM 622 are shown in Figure 33. The coupons had been incubated under sterile conditions or with cells of *A. ferrooxidans* ATCC 23270 or *L. ferrooxidans* DSM 2705.

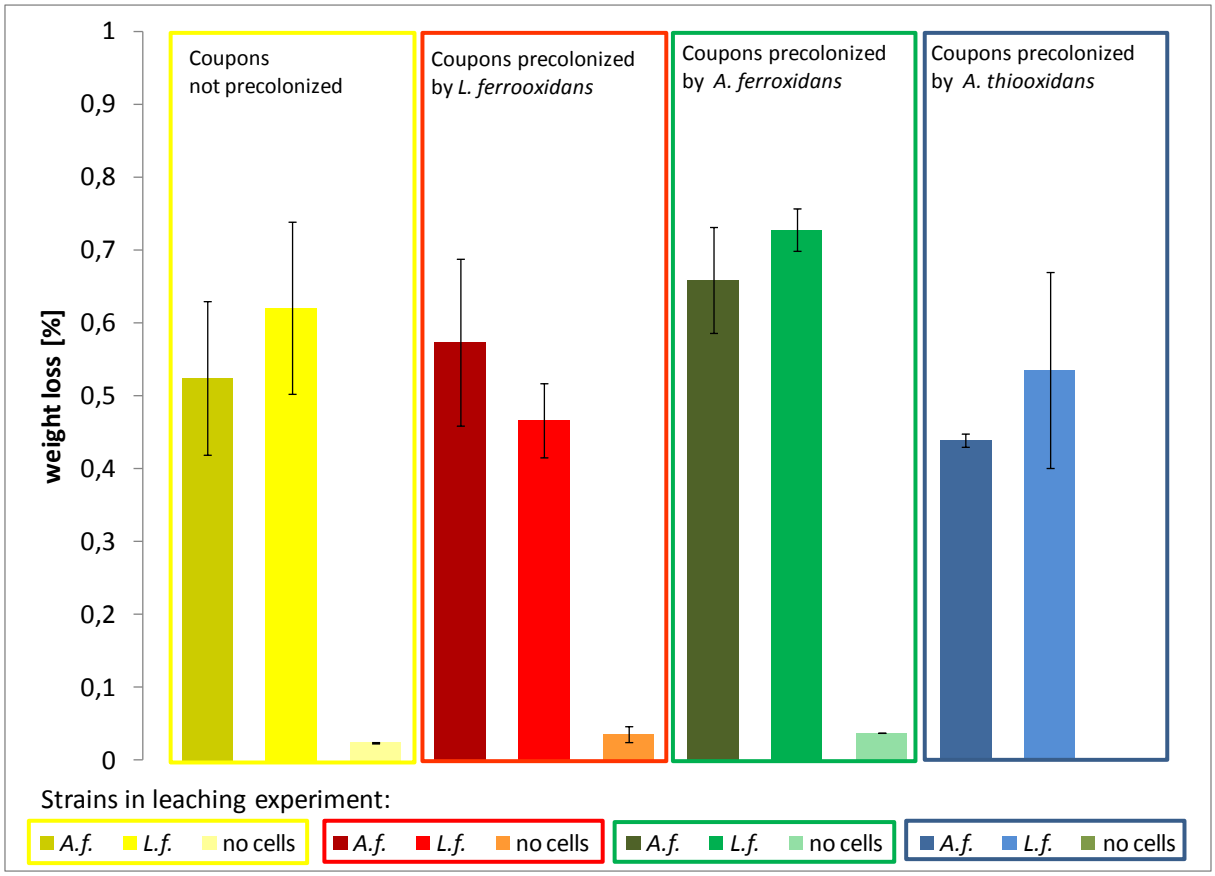

Figure 33: Weight loss of virgin or precolonized pyrite coupons by leaching with *A. ferrooxidans* ATCC 23270 or *L. ferrooxidans* DSM 2705 for 8 weeks
Precolonized pyrite coupons were at first incubated in pure cultures of *L. ferrooxidans* DSM 2705, *A. ferrooxidans* ATCC 23270 or *A. thiooxidans* DSM 622 with an initial cell number of $5 \cdot 10^8$ cells/mL for 3 d for biofilm formation. Afterwards, the biofilm was inactivated by heat-drying at 55 °C for 24 h. Leaching experiment: Initial cell number of *A. ferrooxidans* or *L. ferrooxidans* $5 \cdot 10^8$ cells/mL in 10 mL basal salt solution, 28 °C, shaken (40 rpm).
Yellow bars: uncolonized pyrite coupons leached by *A. ferrooxidans* (*A.f.*), *L. ferrooxidans* (*L.f.*) or abiotic control. Red, green and blue bars: *L. ferrooxidans* (red), *A. ferrooxidans* (green), *A. thiooxidans* (blue) precolonized pyrite coupons, leached by *A. ferrooxidans* (*A.f.*) or *L. ferrooxidans* (*L.f.*), control = without addition of cells (no cells).
(n = 2)

All sterile coupons (virgin or precolonized) exhibited negligible values for weight loss, usually below 0.05 %. Coupons leached by cells of *L. ferrooxidans* or *A. ferrooxidans* lost between 0.4 and 0.7 % of their initial weight. Significant differences between the assay types were not evident.

3.6.2. Iron(III) ion concentration in leaching assays with virgin and precolonized pyrite coupons

In Figure 34 the data for iron(III) ion concentrations of virgin and with a biofilm of heat-inactivated cells of *A. ferrooxidans* ATCC 23270, *L. ferrooxidans* DSM 2705 or *A. thiooxidans* DSM 622 are presented. The coupons had been incubated under sterile conditions or with cells of *A. ferrooxidans* ATCC 23270 or *L. ferrooxidans* DSM 2705.

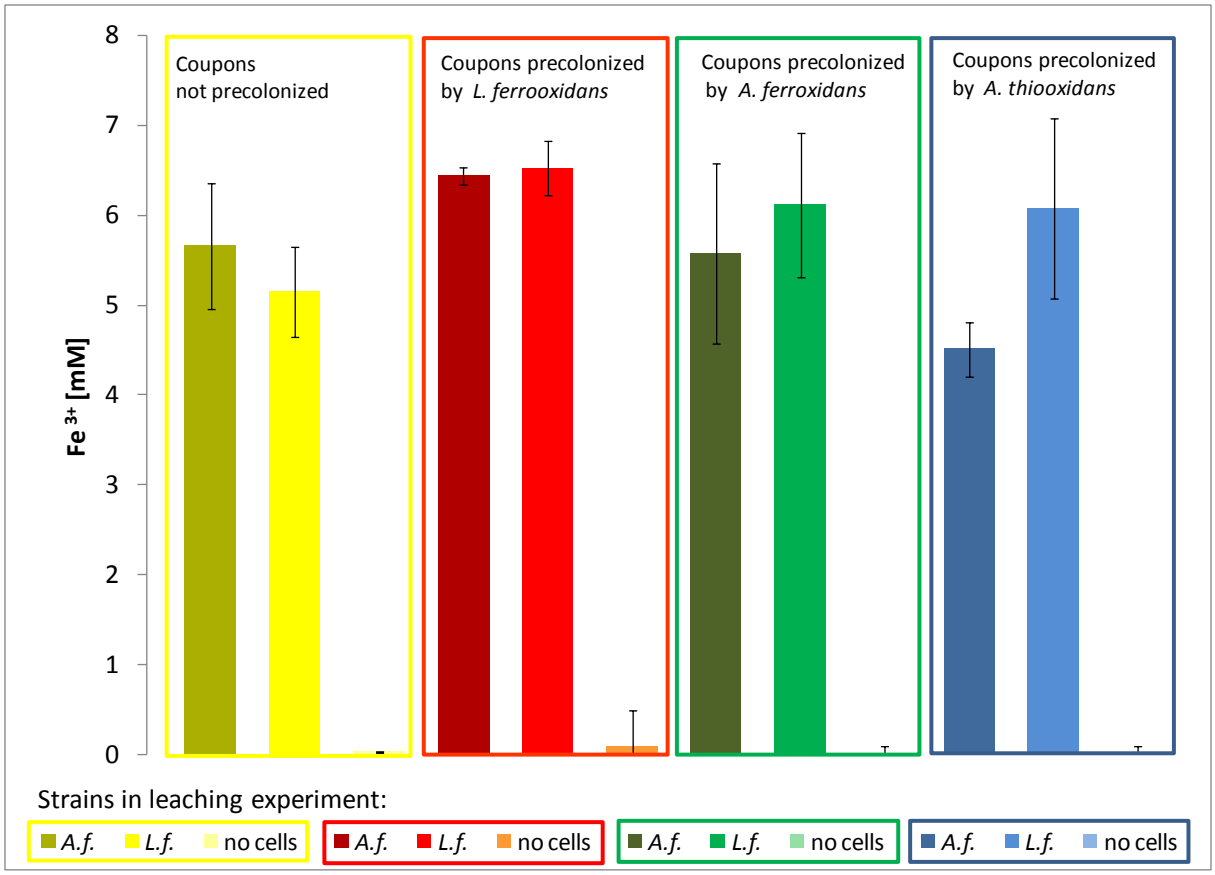

Figure 34: Iron(III) ion concentrations in leaching assays with virgin and precolonized pyrite coupons after 8 weeks of leaching by *A. ferrooxidans* ATCC 23270 or *L. ferrooxidans* DSM 2705

Precolonized pyrite coupons were at first incubated in pure cultures of *L. ferrooxidans* DSM 2705, *A. ferrooxidans* ATCC 23270 or *A. thiooxidans* DSM 622 with an initial cell number of $5 \cdot 10^8$ cells/mL for 3 d for biofilm formation. Afterwards, the biofilm was inactivated by heat-drying at 55 °C for 24 h. Leaching experiment: Initial cell number of *A. ferrooxidans* or *L. ferrooxidans* $5 \cdot 10^8$ cells/mL in 10 mL basal salt solution, 28 °C, shaken (40 rpm). Yellow bars: uncolonized pyrite coupons leached by *A. ferrooxidans* (*A.f.*), *L. ferrooxidans* (*L.f.*) or abiotic control. Red, green and blue bars: *L. ferrooxidans* (red), *A. ferrooxidans* (green), *A. thiooxidans* (blue) precolonized pyrite coupons, leached by *A. ferrooxidans* (*A.f.*) or *L. ferrooxidans* (*L.f.*), control = without addition of cells (no cells).
(n = 2)

It is obvious that in most assays comparable values were obtained (range 5 till 6.5 mM Fe^{3+}). Only the value for *A. thiooxidans* precolonized coupons leached by cells of *A. ferrooxidans* showed a slight decreased output of iron(III) ions. Again, like the previous experiment, the sterile coupons did not have measurable concentrations or very low concentrations of iron(III) ions.

3.6.3. Visualization of leached surfaces of pyrite coupons

Virgin and precolonized surfaces of pyrite coupons after 8 weeks incubation were stained with DAPI and with a lectin to be visualized by combined EFM and AFM.
The images provide information about the spatial arrangement of cells on the mineral surfaces. The differentiation between primary and secondary colonizing cells by the use of DAPI is not possible.

3.6.3.1. Images of pyrite surfaces with attached *A. ferrooxidans* ATCC 23270 or *L. ferrooxidans* DSM 2705 cells

Virgin pyrite coupons incubated with cells of *A. ferrooxidans* ATCC 23270 or *L. ferrooxidans* DSM 2705 as well an abiotic control are presented in Figure 35, Figure 36 and Figure 37.

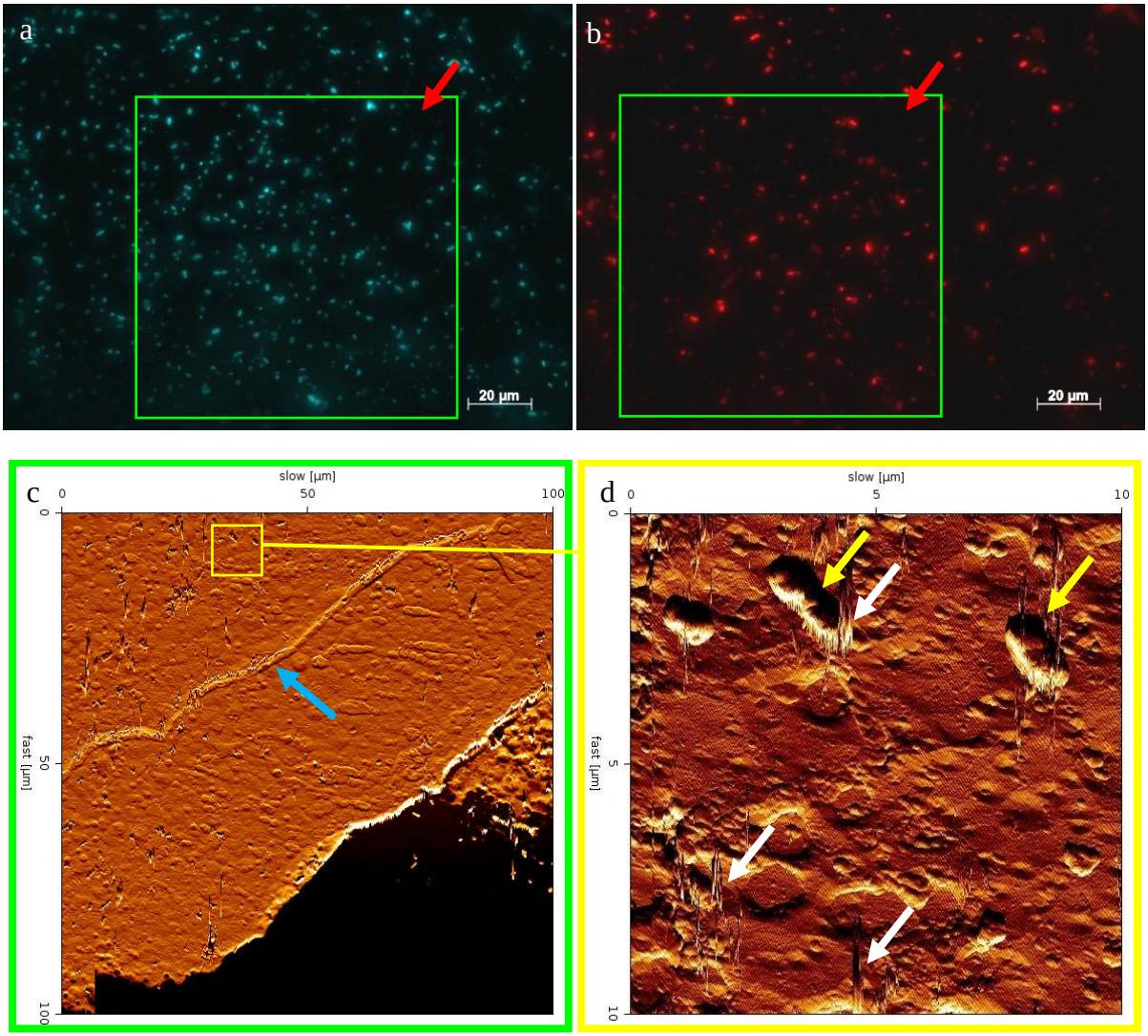

Figure 35 a - d: Selected EFM & AFM images of a pyrite coupon with cells of *A. ferrooxidans* ATCC 23270

After 8 weeks incubation the coupon was stained with DAPI and Lectin (ConA).
Leaching experiment: Initial cell number of *A. ferrooxidans* $5 \cdot 10^8$ cells/mL, 10 mL basal salt solution, 28 °C, shaken (40 rpm).
Fig. a: EFM image; DAPI-stained *A. ferrooxidans* cells; green frame = AFM scan area; red arrow = cell-free area.
Fig. b: EFM image; lectin (Con A) stained biofilm; green frame = AFM scan area; red arrow = EPS-free area.
Fig. c: AFM image; DAPI and lectin (green frames in a & b) stained area; blue arrow = mineral imperfection; black area = exceeding the maximum scanning z range.
Fig. d: AFM image; detail of figure c (yellow frame); white arrows = artifacts produced by scanning; yellow arrows = single cells. AFM images: vertical deflection, contact mode in air.

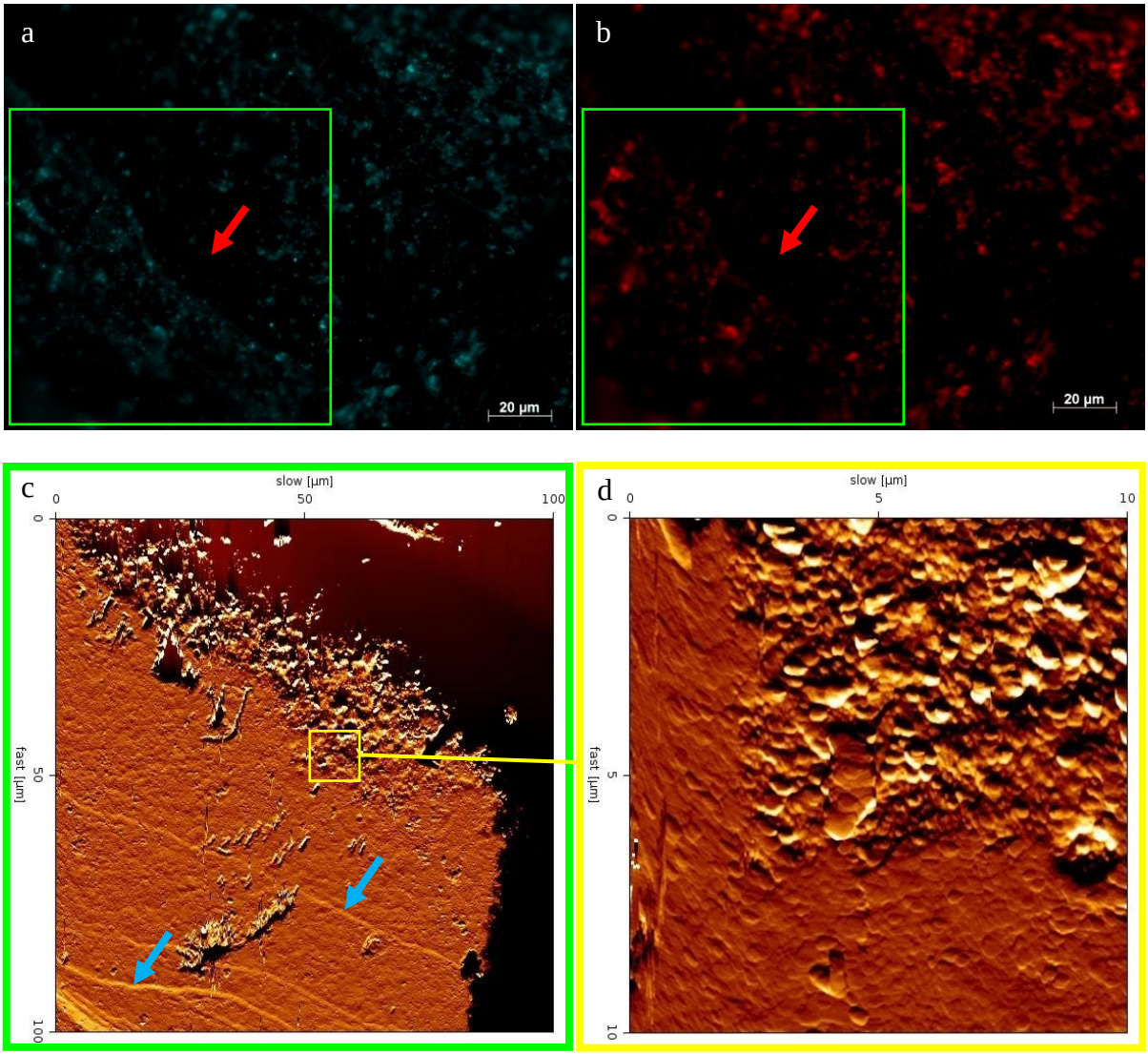

Figure 36 a - d: Selected EFM & AFM images of a pyrite coupon with cells of *L. ferrooxidans* DSM 2705
After 8 weeks incubation the coupon was stained with DAPI and Lectin (ConA).
Leaching experiment: Initial cell number of *L. ferrooxidans* $5 \cdot 10^8$ cells/mL, 10 mL basal salt solution, 28 °C, shaken (40 rpm).
Fig. a: EFM image; DAPI-stained *L. ferrooxidans* cells; green frame = AFM scan area; red arrow = cell-free area.
Fig. b: EFM image; lectin (Con A) stained biofilms; green frame = AFM scan area; red arrow = EPS-free area.
Fig. c: AFM image; DAPI and lectin (green frames in a & b) stained area; blue arrows = mineral imperfections; black/dark brown area: exceeding the maximum scanning z range.
Fig. d: AFM image; detail of figure c (yellow frame); AFM images: vertical deflection, contact mode in air.

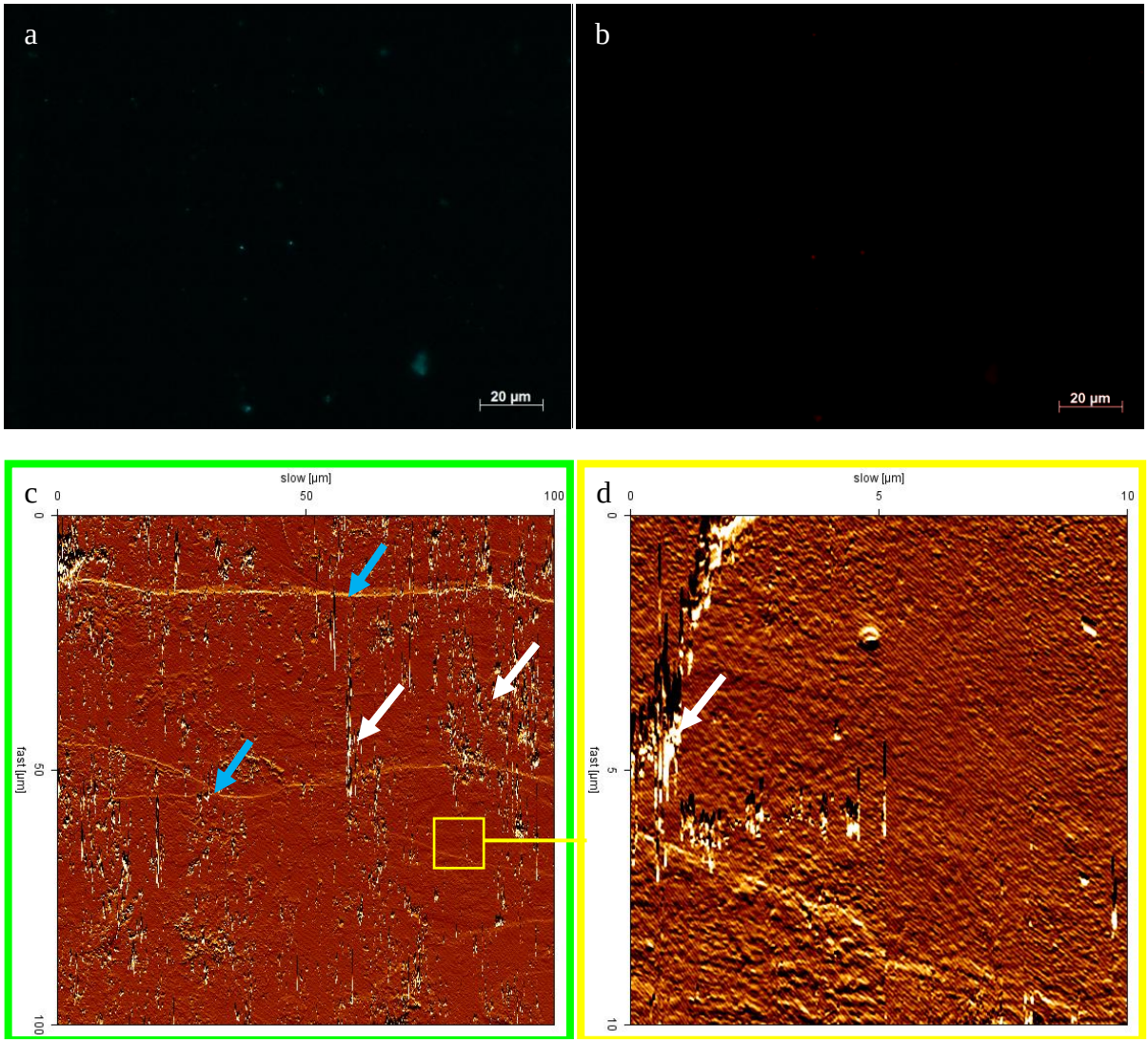

Figure 37 a - d: Selected EFM & AFM images of an abiotic control pyrite coupon

After 8 weeks incubation the coupon was stained with DAPI and Lectin (ConA). Experiment was performed without cells in 10 mL basal salt solution at 28 °C, shaken (40 rpm).

Fig. a: EFM image; DAPI-stained pyrite surface; green frame indicates AFM scan area.

Fig. b: EFM image; lectin (Con A) stained pyrite surface; green frame = AFM scan area.

Fig. c: AFM image; DAPI and lectin (green frames in a & b) stained area; blue arrows = mineral imperfection; white arrows = artifacts produced by scanning.

Fig. d: AFM image; detail of figure c (yellow frame); white arrow = artifacts produced by scanning.

AFM images: vertical deflection, contact mode in air.

On the pyrite coupon colonized by cells of *A. ferrooxidans* the DAPI stain visualizes a low number of cells after 8 weeks incubation. Cells were found to be homogenously distributed without cluster formation (Figure 35a). In contrast, cells of *L. ferrooxidans* occurred inhomogeneously distributed and in cell clusters on the surface of the pyrite coupon (Figure 36a). With cells of *A. ferrooxidans*, the lectin signal (Figure 35b) indicates that only a little part of the coupon surface was covered with EPS, whereas, with cells of *L. ferrooxidans* a considerable coverage of the surface was indicated by the lectin stain.

The AFM images of the colonized pyrite surfaces reveal an uneven surface with small imperfections and steps (blue arrows), as is shown in Figure 35c and Figure 36c. Only a few cells of *A. ferrooxidans* are visible in Figure 35c and (in increased resolution) Figure 35d. Single cells of *L. ferrooxidans* are hardly to identify in Figure 36c. However, the enlargement of this image in Figure 36d indicates cluster a formation of *L. ferrooxidans* with a plentiful of cells.

The black/dark brown areas in Figure 35c and 36c result from the uneven coupon surface exceeding the maximum scanning height of 15 µm for the AFM scanner (z-range). Thus, a complete visualization of areas as large as 100 µm x 100 µm was not possible for these coupons (not even on the duplicates of the coupons). Image imperfections (indicated by white arrows) occur if the scan velocity is too high or particles adhere at the cantilever tip.

In Figure 37 images of the abiotic control are shown. Neither DAPI- nor lectin- signals were detected on the surface, as indicated in Figure 37 a & b. AFM images show an uneven surface with steps (blue arrows). The enlargement in Figure 37d indicates a raw surface without cells.

3.6.3.2. Images of *L. ferrooxidans* DSM 2705 precolonized pyrite surfaces after leaching with *A. ferrooxidans* ATCC 23270 or *L. ferrooxidans* DSM 2705 cells

Pyrite coupon precolonized with a biofilm of cells of *L. ferrooxidans* DSM 2705 (heat-inactivated) were leached by *A. ferrooxidans* ATCC 23270 or *L. ferrooxidans* DSM 2705. In Figure 38, Figure 39 and Figure 40 images are shown of these surfaces as well as an abiotic control after 8 weeks of incubation.

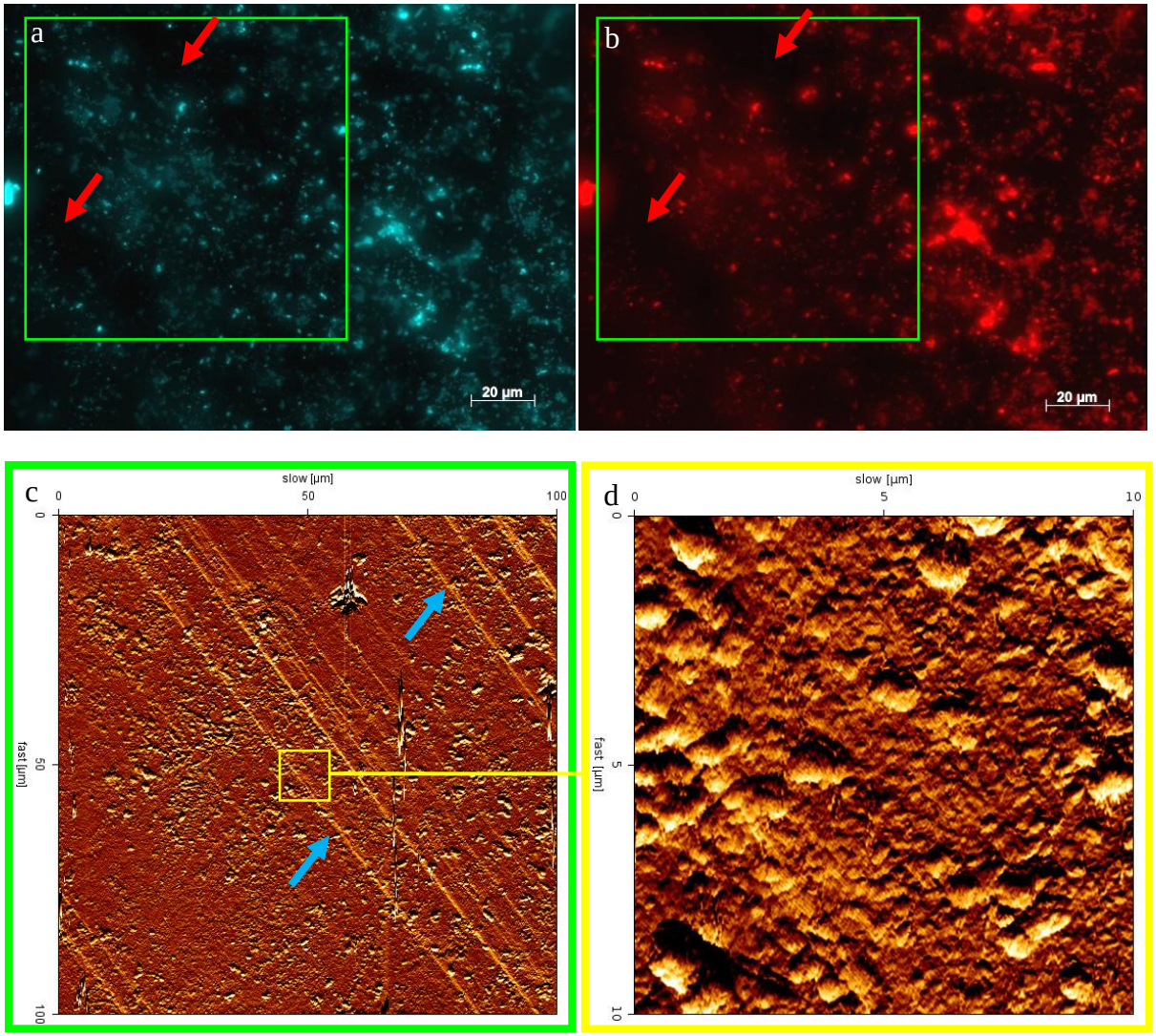

Figure 38 a - d: Selected EFM & AFM images of a pyrite coupon with a heat-inactivated biofilm of cells of *L. ferrooxidans* DSM 2705 after leaching with *A. ferrooxidans* ATCC 23270

After 8 weeks incubation the coupon was stained with DAPI and Lectin (ConA). Pyrite coupon was at first incubated horizontally, naturally grown side up, in 100 mL Erlenmeyer flasks in a pure culture of *L. ferrooxidans* with an initial cell number of $5 \cdot 10^8$ cells/mL, 28°C, aerated, for 3 d for biofilm formation. Afterwards, the biofilm was inactivated by heat-drying at 55 °C for 24 h. Leaching experiment: Initial cell number of *A. ferrooxidans* $5 \cdot 10^8$ cells/mL, 10 mL basal salt solution, 28 °C, shaken (40 rpm).

Fig. a: EFM image; DAPI-stained *L. ferrooxidans* and *A. ferrooxidans* cells; green frame = AFM scan area; red arrows = cell-free area.

Fig. b: EFM image; lectin (Con A) stained biofilms; green frame = AFM scan area; red arrows = EPS-free area.

Fig. c: AFM image; DAPI and lectin (green frames in a & b) stained area; blue arrows = mineral imperfections.

Fig. d: AFM image; detail of figure c (yellow frame).

AFM images: vertical deflection, contact mode in air.

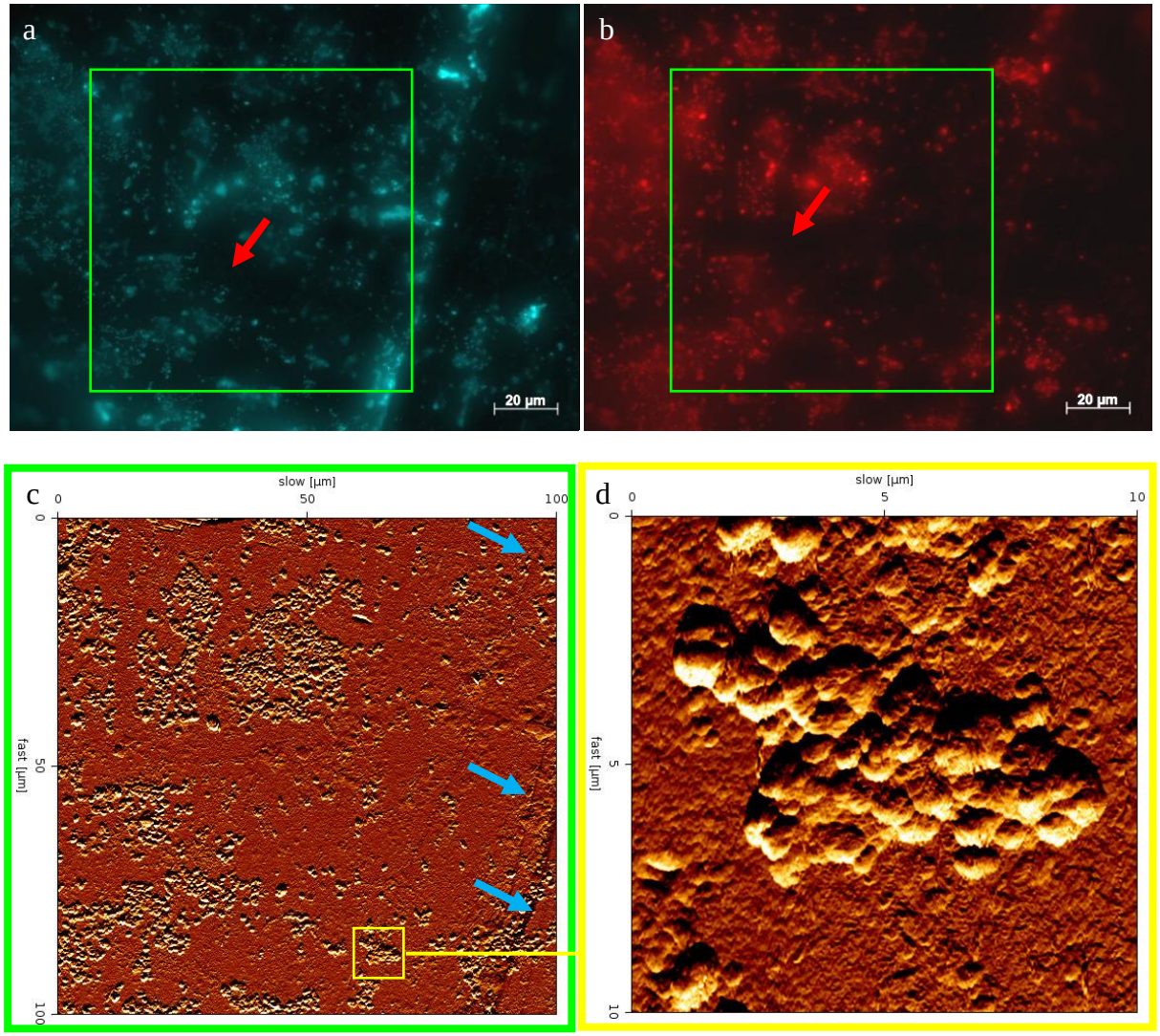

Figure 39 a - d: Selected EFM & AFM images of a pyrite coupon with a heat-inactivated biofilm of cells of *L. ferrooxidans* DSM 2705 after leaching with *L. ferrooxidans* DSM 2705

After 8 weeks incubation the coupon was stained with DAPI and Lectin (ConA). Pyrite coupon was at first incubated horizontally, naturally grown side up, in 100 mL Erlenmeyer flasks in a pure culture of *L. ferrooxidans* with an initial cell number of $5 \cdot 10^8$ cells/mL, 28°C, aerated, for 3 d for biofilm formation. Afterwards, the biofilm was inactivated by heat-drying at 55 °C for 24 h. Leaching experiment: Initial cell number of *L. ferrooxidans* $5 \cdot 10^8$ cells/mL, 10 mL basal salt solution, 28 °C, shaken (40 rpm).

Fig. a: EFM image; DAPI stained *L. ferrooxidans* cells; green frame = AFM scan area; red arrow = cell-free area.

Fig. b: EFM image; lectin (Con A) stained biofilms; green frame = AFM scan area; red arrow = EPS-free area.

Fig. c: AFM image; DAPI and lectin (green frames in a & b) stained area; blue arrows = mineral imperfections.

Fig. d: AFM image; detail of figure c (yellow frame).

AFM images: vertical deflection, contact mode in air.

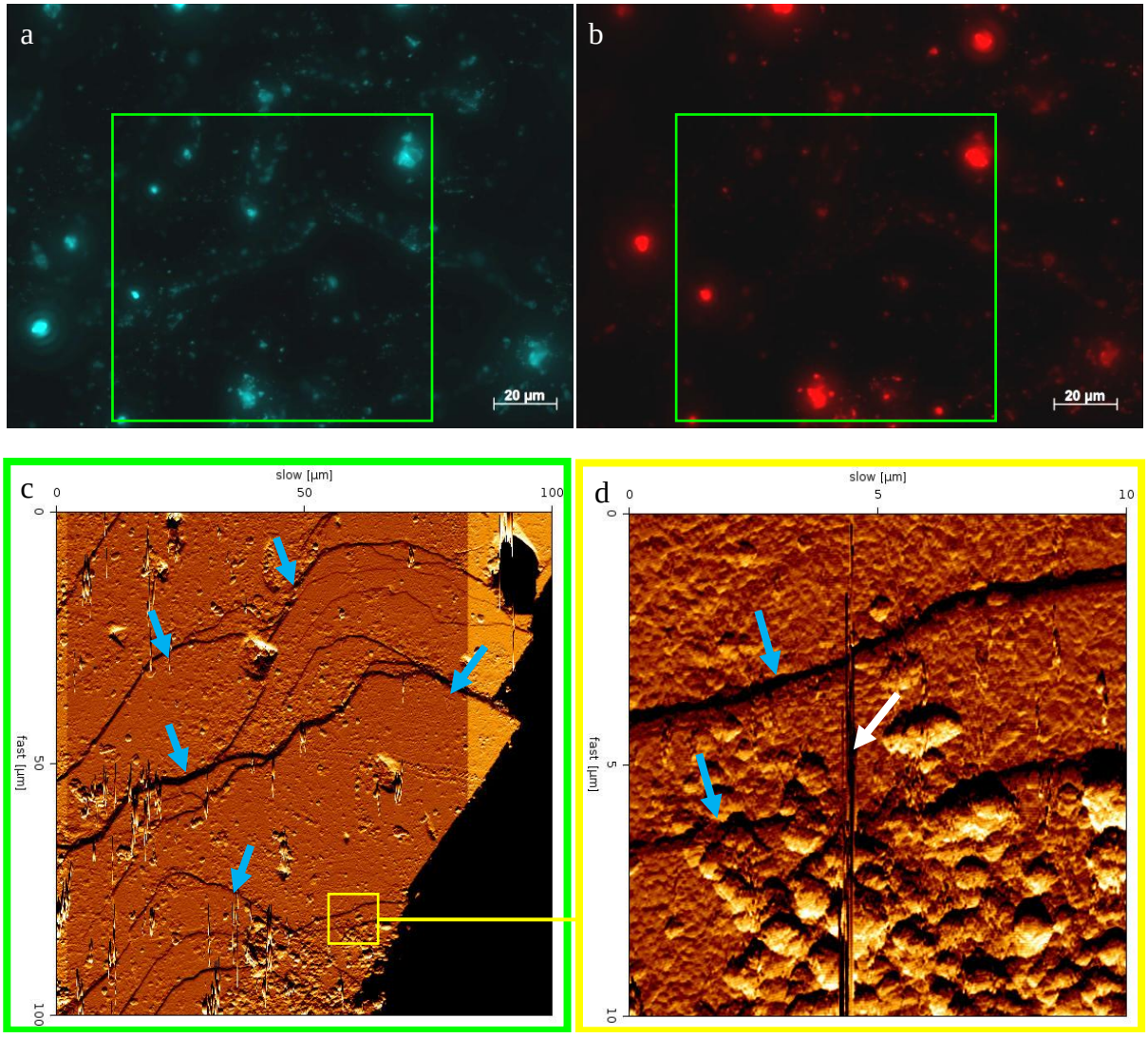

Figure 40 a - d: Selected EFM & AFM images of a pyrite coupon with a heat-inactivated biofilm of cells of *L. ferrooxidans* DSM 2705 after incubation in sterile leach solution

After 8 weeks incubation the coupon was stained with DAPI and Lectin (ConA). Pyrite coupon was at first incubated horizontally, naturally grown side up, in 100 mL Erlenmeyer flasks in a pure culture of *L. ferrooxidans* with an initial cell number of $5 \cdot 10^8$ cells/mL, 28°C, aerated, for 3 d for biofilm formation. Afterwards, the biofilm was inactivated by heat-drying at 55 °C for 24 h. The experiment was performed without secondary addition of cells in 10 mL basal salt solution at 28 °C, shaken (40 rpm).

Fig. a: EFM image; DAPI stained *L. ferrooxidans* cells; green frame = AFM scan area.

Fig. b: EFM image; lectin (Con A) stained biofilms; green frame = AFM scan area.

Fig. c: AFM image; DAPI and lectin (green frames in a & b) stained area; blue arrows = mineral imperfections; black area = exceeding the maximum scanning z range.

Fig. d: AFM image; detail of figure c (yellow frame); blue arrows = mineral imperfections); white arrow = artifacts produced by the scanning method.

AFM images: vertical deflection, contact mode in air.

The EFM images in Figure 38a and Figure 39a of pyrite coupons precolonized with a heat-inactivated biofilm of *L. ferrooxidans* indicate a plentiful of cells and large EPS amounts.
It is obvious from these images that DAPI stained *A. ferrooxidans* and *L. ferrooxidans* cells (Figure 38a) are homogenously distributed over the mineral surface, whereas cells of *L. ferrooxidans* (Figure 39a) appear to be inhomogeneously distributed and occur in many cell-clusters. Still even after 8 weeks areas on the pyrite coupon remained cell-free.
The lectin stain, as shown in Figure 38b, Figure 39b and Figure 40b, indicates EPS of the biofilms on the coupon surfaces. The EPS were found at the same place as the cells. Areas partially marked by a red arrow were still cell- and EPS-free.
The black/dark brown areas in Figure 40c result from the uneven coupon surface exceeding the maximum scanning height of 15 µm for the AFM scanner (z-range). Thus, a complete visualization of areas as large as 100 µm x 100 µm was not possible for these coupons (not even on the duplicate of the coupon). Image imperfections (indicated by white arrows) can occur if the scan velocity is too high or particles adhere at the cantilever tip.

3.6.3.3. Images of *A. ferrooxidans* ATCC 23270 precolonized pyrite surfaces after leaching with *A. ferrooxidans* ATCC 23270 or *L. ferrooxidans* DSM 2705 cells

Pyrite coupon precolonized with a biofilm of cells of *A. ferrooxidans* ATCC 23270 (heat-inactivated) were leached by *A. ferrooxidans* ATCC 23270 or *L. ferrooxidans* DSM 2705. In Figure 41, Figure 42 and Figure 43 images are shown of these surfaces as well as an abiotic control after 8 weeks of incubation.

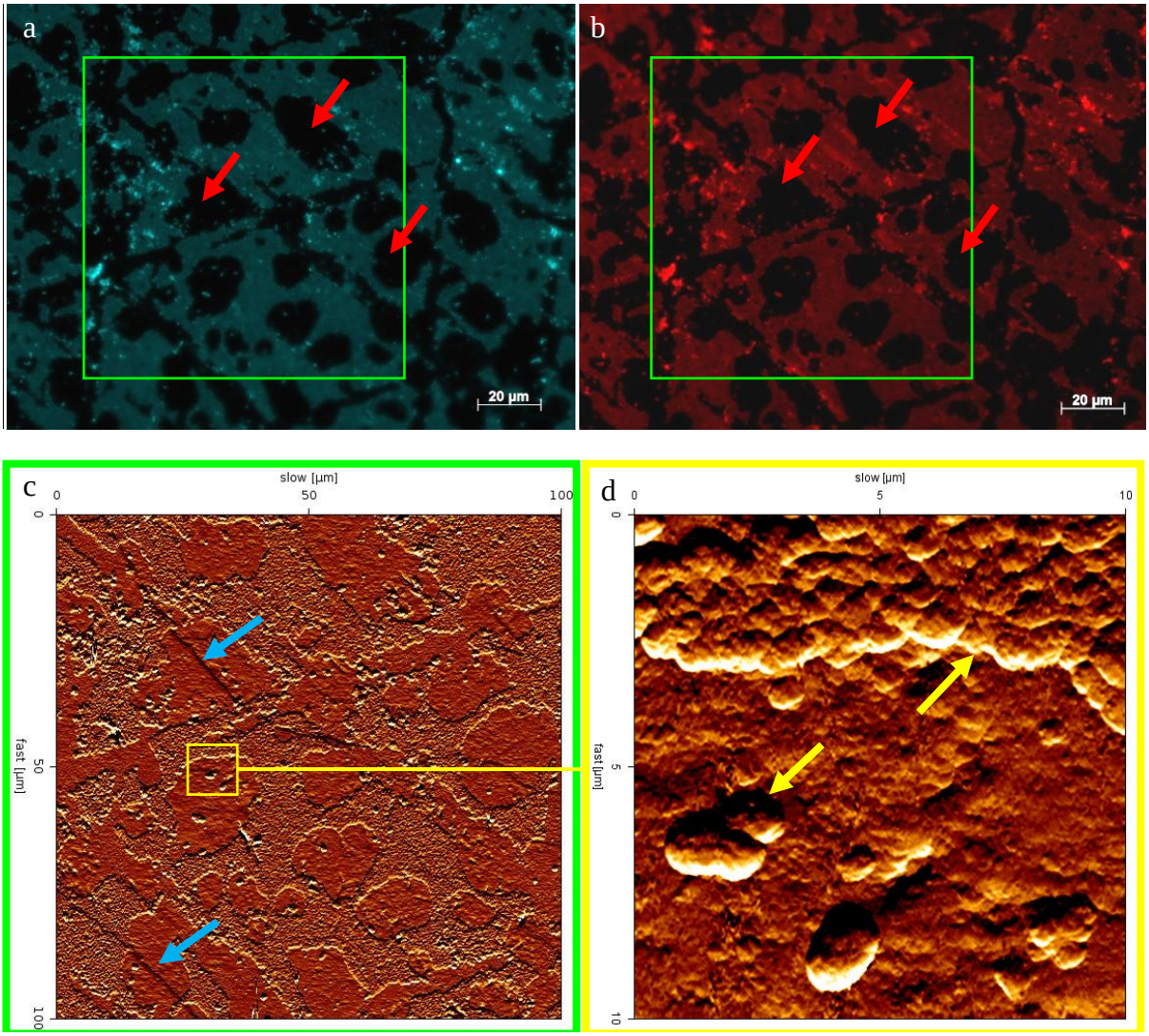

Figure 41 a - d: Selected EFM & AFM images of a pyrite coupon with a heat-inactivated biofilm of cells of *A. ferrooxidans* ATCC 23270 after leaching with *A. ferrooxidans* ATCC 23270

After 8 weeks incubation the coupon was stained with DAPI and Lectin (ConA). Pyrite coupon was at first incubated horizontally, naturally grown side up, in 100 mL Erlenmeyer flasks in a pure culture of *A. ferrooxidans* with an initial cell number of $5 \cdot 10^8$ cells/mL, 28°C, aerated, for 3 d for biofilm formation. Afterwards, the biofilm was inactivated by heat-drying at 55 °C for 24 h. Leaching experiment: Initial cell number of *A. ferrooxidans* $5 \cdot 10^8$ cells/mL, 10 mL basal salt solution, 28 °C, shaken (40 rpm).
Fig. a: EFM image; DAPI stained *A. ferrooxidans* cells; green frame = AFM scan area; red arrows = cell-free area.
Fig. b: EFM image; lectin (Con A) stained biofilms; green frame = AFM scan area; red arrows = EPS-free area.
Fig. c: AFM image; DAPI and lectin (green frames in a & b) stained area; blue arrows = mineral imperfections.
Fig. d: AFM image; detail of figure c (yellow frame); yellow arrows = cells.
AFM images: vertical deflection, contact mode in air.

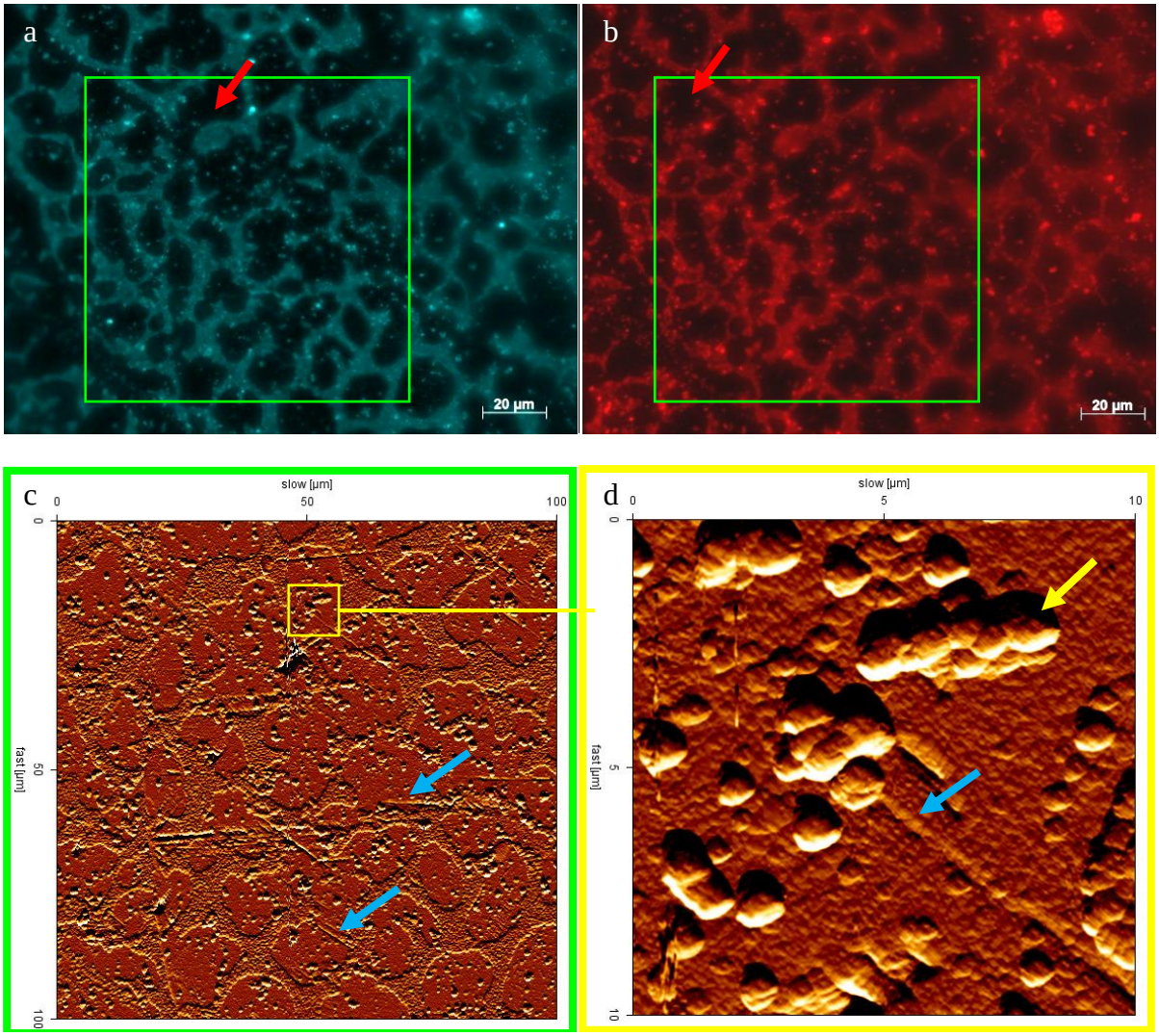

Figure 42 a - d: Selected EFM & AFM images of a pyrite coupon with a heat-inactivated biofilm of cells of *A. ferrooxidans* ATCC 23270 after leaching with *L. ferrooxidans* DSM 2705

After 8 weeks incubation the coupon was stained with DAPI and Lectin (ConA). Pyrite coupon was at first incubated horizontally, naturally grown side up, in 100 mL Erlenmeyer flasks in a pure culture of *A. ferrooxidans* with an initial cell number of $5 \cdot 10^8$ cells/mL, 28°C, aerated, for 3 d for biofilm formation. Afterwards, the biofilm was inactivated by heat-drying at 55 °C for 24 h Leaching experiment: Initial cell number of *L. ferrooxidans* $5 \cdot 10^8$ cells/mL, 10 mL basal salt solution, 28 °C, shaken (40 rpm).

Fig. a: EFM image; DAPI stained *A. ferrooxidans* and *L. ferrooxidans* cells; green frame = AFM scan area; red arrow = cell-free area.

Fig. b: EFM image; lectin (Con A) stained biofilms; green frame = AFM scan area; red arrow = EPS-free area.

Fig. c: AFM image; DAPI and lectin (green frames in a & b) stained area; blue arrows = mineral imperfections.

Fig. d: AFM image; detail of figure c (yellow frame); blue arrow = mineral imperfection; yellow arrow = cells.

AFM images: vertical deflection, contact mode in air.

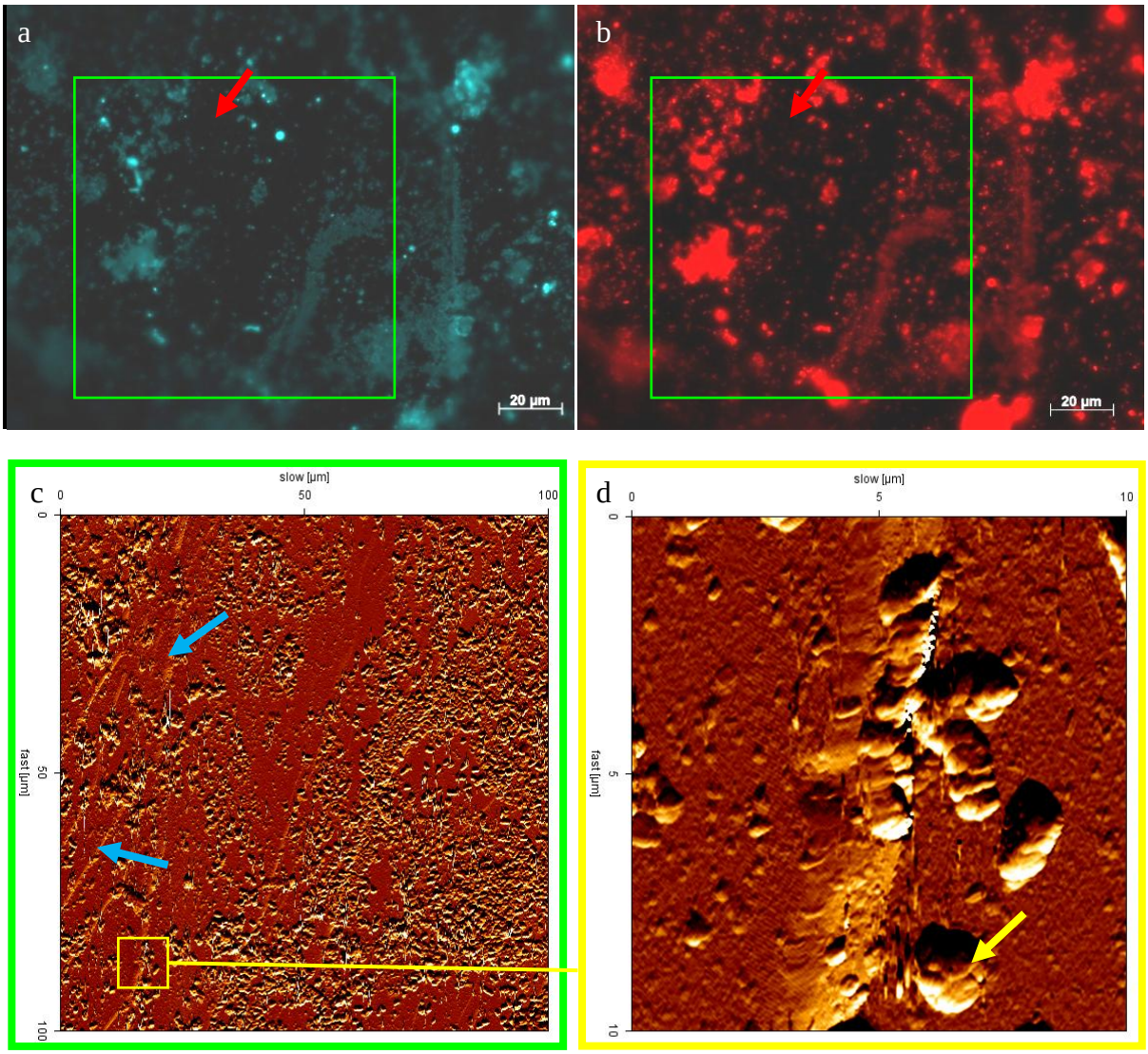

Figure 43 a - d: Selected EFM & AFM images of a pyrite coupon with a heat-inactivated biofilm of cells of *A. ferrooxidans* ATCC 23270 after incubation in sterile leach solution

After 8 weeks incubation the coupon was stained with DAPI and Lectin (ConA). Pyrite coupon was at first incubated horizontally, naturally grown side up, in 100 mL Erlenmeyer flasks in a pure culture of *L. ferrooxidans* with an initial cell number of $5 \cdot 10^8$ cells/mL, 28°C, aerated, for 3 d for biofilm formation. Afterwards, the biofilm was inactivated by heat-drying at 55 °C for 24 h. Experiment was performed without secondary addition of cells in 10 mL basal salt solution at 28 °C, shaken (40 rpm).

Fig. a: EFM image; DAPI stained *A. ferrooxidans* cells; green frame = AFM scan area; red arrow = cell-free area.

Fig. b: EFM image; lectin (Con A) stained biofilms; green frame = AFM scan area; red arrow = EPS-free area.

Fig. c: AFM image; DAPI and lectin (green frames) stained area; blue arrows = mineral imperfections.

Fig. d: AFM image; detail of figure c (yellow frame); yellow arrow = cells. AFM images: vertical deflection, contact mode in air.

The EFM images in Figure 41a and Figure 42a of pyrite coupons precolonized with a heat-inactivated biofilm of *A. ferrooxidans* indicate inhomogeneously distributed biofilms on pyrite surfaces.

A strong DAPI and lectin signal indicates cells and their EPS. They are visible in selected pyrite coupon surfaces, whereas some areas (indicated by red arrows) remained uncolonized even after 8 weeks (Figure 41 a & b, Figure 42 a & b).

On the precolonized control coupon in Figure 43 a large colonization is visible with a pattern, which is different from the one on the other coupons. This may result from the variability of the pyrite crystals.

3.6.3.4. Images of *A. thiooxidans* DSM 622 precolonized pyrite surfaces after leaching with *A. ferrooxidans* ATCC 23270 or *L. ferrooxidans* DSM 2705 cells

Pyrite coupons precolonized with a biofilm of cells of *A. thiooxidans* DSM 622 (heat-inactivated) were leached by *A. ferrooxidans* ATCC 23270 or *L. ferrooxidans* DSM 2705. In Figure 44, Figure 45 and Figure 46 images are shown of these surfaces as well as an abiotic control after 8 weeks of incubation.

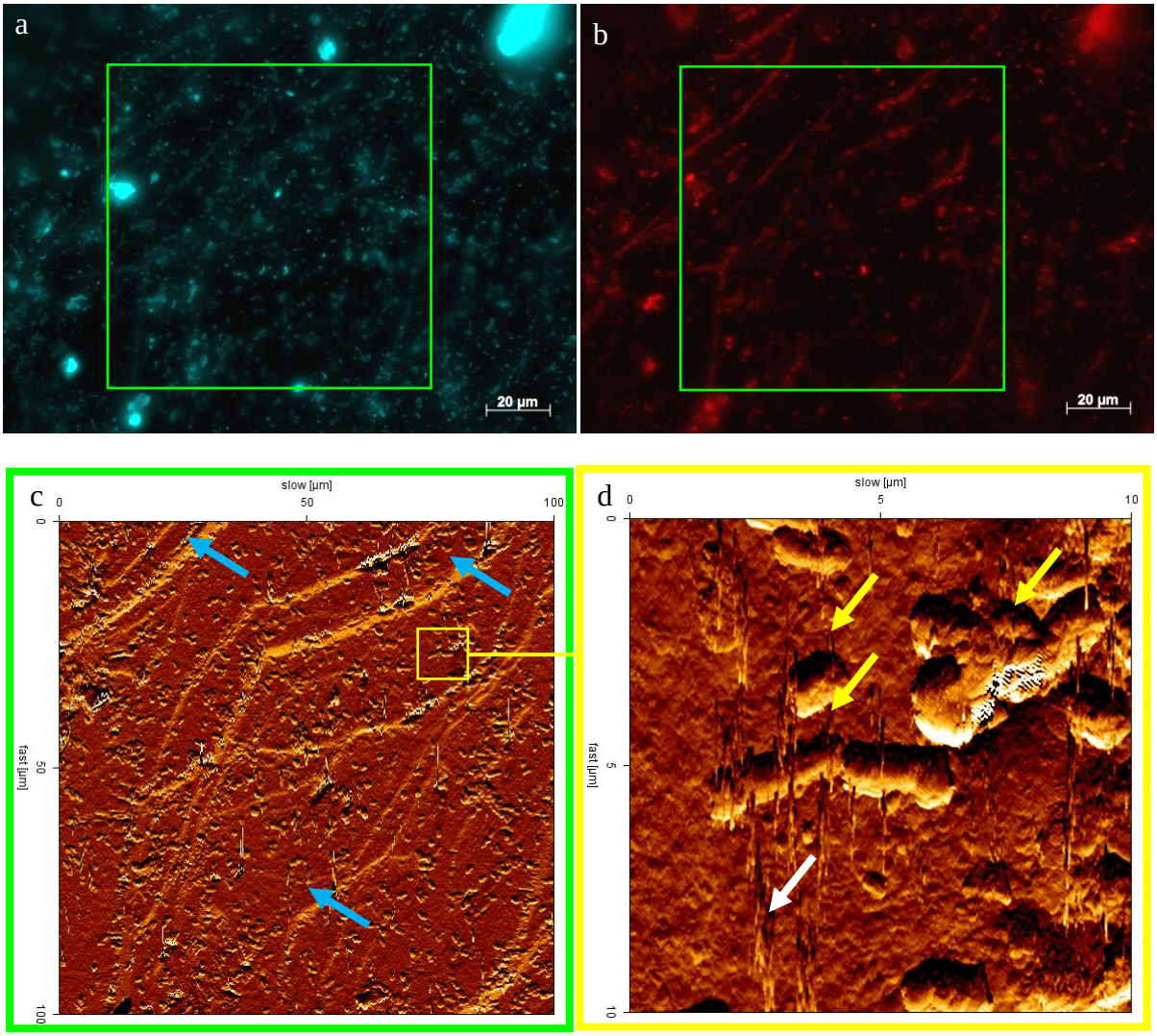

Figure 44 a - d: Selected EFM & AFM images of a pyrite coupon with a heat-inactivated biofilm of cells of *A. thiooxidans* DSM 622 after leaching with *A. ferrooxidans* ATCC 23270

After 8 weeks incubation the coupon was stained with DAPI and Lectin (ConA). Pyrite coupon was at first incubated horizontally, naturally grown side up, in 100 mL Erlenmeyer flasks in a pure culture of *A. thiooxidans* with an initial cell number of $5 \cdot 10^8$ cells/mL, 28°C, aerated, for 3 d for biofilm formation. Afterwards, the biofilm was inactivated by heat-drying at 55 °C for 24 h. Leaching experiment: Initial cell number of *A. ferrooxidans* $5 \cdot 10^8$ cells/mL, 10 mL basal salt solution, 28 °C, shaken (40 rpm).

Fig. a: EFM image; DAPI stained *A. thiooxidans* and *A. ferrooxidans* cells; green frame = AFM scan area.

Fig. b: EFM image; lectin (Con A) stained biofilms; green frame = AFM scan area.

Fig. c: AFM image; DAPI and lectin (green frames in a & b) stained area; blue arrows = mineral imperfections.

Fig. d: AFM image; detail of figure c (yellow frame); yellow arrows = cells; white arrow = artifacts produced by the scanning method.

AFM images: vertical deflection, contact mode in air.

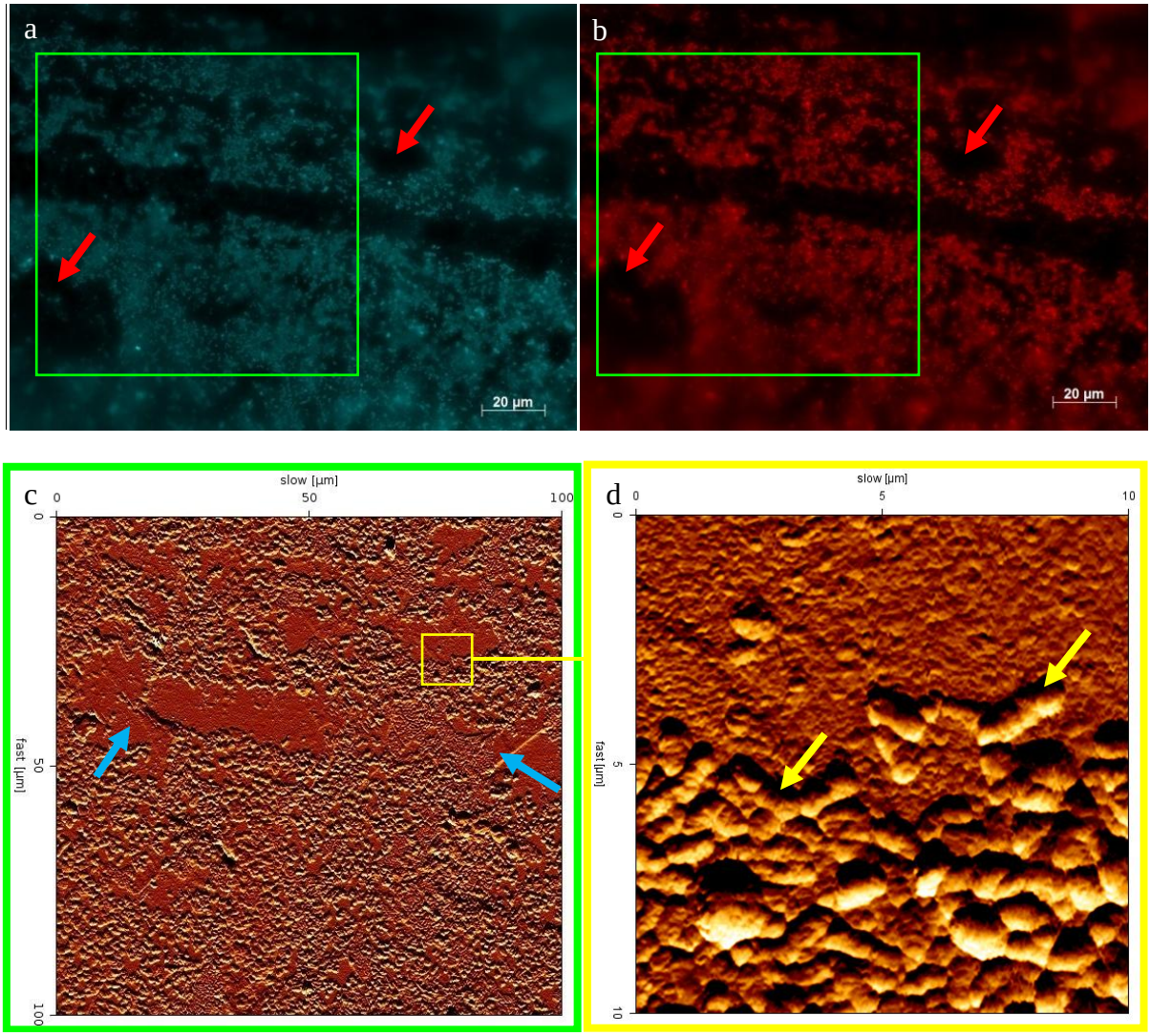

Figure 45 a - d: Selected EFM & AFM images of a pyrite coupon with a heat-inactivated biofilm of cells of *A. thiooxidans* DSM 622 after leaching with *L. ferrooxidans* DSM 2705

After 8 weeks incubation the coupon was stained with DAPI and Lectin (ConA). Pyrite coupon was at first incubated horizontally, naturally grown side up, in 100 mL Erlenmeyer flasks in a pure culture of *A. thiooxidans* with an initial cell number of $5 \cdot 10^8$ cells/mL, 28°C, aerated, for 3 d for biofilm formation. Afterwards, the biofilm was inactivated by heat-drying at 55 °C for 24 h. Leaching experiment: Initial cell number of *L. ferrooxidans* $5 \cdot 10^8$ cells/mL, 10 mL basal salt solution, 28 °C, shaken (40 rpm).

Fig. a: EFM image; DAPI stained *A. thiooxidans* and *L. ferrooxidans* cells; green frame = AFM scan area; red arrows = cell-free area.

Fig. b: EFM image; lectin (Con A) stained biofilms; green frame indicates AFM scan area; red arrows = EPS-free areas.

Fig. c: AFM image; DAPI and lectin (green frames in a & b) stained area; blue arrows = mineral imperfections.

Fig. d: AFM image; detail of figure c (yellow frame); yellow arrows = cells.

AFM images: vertical deflection, contact mode in air.

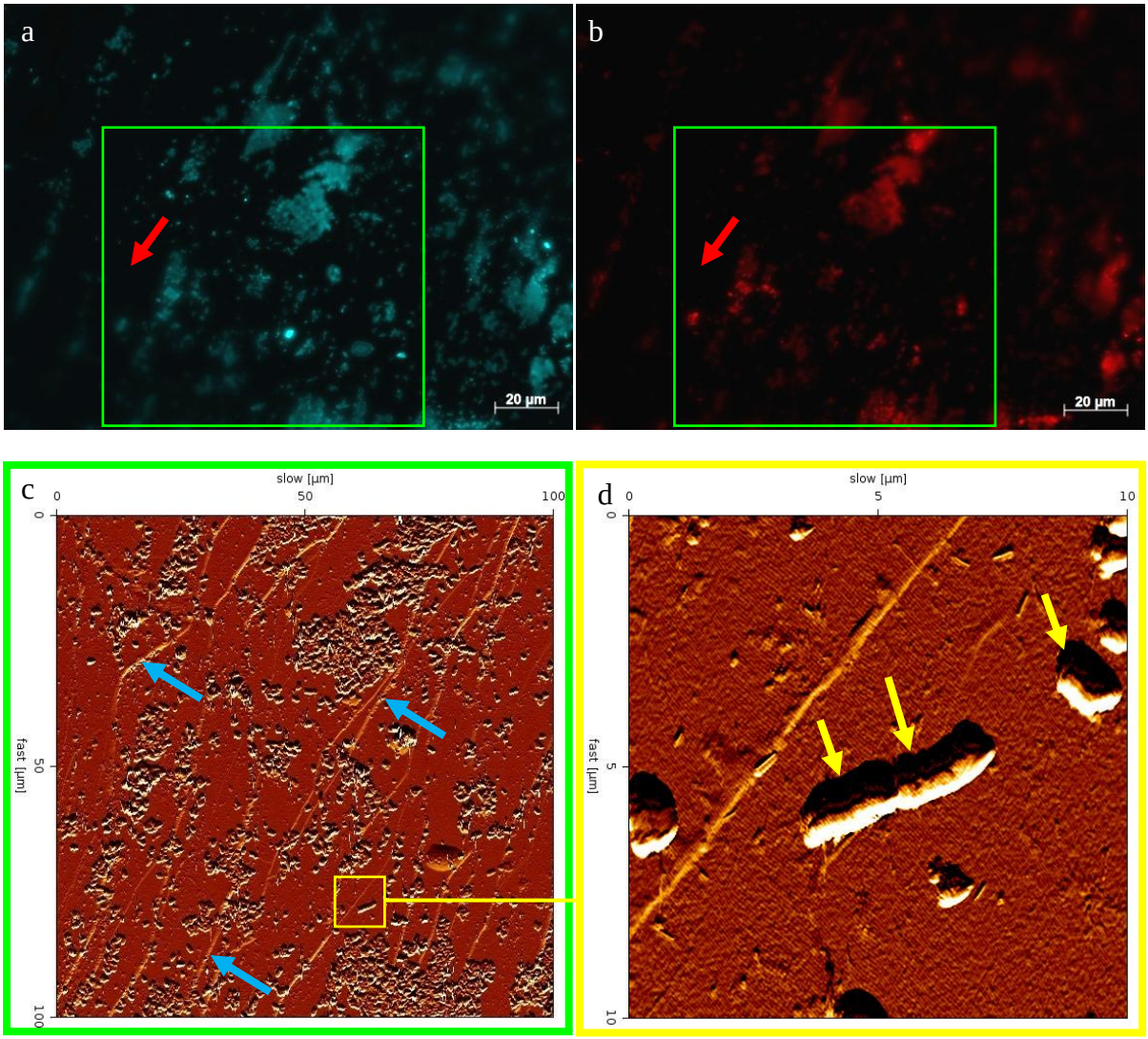

Figure 46 a - d: Selected EFM & AFM images of a pyrite coupon with a heat-inactivated biofilm of cells of *A. thiooxidans* DSM 622 after incubation in sterile leach solution

After 8 weeks incubation the coupon was stained with DAPI and Lectin (ConA). Precolonized pyrite coupons were at first incubated horizontally, naturally grown side up, in 100 mL Erlenmeyer flasks in a pure cultures of *A. thiooxidans* with an initial cell number of $5 \cdot 10^8$ cells/mL, 28°C, aerated, for 3 d for biofilm formation. Afterwards, the biofilm was inactivated by heat-drying at 55 °C for 24 h. Experiment was performed without secondary addition of cells in 10 mL basal salt solution at 28 °C, shaken (40 rpm).

Fig. a: EFM image; DAPI stained *A. thiooxidans* cells; green frame = AFM scan area; red arrow = cell-free area.

Fig. b: EFM image; lectin (Con A) stained biofilms; green frame = AFM scan area; red arrow = EPS-free area.

Fig. c: AFM image; DAPI and lectin (green frames in a & b) stained area; blue arrows = mineral imperfections.

Fig. d: AFM image; detail of figure c (yellow frame); yellow arrows = cells.

AFM images: vertical deflection, contact mode in air.

The EFM image in Figure 44a of a pyrite coupon with a (heat-inactivated) biofilm of cells of *A. thiooxidans* indicate that *A. ferrooxidans* and *A. thiooxidans* cells are homogenously distributed. Cells of *L. ferrooxidans* (and *A. thiooxidans*) appear in a high cell number mainly in cell clusters (Figure 45a) with a high amount of EPS (Figure 45b). On the precolonized control coupon in Figure 46a single cells and cell clusters are visible.

AFM images in Figure 44 c & d and Figure 45 c & d indicate a rougher surface for pyrite coupons leached by *A. ferrooxidans* or *L. ferrooxidans* compared images in Figure 46 c & d of the abiotic control.

Image imperfections (indicated by white arrows) can occur if the scan velocity is too high or particles adhere at the cantilever tip.

4. Discussion

The object of this study was to investigate initial attachment and biofilm formation to pyrite surfaces by pure and mixed cultures of the leaching bacteria *L. ferrooxidans* DSM 2705, *A. ferrooxidans* ATCC 23270 and *A. thiooxidans* DSM 622.

4.1. Bacterial attachment to pyrite

Initial cell attachment and (monolayer) biofilm formation on mineral surfaces play a pivotal role in the whole bioleaching process (Sand et al. 1995, Rodríguez et al. 2003). From previous work it is well known that different strains of leaching bacteria show different rates of attachment to pyrite (Klock 2003, Kock 2003, Stein 2004, Harneit et al. 2006, Mangold 2006, Mafanya 2007). At present, nearly no information is available about the attachment of individual species in mixed cultures to pyrite surfaces and their influence on pyrite dissolution. Song and co-workers quantified the relative amount of pyrite attached cells of strains of *Acidithiobacillus caldus* and *Leptospirillum ferriphilum* in a mixed culture by real-time PCR (Song et al. 2010). However, visual information about the attachment pattern of the individual strains in connection with the pyrite surface was not presented.

Consequently, the first questions are: How to investigate the attachment of pure and mixed cultures and how can single species be identified and enumerated in a mixed culture attached on pyrite surfaces?

4.1.1. Quantification of bacterial attachment

Attachment experiments with pure and mixed cultures to pyrite grains and pyrite coupons were performed.

10 g of pyrite grains with a grain size of 50 – 100 µm were used. The surface area amounts to 0.1111 ± 0.0027 m^2/g. This area will be covered by bacteria only to 2 %, if an inoculum of $5 \cdot 10^8$ cells/mL is used (Mangold 2006). Consequently, the available surface of the pyrite grains is non-limiting for this bacterial attachment experiments.

Shrihari and co-workers described that the attachment of cells of *A. thiooxidans* to chalcopyrite increases with increasing particle size. They proposed that the attachment was a

strong function of the particle size because the actual flow around particles is depending on their size, since the flow pattern in shake flasks is complex (Shrihari et al. 1991).
Consequently, the grain size of pyrite has to be as similar as possible and was standardized for all my experiments. Varying values of attached cells indicate that other, yet undetermined factors influence attachment to mineral sulfides.

Attachment pattern of pure and mixed cultures and single species within the mixed cultures was investigated on pyrite coupons.
For an optimal experimentation different experimental set-ups were tested. For each type of set-up, differences with regard to the extent of cell attachment as well as attachment pattern were observed. E.g. pyrite coupons, which were horizontally incubated without stirring or shaking, exhibited high numbers of attached cells and were accompanied by high amounts of precipitates. Within minutes, the determination of cell numbers on the exposed upper side of the coupon became impossible. In contrast, nearly no cells were observed on the bottom side of such pyrite coupons (6. Appendix; Figure 48). Sedimentation of cells due to gravitation is considered to be the reason for these large differences in surface coverage.
If pyrite coupons were horizontally incubated in Erlenmeyer flasks and subjected to shaking at 50, 100 or 120 rpm, cells were located only at areas with imperfections of the mineral surface or at the edges of the coupons. This may be a result of the influence of shear forces. The total number of cells attached within 24 h was very low, except for the edges of the coupons. Also, nearly no cells were found on the bottom side of the coupons.
In consequence, an own practical method for avoiding cell sedimentation, convection and/or shear forces was developed to overcome this problem.
Pyrite coupons were incubated vertically in a tube. Pressurized sterile air was introduced causing a continuous mixing of the cell suspension (Figure 6). This set-up kept convection low and avoided sedimentation of cells.
Data indicate that with this set-up an attachment to pyrite coupons was particularly significant after 1 h and showed a high variability of cell numbers per counting grid (125 µm x 125 µm) as well as per coupon. It was therefore not possible to calculate a mean value e.g. cells/ mm^2.
Results were evaluated statistically by using frequency distribution histograms. The relative frequency distribution describes the abundance of certain values in percentage within defined classes. The classes were defined as cells per counting grid (125 µm x 125 µm).

All attachment experiments to pyrite coupons as well as to pyrite grains were performed within an experimental time of 8 h. The generation time of *A. ferrooxidans* and *L. ferrooxidans* grown on ferrous iron under optimum conditions is approximately 7 h (Silverman and Lundgren 1959, Sand et al. 1992). For *Acidithiobacillus thiooxidans*, a doubling time of 20 h with sulfur as energy source at pH 3 has been described (Fischer et al. 2002). Since a lag phase occurs after inoculation to a new substrate, the total cell number of bacteria in an experiment should not change within the chosen experimental time.

Increased attachment to mineral sulfides by previous adaption to the substrate/substratum has been observed in several studies (Göksel 2000, Sampson et al. 2000, Stein 2004). An adaption of the test cells to pyrite was avoided in this work in order to keep conditions as similar as possible. *A. ferrooxidans* and *L. ferrooxidans* are able to use e.g. iron(II) ions and pyrite as substrate, whereas *A. thiooxidans* can only grow with sulfur-compounds. Therefore, *A. ferrooxidans* ATCC 23270 and *L. ferrooxidans* DSM 2705 were grown with iron(II) ions as substrate to prevent the adaption of the pyrite-metabolizing species to these surfaces.

All attachment experiments were performed at 28 °C, a temperature which was also used for bacterial growth. Thus, temperature did not influence attachment behavior.

Gehrke and co-workers proposed an increased bacterial attachment, if iron(III) ions are complexed in the capsular EPS. The (negatively charged) cell gains a positive net charge and, thus, is enabled to easily attach to the negatively charged pyrite (Gehrke et al. 1998). Iron(III) ions were detectable in the EPS of iron(II) ion- and pyrite-grown bacteria, but not in the EPS of sulfur-grown bacteria (Harneit et al. 2006). However, during the harvesting procedure cells loose the main amount of their EPS and, thus, also complexed iron- compounds. Previous experiments indicated that EPS are important for attachment (Gehrke et al. 1998, Yu et al. 2010) and cells replenish their capsular EPS within a few hours (Gehrke et al. 1995). Therefore, after cell harvest from work cultures the cell suspensions were kept for 24 h without any substrate to allow the bacteria to replenish their EPS, before an experiment started.

4.1.2. Bacterial attachment to pyrite grains

By the attachment experiment to pyrite grains two questions were partially answered:

- Which pure culture shows the highest initial attachment and in which pattern onto a pyrite surface?
- Which mixed culture shows the highest initial attachment and in which pattern onto a pyrite surface?

The highest amounts of attached cells to pyrite grains after 7 h of experiment were found for pure cultures with nearly to the same numbers for *L. ferrooxidans* DSM 2705 and for *A. thiooxidans* DSM 622. The differences in numbers of attached cells were only 2 %. Taking the standard deviation into account, this difference is negligible. For mixed cultures the highest attachment was found for the combination of *L. ferrooxidans* DSM 2705 with *A. ferrooxidans* ATCC 23270 cells.

Increased attachment of pure cultures of *L. ferrooxidans* DSM 2705 or *A. thiooxidans* DSM 622 could be based on the motility of these strains by means of a polar flagellum. Motility is known and was also observed in this study for *L. ferrooxidans* and *A. thiooxidans* by light microscopy (Doetsch et al. 1967, Harrison and Norris 1985, Hippe 2000). The little attaching strain *A. ferrooxidans* ATCC 23270 showed no motility and is known to be non-flagellated lacking genes for flagellation (Valdés et al. 2007, Li et al. 2010).
It is known that bacteria can attach by use of their polar flagella (Meadows 1971). However, an increased attachment only by adhesive forces of polar flagella of theses bacteria to a pyrite surface is doubtful.
Increased attachment of *L. ferrooxidans* DSM 2705 and *A. thiooxidans* DSM 622 is more likely due to targeted active movement by flagella. Target oriented movement can be induced by quorum sensing molecules and is known for some strains of *A. ferrooxidans*. For strains of *A. thiooxidans* a functional autoinducer-1 (AI-1) quorum sensing system is known, but target orientated movement was not tested and for strains of *L. ferrooxidans* no AHL-signaling molecules or regulator systems have been described up to now.
The increased attachment of *L. ferrooxidans* DSM 2705 may be additionally based on the high amount of EPS produced by these cells. High production of EPS by strains of

L. ferrooxidans has been shown (Klock 2003, Harneit et al. 2006) with a concomitant cluster formation (Norris 1990, Hallmann et al. 1992). Cluster formation by *L. ferrooxidans* DSM 2705 was observed also in growth cultures in this study. The higher the cell numbers the more clusters were found in the growth media. Examination of such cell clusters by light microscopy exhibited cells embedded in a matrix, highly likely EPS (not shown). If bacteria attached in clusters to the pyrite grains by convection forces as a result of the experimental set-up, no assumption of a targeted movement would be necessary to explain such high cell numbers.

Attachment of pure cultures of *A. ferrooxidans, L. ferrooxidans* and *A. thiooxidans* in shake flask experiments has been studied previously (Guidone 1998, Klock 2003, Harneit et al. 2006, Mangold 2006, Mafanya 2007). In order to allow the comparison of attachment data for pure or mixed cultures, experiments with pure cultures were repeated under the same conditions in this work. This repetition should compensate besides varying physical parameters also the possibility of genetical alterations of the strains caused by storage in strain collections which might be cause a change in the attachment behavior.

The attachment of the type strain of *L. ferrooxidans* DSM 2705 has been investigated previously using shake flask experiments. Results indicate an attachment to pyrite grains of more than 90 % after 2 h (Guidone 1998). However, similar experiments in this work resulted in a reduced attachment. After 7 h, 73 % of the cells were found to be attached to the mineral surface. This difference may have been caused by differences in the experimental set up or merely by little variations in previous cell growth. Additionally, genetic changes of *L. ferrooxidans* DSM 2705 cannot be excluded.

Acidithiobacillus thiooxidans does not possess the ability to dissolve pyrite, but is a frequently found member in leaching communities. Attachment to sulfur and pyrite was investigated for different strains of this species and seems to be important for the oxidation of the sulfur moiety (Schaeffer et al. 1963, Göksel 2000, Liu et al. 2003, Harneit et al. 2006). For strain *A. thiooxidans* DSM 622 results obtained by shake flask experiments are not reported in literature.

The data for the attachment experiments of *A. ferrooxidans* ATCC 23270 to pyrite grains are in agreement with those obtained previously. In this study 42 % of the cells attached to pyrite grains after an incubation time of 7 h. Mangold and Mafanya obtained comparable results with approximately 40 % cell attachment of the same strain to pyrite grains (Mangold 2006, Mafanya 2007). In all experiments the main attachment was observed within 120 min.

Other experiments showed that own isolates of *Acidithiobacillus ferrooxidans* attached in increased extent to metal sulfides such as pyrite, chalcopyrite or sphalerite (Kock 2003, Stein 2004, Harneit et al. 2006). In contrast to the type strain, some *Acidithiobacillus ferrooxidans* strains seem to possess flagella (DiSpirito et al. 1982b, Li et al. 2010). This might be a reason for the increased extent of attachment to mineral surfaces as compared to strain *A. ferrooxidans* ATCC 23270. E.g. cells of *A. ferrooxidans* strains R1 and C-52 attached up to 90 % to pyrite after an incubation time of only 10 minutes (Kock 2003). Another study demonstrated a slightly reduced attachment of cells of strain R1 (approx. 80 %) with the equilibrium being established after 2 h (Stein 2004). These different results for the attachment of the same strain, e.g. *A. ferrooxidans* strain R-1, within the same experimental set up can be based upon various factors (e.g. pH, temperature, mineral fraction) which still need to be elucidated. It may be possible that strain R1 belongs to the new species *Acidiferrobacter thiooxydans* (Hallberg et al. 2011) which would explain the different data for attachment. Furthermore, the type strain may have attach-deficiencies due to his long culture collection history.

The experiments using mixed cultures of bacteria including *A. ferrooxidans* ATCC 23270, *L. ferrooxidans* DSM 2705 and *A. thiooxidans* DSM 622 indicate that a combination of strains is an important factor influencing attachment to pyrite grains.

Based on the results for the attachment tests with pure cultures, as discussed above, for each member of the mixed culture the attachment percentage was calculated. The data indicate that in the majority of the combinations of strains of *A. ferrooxidans* ATCC 23270, *L. ferrooxidans* DSM 2705 and *A. thiooxidans* DSM 622 the bacteria influence each other in attachment to pyrite grains.

The attachment of most of the mixed cultures was higher than the calculated values. The highest attachment with 81 % was found for mixed cultures consisting of *L. ferrooxidans* DSM 2705 and *A. ferrooxidans* ATCC 23270. This number is 25 % higher than the calculated one using pure culture values. Also the mixed cultures composed of *A. ferrooxidans* ATCC 23270 with *A. thiooxidans* DSM 622 and *A. ferrooxidans* ATCC 23270 with *A. thiooxidans* DSM 622 plus *L. ferrooxidans* DSM 2705 showed higher attachment than calculated. It is obvious that at least one of these strains benefitted from being a member of the mixed culture.

A modification of a pyrite surface by a secretion of microbial compounds by attached or planktonic cells of *L. ferrooxidans* DSM 2705 or *A. thiooxidans* DSM 622 may have resulted

in a higher attachment of the little attaching cells of the type strain of *A. ferrooxidans* ATCC 23270.

A secretion of a sub class of microbial lipids called microbial surface-active compounds (SACs) are known to be involved in alteration of hydrophobic surfaces. SACs secreted by bacteria into the surrounding media may be responsible for a microbially created conditioning film at an interface (Neu 1996). One of the first examples was reported for a *Thiobacillus* species. The compounds may be involved in the initial stages of adhesion to the hydrophobic surface of extremely hydrophobic elemental sulfur (Jones et al. 1961, Bryant et al. 1984).

The secretion of microbial surface-active compounds can also inhibit bacterial attachment to solid surfaces. The strains *L. ferrooxidans* DSM 2705 and *A. thiooxidans* DSM 622 in a mixed culture showed slightly decreased attachment to pyrite grains. The determined attachment value was 65 %, whereas, the calculated one amounted to 72 % (still statistically significant).

Another cause for such a decreased attachment by at least one of the strains may be based on a competition for attractive (usable) surface areas by the bacteria.

The attachment experiments to pyrite grains provide information about extent and velocity of the cell adhesion to the mineral surface. However, the experiments provide neither information about the attachment behavior of single strains in a mixed culture nor about the attachment patterns on the mineral surface.

In order to overcome this problem, pure and mixed cultures as well as single strains within these mixed cultures attached to pyrite coupons were visualized and investigated by different staining techniques such as DAPI, lectin and FISH in combination with atomic force microscopy.

4.1.3. Bacterial attachment to pyrite coupons

The highest initial attachment for pure cultures to pyrite coupons was determined for cells of *L. ferrooxidans* DSM 2705.

In pure cultures, cells of *L. ferrooxidans* DSM 2705 attached either as single cells or in small clusters. Cluster formation of cells of *L. ferrooxidans* in liquid media is well known (Norris 1990, Hallmann et al. 1992) and was also observed in my experiments. Nevertheless, it is not clear, whether cells attach in clusters to the mineral surface and/or single cells attach to the mineral surface at the same side and form consecutively the clusters. However, due to the

finding of clusters in cultures (Norris 1990, Hallmann et al. 1992) it is probable that preformed cluster attach. This is also supported by the fact that these cells produce large amounts of EPS. The cluster formation in the inoculum increased with increasing cell numbers. The high attachment rates of cells from pure cultures of *L. ferrooxidans* DSM 2705 may be based on the high tendency for cluster formation and the large amount of 'sticky' EPS.

Another typical and frequently observed attachment pattern of leaching bacteria like *L. ferrooxidans* DSM 2705 in pure cultures is evident from the EFM and AFM images (Figure 17 b and c; Figure 41 to 43): large areas are covered with cells, whereas other parts remain virtually cell-free. Obviously, the attachment of cells of *L. ferrooxidans* DSM 2705 is an active process being connected with the mineral surface and/or the conditioning layer on the mineral surface. Furthermore, the composition of the EPS-matrix, the embedded iron(III) ions, chemotaxis, quorum sensing and other factors may participate.

Cells of pure cultures of *L. ferrooxidans* DSM 2705 or *A. ferrooxidans* ATCC 23270 attached mainly within 1 h to the pyrite coupon surface. No significant increase of cell numbers was determined after 8 h. These results are in agreement with those from the attachment experiments to pyrite grains, where cells attached mainly within the first 30 min which reaching an equilibrium after 120 min (Figure 47). However, *A. thiooxidans* DSM 622 showed a significantly higher attachment to pyrite coupons after 8 h as compared to 1 h. This result is different from the one for attachment to pyrite grains, where 30 min were the optimal value. The scientific background is not fully clear, however parameters such as particle size, crystallography of pyrite surfaces, convection forces, chemotaxis and others may play a decisive role.

In pure cultures, *A. ferrooxidans* ATCC 23270 attached mainly in low numbers as single cells on the mineral surface. A flock formation in the bulk solution like the one observed for *L. ferrooxidans* DSM 2705 was not observed. However, after 8 h, small cell clusters consisting of a few cells only were observed infrequently at large surface defects (Figure 18a). The formation of these clusters may have been a result of a preferred attachment to certain areas on the surface of pyrite coupons and an accumulation of cells at those mineral imperfection sides.

Pure cultures of *A. thiooxidans* DSM 622 attached mostly homogenous to the mineral surface. Cluster formation was not observed neither in the bulk solution nor on the mineral surface. Like with the previous strains, large areas of the pyrite surfaces remained cell-free. This

results in the assumption that the initial attachment of *A. thiooxidans* DSM 622 among other things is like the one of *A. ferrooxidans* ATCC 23270 and *L. ferrooxidans* DSM 2705 related to the characteristics of the pyrite coupon surface.

The highest initial attachment to pyrite coupons was detected for the mixed culture composed of all three strains: *A. ferrooxidans* ATCC 23270 with *A. thiooxidans* DSM 622 and *L. ferrooxidans* DSM 2705.

A. thiooxidans DSM 622 was identified to be the strain with the highest attachment within this mixed culture. Furthermore, it showed also the highest attachment within the other mixed culture variants. Taking this into account plus the findings that *L. ferrooxidans* DSM 2705 showed in general reduced attachment in mixed cultures compared to pure cultures, *A. thiooxidans* DSM 622 is identified to be the 'first colonizer' of pyrite coupon surfaces.

A. ferrooxidans ATCC 23270 exhibited generally the lowest attachment in pure and mixed cultures as discussed above. Only in case of the mixed culture composed of *A. ferrooxidans* ATCC 23270 with *A. thiooxidans* DSM 622 and *L. ferrooxidans* DSM 2705 the strain *L. ferrooxidans* DSM 2705 showed the lowest attachment after 8 h. The reasons for this finding remain unclear.

The attachment of cells of single strains to surfaces of pyrite coupons as members of mixed cultures may differ considerably from their attachment in pure culture.

One explanation for increased or decreased attachment of strains in mixed cultures to pyrite coupons is the possible influence of quorum sensing molecules like described above for the attachment to pyrite grains. Attachment experiments with (commercially available) quorum sensing molecules can give further information. Because of time limitation these experiments were not part of this thesis.

Another possibility for the change in the attachment behavior of single species in mixed cultures may be related to the composition of their EPS and embedded components. In the following chapter, the own results obtained on interspecies interactions connected with the EPS composition are discussed in detail.

A significant finding of the attachment of mixed cultures to pyrite coupon surfaces is the strict separation of the species. Cells of one species were found to have physical contact, whereas no physical interspecies contact was observed. Without exception, cells of two (or three) different strains never got mixed or were touching each other on a pyrite surface. Selected

images clearly demonstrate this finding (Figure 21, Figure 23, Figure 25, Figure 27and Figure 28).

The separation of strains on the pyrite coupon surface leads to the idea that *L. ferrooxidans* DSM 2705, *A. ferrooxidans* ATCC 23270 and *A. thiooxidans* DSM 622 may prefer different sides of a pyrite crystal. Another possibility would be that fast cells of attaching strains cover preferred attachment sides and render them unavailable for cells from other strains. Whereas the assumption may explain the data for tests with *L. ferrooxidans* DSM 2705, which showed a decreased attachment in mixed cultures with cells of *A. thiooxidans* DSM 622, this assumption is contrary to the fact that the attachment of little attaching strain like *A. ferrooxidans* ATCC 23270 was increased. It could be that *A. thiooxidans* DSM 622 as the 'first colonizer' may produce a conditioning layer on the pyrite coupon surface. Cells of *A. ferrooxidans* ATCC 23270 who belongs to the same genus could be attract from this conditioning film, whereas, it is repulsive for cells of *L. ferrooxidans* DSM 2705. Further investigations on this phenomenon can give more information about the increased attachment of *A. ferrooxidans* ATCC 23270 and reduced attachment of *L. ferrooxidans* DSM 2705.

The finding of increased attachment of cells of *A. ferrooxidans* ATCC 23270 in a mixed culture containing cells of *A. thiooxidans* DSM 622 allows to answer another question: 'Which member of a mixed culture needs pre-colonization?'. The pure culture of *A. ferrooxidans* ATCC 23270 showed little attachment to a surface of a pyrite coupon. In mixed cultures including *A. thiooxidans* DSM 622 the attachment got increased significantly. However, in the mixed culture only with cells of *L. ferrooxidans* DSM 2705 the attachment of *A. ferrooxidans* ATCC 23270 was decreased. Consequently, cells of *A. ferrooxidans* ATCC 23270 need a precolonization by cells of a 'suitable' member of the leaching community.

Low attachment of the pure culture of *A. ferrooxidans* ATCC 23270 may be explained by the lack of flagella and, consequently, a missing active movement to the mineral surface (Valdés et al. 2007, Li et al. 2010). However, increased attachment of *A. ferrooxidans* ATCC 23270 in mixed cultures indicates that the attachment of this strain is not only limited by the inability of an active movement by flagella. What exactly the reason for increased attachment is, remains to be elucidated. As mentioned, it may be related to pyrite surface modifications or a release of quorum sensing molecules by cells of *A. thiooxidans* DSM 622.

The most frequent attachment of all pure and mixed cultures to pyrite coupons ranged in the class 1 - 50 cells. In addition, large areas of the pyrite surfaces remained cell-free, even after 8

h. This finding is astonishing for the following reason. For pyrite grains the surface is much larger than needed for a colonization by all cells of the inoculum. With pyrite coupons the opposite is true: cells are in excess as compared to the available surface. Cells from the surrounding suspension (V= 50 mL) with a typical size of 0.5 µm width and 3 µm length and population density of $1 \cdot 10^8$ cells/mL could colonize a total area of about 75 cm^2.

Consequently, the low numbers of attached cells plus the remaining cell-free surface areas are not a result of the relation surface area to cell number. Rather it is likely that bacterial attachment is limited by the availability of specific pyrite surface areas. Some areas seem to be more attractive than others, which may caused by e.g. less crystalline and amorphous zones or crystallization patterns (sulfur, iron or mixed surface atoms) on the mineral surface (Andrews 1988, Gehrke et al. 1998, Sanhueza et al. 1999, Gehrke et al. 2001, Kinzler et al. 2003).

In addition, the results of the attachment tests to pyrite coupons differ from the results obtained with pyrite grains. Apparently, some strains were more affected than others e.g. pure cultures of *A. thiooxidans* DSM 622 showed lower attachment to pyrite coupons than pure cultures of *L. ferrooxidans* DSM 2705, whereas the attachment to pyrite grains was similar. Differences may have been caused by the technical set-up. Convection, sedimentation and particle size (available surface with mineral imperfections) play a pivotal role in the ability of the cells to attach to pyrite. Experiments with pyrite grains in an experimental set-up avoiding convection and sedimentation of cells as well as shear forces could give more information about the influence of crystalline structure of pyrite grains. Because of time limitation these experiments were not part of this thesis.

4.1.4. Bacterial attachment to pyrite coupons covered with a pregrown biofilm

Previous studies demonstrated the importance of EPS for the attachment of leaching organisms to metal sulfides (Gehrke et al. 2001, Harneit et al. 2006, Sand and Gehrke 2006, Yu et al. 2010). However, little is known about the interactions between the EPS from various species of leaching bacteria and the influence on the attachment behavior of other species/members of the biocoenosis.

To investigate the influence of EPS on attachment of *L. ferrooxidans* DSM 2705, *A. ferrooxidans* ATCC 23270 or *A. thiooxidans* DSM 622, pyrite coupons were precolonized with these bacteria, heat-inactivated and subsequently used for attachment experiments.

Bacteria in the precolonizing biofilms were heat-inactivated to avoid any influence on the subsequently attaching bacteria like an excretion of QS molecules. Furthermore, by inactivation of the precolonizing cells their rRNA is degraded. This made the identification of the secondary attaching cells by FISH possible. For inactivation heat-drying at 55 °C was selected in order to avoid chemical additions, which could have an influence on bacterial attachment. Since proteins were not detected in the EPS of *A. ferrooxidans, A. thiooxidans* and *L. ferrooxidans* (Gehrke et al. 1998, Harneit et al. 2006), the heat treatment should have not caused any change in bacterial attachment by a denaturation of EPS-proteins. However, it was not tested whether the cells in the heat-inactivated biofilms remained intact. Thus, the release of periplasmic or cytoplasmic proteins cannot be excluded. Since the AFM images indicate intact cells (not collapsed) a release of the above mentioned proteins seems to be unlikely.

The data indicate that the attachment pattern to precolonized pyrite coupons completely differs from the one to virgin coupons. *L. ferrooxidans* DSM 2705 exhibited a decreased attachment to precolonized pyrite coupons as compared to the attachment to virgin coupons. In contrast, *A. ferrooxidans* ATCC 23270 showed a significantly increased attachment to pyrite coupons precovered by biofilms which actually agrees with the hypothesis that cells of *A. ferrooxidans* ATCC 23270 need a precolonization by other leaching bacteria (see above with pure and mixed cultures). Similar to *A. ferrooxidans* ATCC 23270 cells, *A. thiooxidans* DSM 622 showed an increase in attachment to precolonized pyrite coupons. However, an attachment of cells of *A. thiooxidans* DSM 622 in mixed cultures with *L. ferrooxidans* DSM 2705 to virgin pyrite coupons was decreased. These at a first glance contradictory result lead to the assumption that living cells of *L. ferrooxidans* DSM 2705 repel cells of *A. thiooxidans* DSM 622 from pyrite surfaces or cover attractive areas, whereas, the (inactivated) biofilm enhance the attachment.

The distribution of mixed cultures to virgin pyrite coupons indicated a separation of the strains on the pyrite coupon surfaces without physical interspecies contact. In contrast, secondarily attached cells were found on precolonized pyrite coupons in areas with inactivated cells and their EPS. Since these cells were inactivated, it is likely that a modification of the pyrite surface by (inanimate) EPS or embedded components influenced the attachment behavior of these bacteria. E.g. the decreased attachment of cells of *L. ferrooxidans* DSM 2705 to pyrite coupons may be a result of EPS-covered preferential attachment sides on the pyrite by biofilms. The decrease was also detected with precolonized

coupons for this strain. Consequently, attachment of *L. ferrooxidans* DSM 2705 seems to be strictly limited to these specific sides.

The increase of attachment of *A. ferrooxidans* ATCC 23270 and *A. thiooxidans* DSM 622 to precolonized pyrite coupons indicates that in contrast to *L. ferrooxidans* DSM 2705 attachment may not only be related to preferred pyrite surface binding sides. Moreover, the EPS on the mineral surface has an attachment increasing effect. This may be based on EPS-embedded iron- or sulfur compounds, which were enclosed in the capsular EPS during the growth in iron(II) ion or thiosulfate-containing media. Compounds on the pyrite surface like biofilms could be responsible for an increase of the attachment of *A. ferrooxidans* ATCC 23270 and *A. thiooxidans* DSM 622. To clarify this question, attachment experiments with covered pyrite coupons with single biofilm components (e.g. different types of sugars, lipids or free fatty acids) could give more information. They are however, beyond the scope of this work.

4.2. Bacterial leaching of pyrite

Bacterial leaching of mineral sulfides is influenced by several factors such as temperature, concentration of O_2, toxic compounds (molybdenum, silver, arsenic amongst others) and the composition of the leaching biocoenosis.

Leaching of pure and mixed cultures of *L. ferrooxidans* DSM 2705, *A. ferrooxidans* ATCC 23270 or *A. thiooxidans* DSM 622 was investigated to identify the most efficient leaching culture composed of these strains.

Bacterial attachment is known to be important for the whole leaching process. The dependency of initial attachment of pure and mixed cultures of *L. ferrooxidans* DSM 2705, *A. ferrooxidans* ATCC 23270 or *A. thiooxidans* DSM 622 on the efficiency of pyrite dissolution can be evaluated by a correlation of the results of attachment with leaching experiments.

4.2.1. Bacterial leaching of pyrite grains

Bacterial leaching of pyrite grains by pure and mixed cultures was quantified by determining the concentration of iron(III) ions in the bulk solution.

The highest concentration of iron(III) ions and, thus, pyrite dissolution was determined for pure cultures of *L. ferrooxidans* DSM 2705. Coincidently, all mixed cultures containing

L. ferrooxidans DSM 2705 produced high iron(III) ion concentrations. In contrast, the pure culture of *A. ferrooxidans* ATCC 23270 and the mixed culture composed of *A. ferrooxidans* ATCC 23270 and *A. thiooxidans* DSM 622 showed only a low pyrite dissolution.

Concentrations of iron(III) ions of the abiotic controls and in assays with pure cultures of *A. thiooxidans* DSM 622 ranged always below the detection limit of 0.3 mM. This proves that both, abiotic pyrite dissolution as well as biotic dissolution by *A. thiooxidans* DSM 622 are negligible.

Since the iron(III) ion concentration is representative for the amount of pyrite dissolution, the data indicate that bacteria of the strain *L. ferrooxidans* DSM 2705 are the most important species as compared to *A. ferrooxidans* ATCC 23270 and *A. thiooxidans* DSM 622.

One possible explanation for higher leaching rates by cells of *L. ferrooxidans* DSM 2705 or mixed cultures including *L. ferrooxidans* DSM 2705 could be a higher cell number of *L. ferrooxidans* DSM 2705. The determination of cell number of *L. ferrooxidans* DSM 2705 on pyrite grains by microscopy is not possible. The determination of the relative amount of cells by real-time PCR could give more information, however, it was beyond the scope of this work.

A more likely explanation for increased leaching rates of *L. ferrooxidans* DSM 2705 is based on the kinetics of the bioleaching/biooxidation of pyrite (Rawlings et al. 1999). It was shown by Norris et al. that *L. ferrooxidans* has a higher affinity for ferrous iron than cells of *A. ferrooxidans* (Norris et al. 1988). In agreement with this report were the findings that *L. ferrooxidans* has a lower maximum specific utilization rate than *A. ferrooxidans* at low redox potential but can sustain higher activity up to a high redox potential. The redox potential (ferrous to ferric iron concentration) in a batch culture is low at the start of oxidation process but increases during the leaching of pyrite and became more favorable for *L. ferrooxidans* (Rawlings et al. 1999).

A careful examination combining the results from both, the attachment and the leaching experiments with pyrite grains, provides more in depth information whether a connection between initial bacterial attachment and mineral dissolution exists.

71 % of the cells of pure cultures of *A. thiooxidans* DSM 622 attached to pyrite grains, albeit their inability to dissolve pyrite. Furthermore, mixed cultures composed of *A. ferrooxidans* ATCC 23270 and *A. thiooxidans* DSM 622 showed similar attachment numbers as mixed cultures including *L. ferrooxidans* DSM 2705, but the dissolution by the latter one is much

higher. Consequently, high rates of bacterial attachment to pyrite grains are not necessarily concomitant with high pyrite grain dissolution rates (at least under -shaken flask- experimental conditions).

4.2.2. Bacterial leaching of pyrite coupons

In addition to the attachment experiments, bacterial leaching experiments with virgin and precolonized pyrite coupons were performed. The data were analyzed for a possible impact of colonization patterns on pyrite dissolution.

The attachment experiments indicated significant differences in cell adhesion, whereas, the amount of dissolution amongst the assays did not differ significantly.

Determinations of weight loss as well as of the concentrations of iron(III) ions in the bulk solutions indicated comparable bacterial leaching rates for living cells independent of the strain or a precolonization of pyrite coupons.

Pyrite dissolution is clearly dependent on living bacteria. This result is in agreement with those of Gehrke et al., where killed bacteria with EPS caused no significant pyrite dissolution (Gehrke et al. 1998). The influence of a precolonization with killed cells or at least on pyrite dissolution needs to be analyzed more precisely including large pyrite amounts and surfaces. Due to time constraints, no further experiments were performed.

For the visualization of biofilms on leached pyrite surfaces the experimental set-up including pyrite coupons was chosen. The pyrite coupons of these experiments were subjected to epifluorescence- and atomic force microscopy in order to gain information about the mineral surface as well as on bacterial attachment patterns and on biofilm formation.

Again the finding was made that large areas of the pyrite surfaces remained free of cells and EPS, even after 8 weeks incubation.

It is known that bacterial attachment is orientated to the crystallographic structure of the pyrite surface. Sanhueza and coworkers investigated the attachment of *Acidithiobacillus ferrooxidans* on synthetic pyrite with varying structural and electronic properties. They found that areas of amorphous pyrite were more attractive for bacterial attachment of cells of *A. ferrooxidans* than areas which were fully crystalline (Sanhueza et al. 1999). Accordingly, the patterns with attached cells and large cell-free areas can be interpreted by a coexistence of crystalline and amorphous pyrite phases.

Attachment to visible imperfections such as cracks, steps or cleavages as described in earlier studies was observed (Gehrke et al. 1998, Edwards and Rutenberg 2001) but was not always detectable. However, the AFM image resolution (scale) in my study was too low to allow the identification of surface defects securely (small mineral imperfections were not visible). A resolution in nm-range on the crystallography of the pyrite coupon surfaces could give more information.

4.3. Conclusion

In order to enhance bioleaching for precious metal winning, or to inhibit bioleaching for the reduction of the environmental impact of acid mine- or acid rock drainage it is important to know whether bacterial attachment and biofilm formation will have an influence on mineral dissolution.

Highly efficient leaching communities can be constructed in vitro, if the efficiency of single strains and their influence on the whole leaching community is known. *L. ferrooxidans* DSM 2705 is the most efficient strain in pyrite dissolution, as my results indicate. However, attachment of *L. ferrooxidans* DSM 2705 was decreased, if it was combined with cells of *A. thiooxidans* DSM 622. Nevertheless, a decrease of pyrite leaching was not observed. If leaching shall be optimized, this result should be considered in combinations of the biocoenosis for further investigations.

The inhibition of unwanted leaching like AMD/ARD could be achieved by the inhibition of most effective leaching bacteria such as *L. ferrooxidans* DSM 2705.

5. Literature

Acuña, J., Rojas, J., Amaro, A., Toledo, H., Jerez, C. (1992). Chemotaxis of *Leptospirillum ferrooxidans* and other acidophilic chemolithotrophs: comparison with the *Escherichia coli* chemosensory system. FEMS Microbiol. Lett., 96, pp. 37 - 42.

Akcila, A., Ciftcia, H., Devecib, H. (2007). Role and contribution of pure and mixed cultures of mesophiles in bioleaching of a pyritic chalcopyrite concentrate. Miner. Eng., 20, pp. 310 - 318.

Amann, R., Fuchs, B., Behrens, S. (2001). The identification of microorganisms by fluorescence in situ hybridisation. Curr. Opin. Biotechnol., 12, pp. 231 - 236.

Amann, R., Krumholz, L., Stahl, D. (1990). Fluorescent-oligonucleotide probing of whole cells for determinative, phylogenetic, and environmental studies in microbiology. J. Bacteriol., 172, pp. 762 - 770.

Amann, R., Ludwig, W., Schleifer, K.-H. (1995). Phylogenetic identification and in situ detection of individual microbial cells without cultivation. Microbiol. Rev., 59, pp. 143 - 169.

Andrews, G. (1988). The selective adsorption of *Thiobacilli* to dislocation sites on pyrite surfaces. Biotechnol. Bioeng., 31, pp. 378 - 381.

Anonymous. (1984). Bestimmung von Eisen, E1, In: Deutsche Einheitsverfahren zur Wasser-, Abwasser- und Schlammuntersuchung. Weinheim, Germany: Verlag Chemie.

Bacela-Nicolau, P., Johnson, D. (1999). Leaching of pyrite by acidophilic heterotrophic iron-oxidizing bacteria in pure and mixed cultures. Appl. Environ. Microbiol., 65, pp. 585 - 590.

Balashova, V., Vedinina, I. Y., Markosyan, G., Zavarzin, G. (1974). The autotrophic growth of *Leptospirillum ferrooxidans*. Microbiology (English translation of Mikrobiologiya), 43, pp. 491 - 494.

Barker, B., Banfield, J. (2003). Microbial communities in acid mine drainage. FEMS Microbiol. Ecol., 44, pp. 139 - 152.

Barnes, H., Romberger, S. (1968). The chemical aspects of acid mine drainage. J. Water Pollut. Control Fed., 40, pp. 371 - 384.

Barton, L., Shively, J. (1968). Thiosulfate utilization by *Thiobacillus thiooxidans* ATCC 8085. J. Bacteriol., 95, p. 720.

Battaglia, F., Morin, D., Garcia, J.-L., Ollivier, P. (1994). Isolation and study of two strains of *Leptospirillum*-like bacteria from a natural mixed population cultured on a cobaltiferrous pyrite substrate. Antonie van Leeuwenhoek, 66, pp. 295 - 302.

Beard, S., Paradela, A., Albar, J., Jerez, C. (2011). Growth of *Acidithiobacillus ferrooxidans* ATCC 23270 in thiosulfate under oxygen-limiting conditions generates extracellular sulfur globules by means of a secreted tetrathionate hydrolase. Front. Microbio., 2, doi: 10.3389/fmicb.2011.00079.

Beech, I., Smith, J., Steele, A., Penegar, I., Campbell, S. (2002). The use of atomic force microscopy for studying interactions of bacterial biofilms with surfaces. Colloid. Surface. B, 23, pp. 231 - 247.

Bevilaqua, D., Garcia, O., Tuovinen, O. (2010). Oxidative dissolution of bornite by *Acidithiobacillus ferrooxidans*. Process. Biochem., 45, pp. 101 - 106.

Binning, G., Quate, C., Gerber, C. (1986). Atomic force microscopy. Rev. Lett., 56, pp. 930 - 933.

Bird, L., Bonnefoy, V., Newman, D. (2011). Bioenergetic challenges of microbial iron metabolisms. Trends. Microbiol., 19, pp. 330 - 340.

Bond, P., Banfield, J. (2001). Design and performance of rRNA targeted oligonucleotide probes for in situ detection and phylogenetic identification of microorganisms inhabiting acid mine drainage environments. Microb. Ecol., 41, pp. 149 - 161.

Bond, P., Smriga, S., Banfield, J. (2000). Phylogeny of microorganisms populating a thick, subaerial, predominantly lithotrophic biofilm at an extreme acid mine drainage site. Appl. Environ. Microbiol., 66, pp. 3842 - 3849.

Bosecker, K. (1997). Bioleaching: metal solubilization by microorganisms. FEMS Microbiol. Rev., 20, pp. 591 - 604.

Brierley, C. (1997). Mining Biotechnology: Research to commercial development and beyond. In D. Rawlings, Biomining: Theory, Microbes and Industrial Processes (pp. 3 - 17). Berlin, Deutschland: Springer.

Bryant, R., Costerton, J., Laishley, E. (1984). The role of *Thiobacillus albertis* glycocalyx in the adhesion of cells to elemental sulfur. Can. J. Microbiol., 30, pp. 81 - 90.

Brock, T., Gustafson, J. (1976). Ferric iron reduction by sulfur- and iron-oxidizing bacteria. Appl. Environ. Mirobiol., 32, pp. 567 - 571.

Brunauer, S., Emmett, P., Teller, E. (1938). Adsorption of gases in multimolecular layers. J. Amer. Chem. Soc., 30, pp. 309 - 319.

Busscher, H., Sjollema, J., van der Mei, H. (1990). Relative importance of surface free energy as a measure of hydrophobicity in bacterial adhesion to solid surfaces. In R. Doyle, M. Rosenberg, Microbial Cell Surface Hydrophobicity (pp. 335 - 359). Washington: American Society for Microbiology.

Chan, C., Suzuki, I. (1994). Thiosulfate oxidation by sulfur-grown *Thiobacillus thiooxidans* cells, cell-free extracts, and thiosulfate-oxidizing enzyme. Can. J. Microbiol., 40, pp. 816 - 822.

Chen, Y., Busscher, H., van der Mei, H., Norde, W. (2011). Statistical analysis to substratum surfaces as measured using atomic force microscopy. Appl. Environ. Microbiol., 77, pp. 5065 - 5070.

Colmer, A., Hinkel, M. (1947). The role of microorganisms in acidic mine drainage: a preliminary report. Science, 106, pp. 253 - 256.

Cullander, C. (1999). Fluorescent probes for confocal microscopy. Methods Mol. Biol., 122, pp. 59 - 73.

Curutchet, G., Pogliani, C., Donati, E. (1995). Indirect bioleaching of covellite by *Thiobacillus thiooxidans* with an oxidant agent. Biotechnol. Lett., 17, pp. 1251 - 1256.

DeLong, E., Wickham, G., Pace, N. (1989). Phylogenetic strains: ribosomal RNA-based probes for the identification of single cells. Science, 243, pp. 1360 - 1363.

DiSpirito, A., Tuovinen, O. (1982a). Uranous ion oxidation and carbon dioxide fixation by *Thiobacillus ferrooxidans*. Arch. Microbiol., 133, pp. 28 - 32.

DiSpirito, A., Silver, M., Voss, L., Tuovineni, O. (1982b). Flagella and pili of iron-oxidizing *Thiobacilli* isolated from an uranium mine in northern Ontario, Canada. Appl. Environ. Mirobiol., 43, pp. 1196 - 1200.

Doetsch, R., Cook, T., Vaituzis, Z. (1967). On the uniqueness of the flagellum of *Thiobacillus thiooxidans*. Antonie van Leeuwenhoek J. Microbiol. Serol., 33, pp. 196 - 202.

Donlan, R. (2002). Biofilms: Microbial life on surfaces. Emerg. Infectious. Dis., 8, pp. 881 - 890.

Dopson, M., Lindström, E. (1999). Potential role of *Thiobacillus caldus* in arsenopyrite bioleaching. Appl. Environ. Microbiol., 65, pp. 36 - 40.

Drobner, E., Huber, H., Stetter, K. (1990). *Thiobacillus ferrooxidans*, a facultative hydrogen oxidizer. Appl. Environ. Mirobiol., 56, pp. 2922 - 2923.

Edelbro, R., Sandström, Å., Paul, J. (2003). Full potential calculations on the electron bandstructures of sphalerite, pyrite and chalcopyrite. Appl. Surf. Sci., 206, pp. 300 - 313.

Edwards, K., Rutenberg, A. (2001). Microbial response to surface microtopography: The role of metabolism in localized mineral dissolution. Chem. Geol., 180, pp. 19 - 32.

Edwards, K., Bond, P., Banfield, J. (2000). Characteristics of attachment and growth of *Thiobacillus caldus* on sulphide minerals: a chemotactic response to sulphur minerals. Environ. Microbiol., 2 (3), pp. 324 - 332.

Edwards, K., Gihring, T., Banfield, J. (1999). Seasonal variations in microbial populations and environmental conditions in an extreme acid mine drainage environment. Appl. Environ. Microbiol., 65, pp. 3627 - 3632.

Edwards, K., Schrenk, M., Hamers, R., Banfield, J. (1998). Microbial oxidation of pyrite: Experiments using microorganisms from an extreme acidic environment. Am. Mineral., 83, pp. 1444 - 1453.

Ehrhardt, C., Banas, E., Janik, J. (1968). Application of spherically curved chrystals for X-ray fluorescence. Appl. Spectrosc., 22, pp. 730 - 735.

Engel, A., Schoenenberger, C.-A., Müller, D. (1997). High-resolution imaging of native biological sample surfaces using scanning probe microscopy. Curr. Opin. Struc. Biol., 7, pp. 279 - 284.

Espejo, R., Romer, P. (1987). Growth of *Thiobacillus ferrooxidans* on elemental sulfur. Appl. Environ. Microbiol., 53, pp. 1907 - 1912.

Etzel, K. (2008). Biological and abiotic dissolution of natural, cut and synthetic pyrite surfaces. Dissertation. Kiel.

Farah, C., Vera, M., Morin, D., Haras, D., Jerez, C., Guiliani, N. (2005). Evidence for a functional quorum-sensing type Al-1 system in the extremophilic bacterium *Acidithiobacillus ferrooxidans*. Appl. Environ. Microbiol., 71, pp. 7033 - 7040.

Fife, D., Bruhn, D., Miller, K., Stoner, D. (2000). Evaluation of a fluorescent lectin-based staining technique for some acidophilic mining bacteria. Appl. Environ. Microbiol., 66, pp. 2208 - 2210.

Fischer, J., Quentmeier, A., Gansel, S., Sabados, V., Friedrich, C. (2002). Inducible aluminium resistance of *Acidiphilum cryptum* and aluminium tolerance of other acidophilic bacteria. Arch. Microbiol. , 178, pp. 554 - 558.

Florian, B., Noël, N., Thyssen, C., Felschau, I., Sand, W. (2011). Some quantitative data on bacterial attachment to pyrite. Miner. Eng., 24, pp. 1132 - 1138.

Florian, B., Noël, N., Sand, W. (2010). Visualization of initial attachment of bioleaching bacteria using combined atomic force and epifluorescence microscopy. Min. Eng., 23, pp. 532 - 535.

Florian, B. (2007). Study of the attachment behavior of moderate thermophilic bacteria to metal sulfides. Master thesis. Aquatische Biotechnologie, Universität Duisburg-Essen, Duisburg.

Fub, B., Zhoua, H., Zhanga, R., Qiua, G. (2008). Bioleaching of chalcopyrite by pure and mixed cultures of *Acidithiobacillus spp*. and *Leptospirillum ferriphilum*. Int. Biodeter. Biodegr., 62, pp. 109 - 115.

Garcia, O., Bigham, J., Tuovinen, O. (1995). Oxidation of galena by *Thiobacillus ferrooxidans* and *Thiobacillus thiooxidans*. Can. J. Microbiol., 41, pp. 508 - 514.

Gehrke, T., Hallmann, R., Kinzler, K., Sand, W. (2001). The EPS of *Acidithiobacillus ferrooxidans* - a model for structure-function relationships of attached bacteria and their physiology. Water. Sci. Technol., 43, pp. 159 - 167.

Gehrke, T., Hallmann, R., Sand, W. (1995). Importance of exopolymers from *Thiobacillus ferrooxidans* and *Leptospirillum ferrooxidans* for bioleaching. In T. Vargas, C. Jerez, J. Wiertz, H. Toledo, Biohydrometallurgy processing. Santiago.

Gehrke, T., Telegdi, J., Thierry, D., Sand, W. (1998). Importance of extracellular polymeric substances from *Thiobacillus ferrooxidans* for bioleaching. Appl. Environ. Microbiol., 64, pp. 2743 - 2747.

Goebel, B., Stackebrandt, E. (1994). Cultural and phylogenetic analysis of mixed microbial populations found in natural and commercial bioleaching environments. Appl. Environ. Microbiol., 60, pp. 1614 - 1621.

Göksel, A. (2000). Einfluss der extracellulären, polymeren Substanzen (EPS) auf die Oxidation von Elementarschwefel von acidophilen Laugungsbakterien. Diplomarbeit. Bteilung Mikrobiologie, Institut für Allgemeine Botanik, Universität Hamburg.

Gomez, C., Bosecker, K. (1999). Leaching heavy metals from contaminated soil by using *Thiobacillus ferrooxidans* or *Thiobacillus thiooxidans*. Geomicobiol. J., 16, pp. 233 - 244.

González-Toril, E., Gómez, F., Malki, M., Amils, R. (2006). The isolation and study of acidophilic microorganisms. In F. Rainey, A. Oren, Extremeophiles- Methods in Microbiology (Vol. 35, pp. 471 - 510). Amsterdam, Netherlands: Elsevier/Academic Press.

Gray, N. (1996). Environmental impact and remediation of acid mine drainage: a management problem. Environ. Geol., 30, pp. 62 - 71.

Grundwell, F. (1988). The influence of the electronic structure of solids on the anodic dissolution and leaching of semiconducting sulphide minerals. Hydrometallurgy, 21, pp. 155 - 190.

Guidone, G. (1998). Physiologische Untersuchungen an vier Stämmen der Gattung "*Leptospirillum*". Diplomarbeit. Institut für Allgemeine Botanik, Universität Hamburg.

Hallberg, K., Hedrich, S., Johnson, D. (2011). *Acidiferrobacter thiooxydans*, gen. nov. sp. nov.; an acidophilic, thermo-tolerant, facultatively anaerobic iron- and sulfur-oxidizer of the family *Ectothiorhodospiraceae*. Extremophiles, 15, 271–279.

Hallmann, R., Friedrich, A., Koops, H.-P., Pommerening-Roeser, A., Rohde, K., Zenneck, C., et al. (1992). Physiological characteristics of *Thiobacillus ferrooxidans* and *Leptospirillum ferrooxidans* and physicochemical factors influence microbial metal leaching. Geomicrobiol. J., 10, pp. 193 - 206.

Harneit, K., Göksel, A., Kock, D., Klock, J., Gehrke, T., Sand, W. (2006). Adhesion to metal sulfide surfaces by cells of *Acidithiobacillus ferrooxidans*, *Acidithiobacillus thiooxidans* and *Leptospirillum ferrooxidans*. Hydrometallurgy, 83, pp. 245 - 254.

Harrison, A., Norris, P. (1985). *Leptospirillum ferrooxidans* and similar bacteria: some characteristics and genomic diversity. FEMS Microbiol. Biotechnol. Let., 30, pp. 99 - 102.

Harrison, A. (1982). Genomic and physiological diversity amongst strains of *Thiobacillus ferrooxidans*, and genomic comparison with *Thiobacillus thiooxidans*. Arch. Microbiol., 131, pp. 68 - 76.

Harrison, A. (1981). *Acidiphilium cryptum* gen. nov., sp. nov., heterotrophic bacterium from acidic mineral environments. Int. J. Syst. Bacteriol., 31, pp. 327 - 332.

Hazeu, W., Batenburg-van der Vegte, W., Bos, P., van der Pas, R., Kuenen, J. (1988). The production and utilization of intermediary elemental sulfur during the oxidation of reduced sulfur compounds by *Thiobacillus ferrooxidans*. Arch. Microbiol., 150, pp. 574 - 579.

Hippe, H. (2000). *Leptospirillum* gen. nov. (ex Markosyan 1972), nom. rev., including *Leptospirillum ferrooxidans* sp. nov. (ex Markosyan 1972), nom. rev. and *Leptospirillum*

thermoferrooxidans sp. nov. (Golovacheva et al. 1992). Int. J. Syst. Evol. Microbiol., 50, pp. 501 - 503.

Holuscha, D. (2010). Visualization of extracellular polymeric substances during attachment to metal sulfides by acidophilic microorganisms. Master Thesis, Universität Duisburg-Essen .

Hongyu, M., Chen, Q., Du, J., Tang, L., Qin, F., Miao, B., et al. (2011). Ferric reductase activity of the ArsH protein from *Acidithiobacillus ferrooxidans*. J. Microbiol. Biotechnol., 21, pp. 464 - 469.

Ingledew, W. (1982). *Thiobacillus ferrooxidans* the bioenergetics of an acidophilic chemolithotroph. Bioch. Biophys. Acta., 683, pp. 89-117.

Jiao, Y., Cody, G., Harding, A., Wilmes, P., Schrenk, M., Wheeler, K., et al. (2010). Characterization of extracellular polymeric substances from acidophilic microbial biofilms. Appl. Environ. Microbiol., 76, pp. 2916 - 2922.

Jones, G., Starkey, R. (1961). Surface-active substances produced by *Thiobacillus thiooxidans*. J. Bacteriol., 81, pp. 788 - 789.

Jones, D., Albrecht, H., Dawson, K., Schaperdoth, I. (2011). Community genomic analysis of an extremely acidophilic sulfur-oxidizing biofilm. ISME J online publication, p. doi:10.1038/ismej.2011.75.

Karavaiko, G., Turova, T., Kondrat'eva, T., Lysenko, A., Kolganova, V., Ageeva, S., et al. (2003). Phylogenetic heterogeneity of the species *Acidithiobacillus ferrooxidans*. Int. J. Syst. Evol. Micr., 53, pp. 113 - 119.

Kelly, D., Wood, A. (2000). Reclassification of some species of *Thiobacillus* to the newly designated genera *Acidithiobacillus* gen. nov., *Halothiobacillus* gen. nov. and *Thermithiobacillus* gen. nov. Int. J. Syst. Evol. Microbiol., 50, pp. 511 - 516.

Kimura, S., Coupland, K., Hallberg, K., Johnson, D. (2003). Composition of biofilm communities in acidic mine waters as revealed by combined cultivation and biomolecular approaches. Proceedings of the 15th International Biohydrometallurgy Symposium, pp. 1057 - 1065.

Kinzler, K., Gehrke, T., Telegdi, J., Sand, W. (2003). Bioleaching - a result of interfacial processes caused by extracellular polymeric substances (EPS). Hydrometallurgy, 71, pp. 83 - 88.

Klock, J.-H. (2003). Oxidationsaktivität, extracelluläre polymere Substanzen und Anheftung an Metallsulfide bei *Leptospirillum ferrooxidans*. Diplomarbeit. Abteilung Mikrobiologie, Institut für Allgemeine Botanik, Universität Hamburg.

Kock, D., Schippers, A. (2008). Quantitative microbial community analysis of three different sulfidic mine tailing dumps generating acid mine drainage. Appl. Environ. Mircrob., 74, pp. 5211 - 5219.

Kock, D., Graupner, T., Rammlmair, D., Schippers, A. (2007). Quantification of microorganisms involved in cemented layer formation in sulfidic mine waste tailings. Adv. Mater. Res., 20/21, pp. 481 - 484.

Kock, D. (2003). Untersuchung zur Anheftung von *Acidithiobacillus ferrooxidans* an verschiedenen Mineralen. Diplomarbeit. Abteilung Mikrobiologie, Institut für Allgemeine Botanik, Universität Hamburg.

König, R., Winkler, G. (1989). C. Plinius Secundus d. Ä. Naturkunde. In R. König, K. Bayer, Lateinisch-Deutsch Buch XXXIV. Metallurgie. München.

Landesman, J., Duncan, D., Walden, C. (1966). Oxidation of inorganic sulfur compounds by washed cell suspensions of *Thiobacillus ferrooxidans*. Can. J. Microbiol., 12, pp. 957 - 964.

Leduc, L., Ferroni, G. (1994). The chemolithotrophic bacterium *Thiobacillus ferrooxidans*. FEMS Microbiol., 14, pp. 103 - 120.

Li, Y.-Q., Wan, D.-S., Huang, S.-S., Leng, F.-F., Yan, L., Ni, Y.-Q., et al. (2010). Type IV pili of *Acidithiobacillus ferrooxidans* are necessary for sliding, twitching motility, and adherence. Curr. Microbiol., 60, pp. 17 - 24.

Liu, H.-L., Chen, B.-Y., Lan, Y.-W., Cheng, Y.-C. (2003). SEM and AFM images after bioleaching by the indigenous *Thiobacillus thiooxidans*. Appl. Microbiol. Biotechnol., 62, pp. 414 - 420.

Lizama, H., Suzuki, I. (1991). Interaction of chalcopyrite and sphalerite with pyrite during leaching by *Thiobacillus ferrooxidans* and *Thiobacillus thiooxidans*. Can. J. Microbiol., 37, pp. 304 - 311.

Loosdrecht, M., Lyklema, J., Norde, W., Zehnder, J. (1990). Influence of interfaces on microbial activity. Microbiol. Rev., 54, pp. 75 - 87.

Luther III, G. (1987). Pyrite oxidation and reduction: Molecular orbital theory consideration. Geochim. Cosmochim. Acta., 51, pp. 3193-3199.

Mackintosh, M. (1978). Nitrogen fixation by *Thiobacillus ferrooxidans*. J. Gen. Microbiol., 105, pp. 215 - 218.

Mafanya, K. (2007). The study of the attachment behaviour of different strains of *Acidithiobacillus* spp. to pyrite. Master thesis. Aquatische Biotechnologie, Universität Duisburg-Essen, Duisburg.

Mangold, S., Harneit, K., Rohwerder, T., Claus, G., Sand, W. (2008 a). Novel combination of atomic force microscopy and epifluorescence microscopy for visualization of leaching bacteria on pyrite. Appl. Environ. Microbiol., 74, pp. 410 - 415.

Mangold, S., Laxander, M., Harneit, K., Rohwerder, T., Claus, G., Sand, W. (2008 b). Visualization of *Acidithiobacillus ferrooxidans* biofilms on pyrite by atomic force microscopy and epifluorescence microscopy under various conditions. Hydrometallurgy, 94, pp. 127 - 132.

Mangold, S. (2006). Attachment and leaching rate of different strains of *Acidithiobacillus ferrooxidans* on sulfide minerals. Laboratory project report, University of Duisburg-Essen, Duisburg.

Markosyan, G. (1972). A new iron-oxidizing bacterium - *Leptospirillum ferrooxidans* nov. gen. sp. Biol. J. Armenia, 25, pp. 26 - 29.

Meadows, P. (1971). The attachment of bacteria to solid surfaces. Arch. Microbiol. , 75, pp. 374 - 381.

Medvedev, D., Stuchebrukhov, A. (2001). DNA repair mechanism by photolyase: Electron transfer path from the photolyase catalytic cofactor FADH- to DNA thymine dimer. J. Ther.Biol., 210, pp. 237 - 248.

Moses, C., Nordstrom, D., Herman, J., Mills, A. (1987). Aqueous pyrite oxidation by dissolved oxygen and ferric iron. Geochim. Cosmochim. Acta., 51, pp. 1561 - 1571.

Moter, A., Göbel, U. (2000). Fluorescence in situ hybridization (FISH) for direct visualization of microorganisms. J. Microbiol. Meth., 41, pp. 85 - 112.

Murowchick, J., Barnes, H. (1987). Effect of temperature and degree of supersaturation on pyrite morphology. Am. Mineral., 72, pp. 11 - 12.

Nagaoka, T., Ohmura, N., Saiki, H. (1999). A novel mineral floating process using *Thiobacillus ferrooxidans*. Appl. Environ. Mirobiol., 65, pp. 3588 - 3593.

Natarajan, K. (1990). Electrochemical aspects of bioleaching of base-metal sulfides. In H. Ehrlich, C. Brierley, Microbial Mineral Recovery (pp. 79 - 106). New York: McGraw-Hill.

Neu, T. (1996). Significance of bacterial surface-active compounds in interaction of bacteria with interfaces. Microbiol. Rev., 60, pp. 151 - 166.

Noël, N., Florian, B., Sand, W. (2010). AFM EFM study on attachment of acidophilic leaching organisms. Hydrometallurgy, 104, pp. 370 - 375.

Noël, N. (2008). Comparative study of planktonic and sessile cells in cultures of *Leptospirillum ferriphilum* and *Acidithiobacillus caldus* on pyrite. Master thesis. Aquatische Biotechnologie, Universität Duisburg-Essen, Duisburg.

Norris, P., Murrell, J., Hinson, D. (1995). The potential for diazotrophy in iron- and sulfur oxidizing acidophilic bacteria. Arch. Microbiol., 164, pp. 294 - 300.

Norris, P. (1990). Acidophilic bacteria and their activity in mineral sulfide oxidation. In H. Ehrlich, C. Brierley, Microbial mineral recovery (pp. 3 - 27). New York: McGraw-Hill.

Norris, P., Barr, D., Hinson, D. (1988). Iron and mineral oxidation by acidophilic bacteria: affinities for iron and attachment to pyrite. In P. Norris, D. Kelly. In: Biohydrometallurgy,

proceedings of the international symposium (pp. 43 – 59). Warwick, Antony Rowe Ltd. Chippenham, Wiltshire, UK.

Norris, P. (1983). Iron and mineral oxidation with *Leptospirillum ferrooxidans*. In G. Rossi, A. Torma, Progress in Biohydrometallurgy (pp. 83 - 96). Iglesias, Italy: Associazone Mineraria Sarda.

Norris, P., Kelly, D. (1978). Dissolution of pyrite (FeS2) by pure and mixed cultures of some acidophilic bacteria. FEMS Microbiol. Lett., 4, pp. 143 - 146.

Okibe, N., Johnson, D. (2009). Biooxidation of pyrite by defined mixed cultures of moderately thermophilic acidophiles on pH-controlled bioreactors: significance of microbial interactions. Biotechnol. Bioeng., 87, pp. 574 - 583.

Okibe, N., Gericke, M., Hallberg, K., Johnson, D. (2003). Enumeration and characterization of acidophilic microorganisms isolated from pilot plant stirred-tank bioleaching operation. Appl. Environ. Microbiol., 69, pp. 1936 - 1943.

Pace, D., Mielke, R., Southam, G., Porter, T. (2005). Scanning force microscopy studies of the colonization and growth of A. ferrooxidans on the surface of pyrite minerals. Scanning, 27, pp. 136 - 140.

Parro, V., Moreno-Paz, M. (2004). Nitrogen fixation in acidophile iron-oxidizing bacteria: The nif regulon of *Leptospirillum ferrooxidans*. Res. Microbiol. , 155, pp. 703 - 709.

Parro, V., Moreno-Paz, M. (2003). Gene function analysis in environmental isolates: the nif regulon of the strict iron oxidizing bacterium *Leptospirillum ferrooxidans*. PNAS., 100, pp. 7883 - 7888.

Pistorio, M., Curutchet, G., Donati, E., Tedesco, P. (1994). Direct zinc sulfide bioleaching by *Thiobacillus ferrooxidans* and *Thiobacillus thiooxidans*. Biotechnol. Lett., 16, pp. 419 - 424.

Pivovarova, T., Markosyan, G., Karavaiko, G. (1981). Morphogenesis and fine structure of *Leptospirillum ferrooxidans*. Microbology, 50, pp. 339 - 344.

Porter, K., Feig, Y. (1980). The use of DAPI for identification and counting aquatic microflora. Limnol. Oceanogr., 25, pp. 943 - 948.

Pronk, J., De Bruyn, J., Bos, P., Kuenen, J. (1992). Anaerobic growth of T*hiobacillus ferrooxidans*. Appl. Environ. Microbiol., 58, pp. 2227 - 2230.

Quatrini, R., Appia-Ayme, C., Denis, Y., Jedlicki, E., Holmes, D., Bonnefoy, V. (2009). Extending the model for iron and sulfur oxidation in the extreme acidophilic *Acidithiobacillus ferrooxidans*. BMC Genomics, 10:394, pp. doi:10.1186/1471-2164-10-394.

Qui, M.-Q., Xiong, S.-Y., Zhang, W.-M., Wang, G.-X. (2005). A comparison of bioleaching of chalcopyrite using pure culture or a mixed culture. Miner. Eng., 18, pp. 987 - 990.

Rawlings, D. (2005). Characteristics and adaptability of iron- and sulfur-oxidizing microorganisms used for the recovery of metals from minerals and their concentrates. Microb. Cell Fact. 4. doi:10.1186/1475-2859-4-13

Rawlings, D. (2002). Heavy metal mining using microbes. Annu. Rev. Microbiol., 56, pp. 65 - 91.

Rawlings, D., Tributsch, H., Hansford, G. (1999). Reason why '*Leptospirillum*' -like species rather than *Thiobacillus ferrooxidans* are the dominant iron-oxidizing bacteria in many commercial processes for the biooxidation of pyrite and related ores. Microbiology , 145, pp. 5 - 13.

Rittenberg, S., Grady, R. (1950). Induced mutants of *Thiobacillus thiooxidans* requiring organic growth factors. J. Bacteriol., 60, pp. 509 - 510.

Rodríguez, Y., Ballester, A., Balázquez, M., González, F., Muñoz, J. (2003). Study of bacterial attachment during the bioleaching of pyrite, chalcopyrite, and sphalerite. Geomicrobiol. J., 20, pp. 131 - 141.

Rohwerder, T., Sand, W. (2007a). Mechanisms and biochemical fundamentals of bacterial metal sulfide oxidation. In E. Donati, W. Sand, Microbial Processing of Metal Sulfides (pp. 35 - 58). Dordrecht, Netherlands: Springer.

Rohwerder, T., Sand, W. (2007b). Oxidation of inorganic sulfur compounds in acidophilic prokaryotes. Eng. Life Sci. , 7, pp. 301 - 309.

Rohwerder, T., Sand, W. (2003a). The sulfane sulfur of persulfates is the actual substrate of the sulfur-oxidizing systems from *Acidithiobacillus* and *Acidiphilum* spp. Microbiology, 149, pp. 1699 - 1709.

Rohwerder, T., Gehrke, T., Kinzler, K., Sand, W. (2003b). Bioleaching review part A: Progress in bioleaching: fundamentals and mechanisms of bacterial metal sulfide oxidation. Appl. Microbiol. Biotechnol., 63, pp. 239 - 248.

Rohwerder, T., Schippers, A., Sand, W. (1998). Determination of reaction energy values for biological pyrite oxidation by calorimetry. Thermochim. Acta., 309, pp. 19 - 29.

Rojas-Chapana, J., Tributsch, H. (2004). Interfacial activity and leaching patterns of *Leptospirillum ferrooxidans* on pyrite. FEMS Microbiol. Ecol., 47, pp. 19 - 29.

Ruiz, L., Gonzalez, A., Frezza, M., Soulere, L., Queneau, Y., Doutheau, A., Rohwerder, T., Sand, W., Jerez, C.A., Guiliani, N. (2007). Is the quorum sensing type Al-1 system of *Acidithiobacillus ferrooxidans* involved in its attachment to mineral surfaces? Adv. Mat. Res., 20-21, pp. 345 - 349.

Rzhepishevska, O., Lindstrom, E., Tuovinen, O., Dopson, M. (2005). Bioleaching of sulfidic tailing samples with a novel, vacuum-positive pressure driven bioreactor. Biotechnol. Bioeng., 92, pp. 559 - 567.

Sakaguchi, H., Torma, A., Silver, M. (1976). Microbiological oxidation of synthetic chalcocite and covellite by *Thiobacillus ferrooxidans*. Appl. Environ. Microbiol., 31, pp. 7 - 10.

Sampson, M., Phillips, C., Blake II, R. (2000). Influence of the attachment of acidophilic bacteria during the oxidation of mineral sulfides. Miner. Eng., 13, pp. 373 - 389.

Sand, W., Gehrke, T. (2006). Extracellular polymeric substances mediate bioleaching/biocorrosion via interfacial processes involving iron(III) ions and acidophilic bacteria. Res. Microbiol., 157, pp. 49 - 56.

Sand, W., Gehrke, T., Jozsa, P.-G., Schippers, A. (2001). (Bio)chemistry of bacterial leaching- direct vs. indirect bioleaching. Hydromet., 59, pp. 159 - 175.

Sand, W., Gehrke, T., Hallmann, R., Schippers, A. (1998). Towards a novel bioleaching mechanism. Min. Pro. Ext. Met. Rev. , 19, pp. 97 - 106.

Sand, W., Gehrke, T., Hallmann, R., Schippers, A. (1995). Sulfur chemistry, biofilm, and the (in)direct attack mechanism - a critical evaluation of bacterial leaching. Appl. Microbiol. Biotechnol., 43, pp. 961 - 966.

Sand, W., Rohde, K., Sobotke, B., Zenneck, C. (1992). Evaluation of *Leptospirillum ferrooxidans* for leaching. Appl. Environ. Microb., 58, pp. 85 - 92.

Sand, W. (1989). Ferric iron reduction by *Thiobacillus ferrooxidans* at extremely low pH-values. Biogeochemistry, 7, pp. 195 - 201.

Sanhueza, A., Ferrer, I., Vargas, T., Amils, R., Sanchez, C. (1999). Attachment of *Thiobacillus ferrooxidans* on synthetic pyrite of varying structural and electronic properties. Hydrometallurgy, 51, pp. 115 - 129.

Sauer, K., Camper, A., Ehrlich, G., Costerton, J., Davies, D. (2002). *Pseudomonas aeruginosa* displays multiple phenotypes during development as a biofilm. J. Bacteriol., 184, pp. 1140 - 1154.

Schaeffer, W., Holbert, P., Umbreit, W. (1963). Attachment of *Thiobacillus thiooxidans* to sulfur christals. J. Bacteriol., 85, pp. 137 - 140.

Schippers, A., Breuker, A., Blazejak, K., Bosecker, K., Kock, D., Wright, T. (2010). The biogeochemistry and microbiology of sulfuric mine waste and bioleaching dumps and heaps, and novel Fe(II)-oxidizing bacteria. Hydrometallurgy, 104, pp. 342 - 350.

Schippers, A. (2007). Microorganisms involved in bioleaching and nucleic acid-based molecular methods for their identification and quantification. In E. Donati, W. Sand, Microbial Processing of Metal Sulfides (pp. 3 - 34). Dordrecht, Netherlands: Springer.

Schippers, A., Bosecker, K. (2005). Bioleaching: Analysis of microbial communities dissolving metal sulfides. In J.-L. Barredo, Methods in Biotechnology (Vol. 18: Microbial Processes and Products, pp. 405 - 412). Totowa, New York: Humana Press.

Schippers, A., Sand, W. (1999a). Bacterial leaching of metal sulfides proceeds by two indirect mechanisms via thiosulfate or via polysulfides and sulfur. Appl. Environ. Microbiol., 65, pp. 319 - 321.

Schippers, A., Rohwerder, T., Sand, W. (1999b). Intermediary sulfur compounds in pyrite oxidation: implications for bioleaching and biodepyritization of coal. Appl. Microbiol. Biot., 52, pp. 104 - 110.

Schippers, A. (1998). Untersuchungen zur Schwefelchemie der biologischen Laugung von Metallsulfiden. Dissertation. Hamburg.

Schippers, A., Jozsa, P.-G., Sand, W. (1996). Sulfur chemistry in bacterial leaching of pyrite. Appl. Environ. Microbiol. , 62, pp. 3424 - 3431.

Schippers, A., Hallmann, R., Wentzien, S., Sand, W. (1995). Microbial diversity in uranium mine waste heaps. Appl. Environ. Microbiol., 61, pp. 2930 - 2935.

Schrenk, M., Edwards, K., Goodman, R., Hamers, R., Banfield, J. (1998). Distribution of *Thiobacillus ferrooxidans* and *Leptospirillum ferrooxidans*-implications for generation of acid mine drainage. Science, 279, pp. 1519 - 1522.

Shao, Z., Mou, J., Czajkowsky, D., Yang, J., Yuan, J.-Y. (1996). Biological atomic force microscopy: what is achieved and what is needed. Adv. Phys., 45, pp. 1 - 86.

Shrihari, J., Modak, M., Kumar, R., Gandhi, K. (1995). Dissolution of particles of pyrite mineral by direct attachment of *Thiobacillus ferrooxidans*. Hydrometallurgy, 38, pp. 175 - 187.

Shrihari, J., Kumar, R., Gandhi, K., Natarajan, K. (1991). Role of cell attachment in leaching of chalcopyrite mineral by *Thiobacillus ferrooxidans*. Appl. Microbiol. Biotechnol., 36, pp. 278 - 282.

Silver, S., Thorma, A. (1974). Oxidation of metal sulfides by *Thiobacillus ferrooxidans* grown on different substrates. Can. J. Mirobiol., 20, pp. 141-147.

Silverman, M., Lundgren, D. (1959). Studies on the chemoautotrophic iron bacterium *Ferrooxidans ferrooxidans*. I. An improved medium and harvesting procedure for securing high cell yields. J. Bacteriol., 77, pp. 642 - 647.

Singer, P., Stumm, W. (1970). Acid mine drainage: the rate-determining step. Science, 167, pp. 1121 - 1123.

Stein, S. (2004). Anheftung von *Acidithiobacillus ferrooxidans* an Mineraloberflächen nach Anzucht auf unterschiedlichen Substraten. Diplomarbeit. Biozentrum Klein Flottbek und Botanischer Garten, Universität Hamburg.

Stevens, C., Noaha, K., Andrewsa, G. (1993). Large laboratory scale demonstration of combined bacterial and physical coal depyritization. Fuel, 72, pp. 1601 - 1606.

Strathmann, M., Wingender, J., Flemming, H.-C. (2002). Application of fluorescently labeled lectins for the visualisation and biochemical characterization of polysaccharides in biofilms of Pseudomonas aeruginosa. J. Microbiol. Meth., 50, pp. 237 - 248.

Streudel, R. (1996). Mechanism for the formation of elemental sulfur from aqueous sulfide in chemical and microbiological desulfurization processes. Ind. Eng. Chem. Res., 35, pp. 1417 - 1423.

Suzuki, I., Chan, C., Takeuchi, T. (1992). Oxidation of elemental sulfur to sulfite by *Thiobacillus thiooxidans* cells. Appl. Environ. Microbiol., 58, pp. 3767-3769.

Suzuki, I. (1965). Oxidation of elemental sulfur by an enzyme system of *Thiobacillus thiooxidans*. Biochim. Biophys. Acta., 104, pp. 359 - 371.

Tayler, E., Lower, S. (2008). Thickness and surface density of extracellular polymers on *Acidithiobacillus ferrooxidans*. Appl. Environ. Microbiol., 74, pp. 309 - 311.

Telegdi, J., Keresztes, Z., Pálinkás, G., Kálmán, E., Sand, W. (1998). Microbially influenced corrosion visualized by atomic force microscopy. Appl. Phys., 66, pp. 639 - 642.

Temple, K., Colmer, A. (1951). The autotrophic oxidation of iron by a new bacterium, *Thiobacillus ferrooxidans*. J. Bacteriol., 62, pp. 605 - 611.

Torma, A., Sakaguchi, H. (1978). Relation between the solubility product and the rate of metal sulfide oxidation by *Thiobacillus ferrooxidans*. J. Ferment. Technol., 56, pp. 173 - 178.

Tributsch, H., Bennett, J. (1981a). Semiconductor-electrochemical aspects of bacterial leaching. I. Oxidation of metal sulphides with large energy gaps. J. Chem. Technol. Biotechnol., 31, pp. 565 - 577.

Tributsch, H., Bennett, J. (1981b). Semiconductor-Electrochemical Aspects of Bacterial Leaching. Part 2. Survey of rate-controlling Sulphide Properties. J. Chem. Technol. Biotechnol., 31, pp. 627 - 635.

Tuovinen, O., Bhatti, T., Bigham, J., Hallberg, K., Garcia, J., Lindström, E. (1994). Oxidative dissolution of arsenopyrite by mesophilic and moderately acidophilic thermophiles. Appl. Environ. Mirobiol., 60, pp. 3268 - 3274.

Tyson, G., Chapman, J., Hugenholtz, P., Allen, E., Ram, R., Richardson, P., et al. (2004). Community structure and metabolism through reconstruction of microbial genomes from the environment. Nature, 428, pp. 37 - 43.

Valdés, J., Pedroso, I., Quatrini, R., Hallberg, K., Valenzuela, P., Holmes, D. (2007). Insights into the metabolism and ecophysiology of three *Acidithiobacilli* by comparative genome analysis. Adv. Mat. Res., 20-21, pp. 439 - 442.

van der Aa, B., Dufrêne, Y. (2002). In situ characterization of bacterial extracellular polymeric substances by AFM. Colloid. Surface. B, 23, pp. 173 - 182.

Waksman, S., Joffe, J. (1922). Microorganisms concerned in the oxidation of sulfur in the soil: II. *Thiobacillus thiooxidans*, a new sulfur-oxidizing organism isolated from the soil. J. Bacteriol., 7, pp. 239 - 256.

Weiß, J. (1991). Ionenchromatographie. Weinheim: VCH-Verlagsgesellschaft.

Winans, S., Bassler, B. (2002). Meeting Review: Mob Psychology. J. Bacteriol., 184, pp. 873 - 883.

Wingender, J., Neu, R., Flemming, H.-C. (1999). What are bacterial extracellular polymeric substances? In J. Wingender, R. Neu, H.-C. Flemming, Microbial Extracellular Substances. Characterization, Structure and Function (pp. 1-15). Berlin Heidelberg: Springer-Verlag.

Woese, C. (1987). Bacterial evolution. Microbiol. Rev., 51, pp. 221 - 271.

6. Appendix

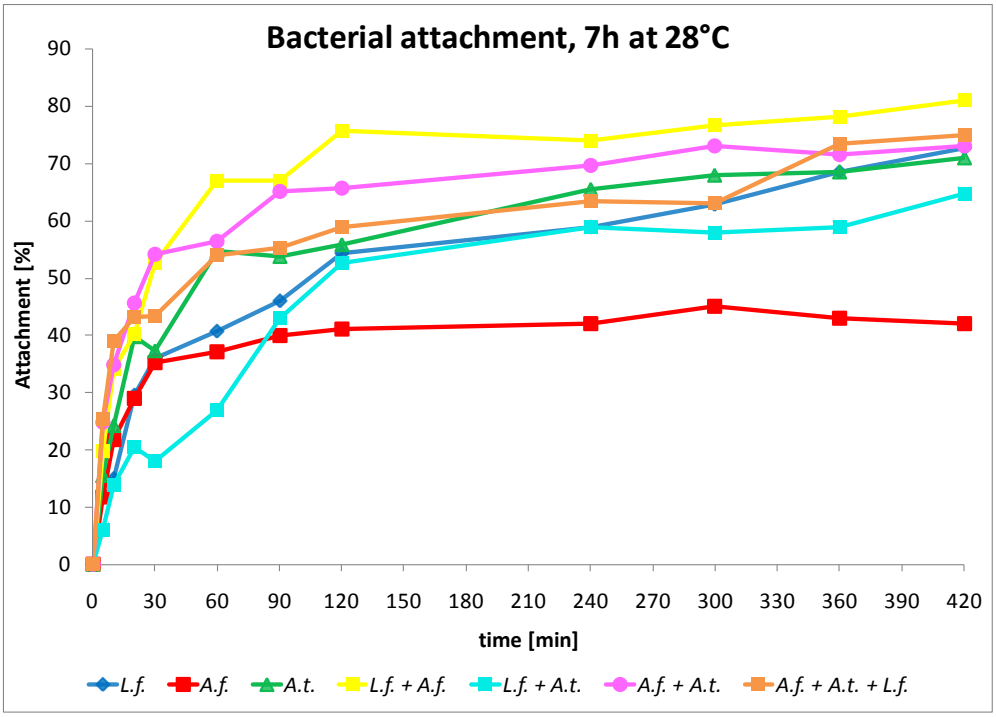

Figure 47: Bacterial attachment to pyrite grains, 7 h at 28 °C
Attachment of *L. ferrooxidans* DSM 2705 (*L.f.*), *A. ferrooxidans* ATCC 23270 (*A.f.*), *A. thiooxidans* DSM 622 (*A.t.*) in pure and mixed cultures to pyrite grains. Initial total cell number $5 \cdot 10^8$ cells/mL (two strains: 50 % each strain respectively; three strains: 33 % each strain respectively), 50 mL basal salt solution, 10 g pyrite grains (50 - 100 µm), 28 °C, shaken (120 rpm).
Standard error (n=6): *L.f.* 17 %, *A.f.* 13 %, *A.t.* 12 %, *L.f.* + *A.f.* 10 %, *L.f.* + *A.t.* 14 %, *A.f.* + *A.t.* 10 %, *A.f.* + *A.t.* + *L.f.* 14 %.

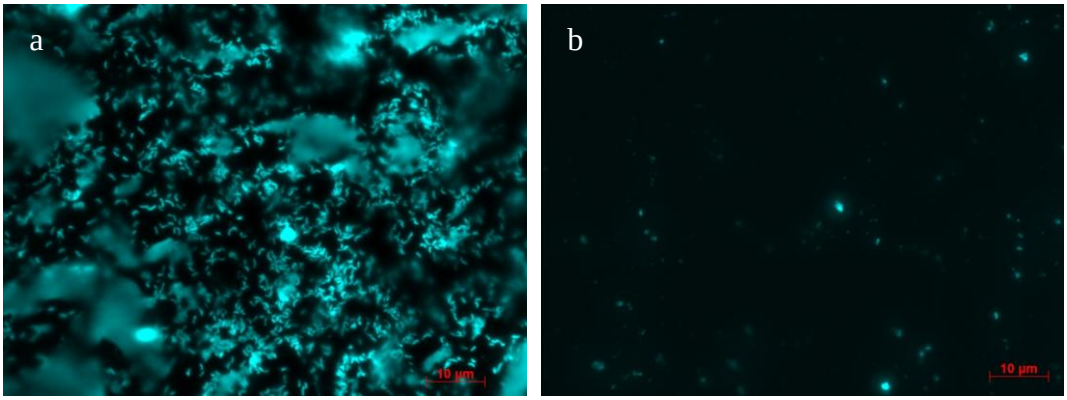

Figure 48 a - b: DAPI stained *L. ferrooxidans* cells on pyrite coupon surface after 1 h
Cells of pure cultures of *L. ferrooxidans* on pyrite coupons. Initial cell number of $1 \cdot 10^8$ cells/mL in 50 mL Mackintosh basal salt solution at 28 °C. Coupon was horizontally incubated in Erlenmeyer flask. Figure a: upper side of the pyrite coupon, figure b: lower side.

List of publication

Book chapter

Rohwerder, T., Florian, B., Bellenberg, S., Wentzien, S., Sand, W. (2008). Monitoring activities of leaching microorganisms at coal sites. In Gerald B. Fosdyke, Coal Mining Research, Technology and Safety. Nova Science Publisher, Inc.

Referenced publications

Florian, B., Noël, N., Bellenberg, S., Huergo, J., Rohwerder, T., Sand, W. (2009). Attachment behavior of leaching bacteria to metal sulfides elucidated by combined atomic force and epifluorescence microscopy. Advanced Materials Research., 71 - 73, pp. 337 - 340.

Sand, W., Florian, B., Noël, N. (2009). Mechanisms of bioleaching and the visualization of these by combined AFM & EFM. Advanced Materials Research., 71 - 73, pp. 297 - 302.

Bellenberg, S., Florian, B., Vera, M.A., Rohwerder, T., Sand, W. (2009). Comparative study of planktonic and sessile cells from pure and mixed cultures of *Acidithiobacillus ferrooxidans* and *Acidiphilium cryptum* growing on pyrite. Advanced Materials Research., 71 - 73, pp. 333 - 336.

Florian, B., Noël, N., Sand, W. (2010). Visualization of initial attachment of bioleaching bacteria using combined atomic force and epifluorescence microscopy. Miner. Eng., 23 pp. 532 - 535

Noël, N., Florian, B., Sand, W. (2010). AFM & EFM study on attachment of acidophilic leaching organisms. Hydrometallurgy, 104, pp. 370 - 375.

Florian, B., Noël, N., Thyssen, C., Felschau, I., Sand, W. (2011). Some quantitative data on bacterial attachment to pyrite. Miner. Eng., 24, pp. 1132 - 1138

Oral presentations

Florian, B., Bellenberg, S., Noël, N., Rohwerder, T., Sand, W. (2008) Visualization and quantification of the initial colonization and biofilm formation on metal sulfides by leaching bacteria. 3rd International Biofilms Conference, 06. - 08.10.2008., Munich, Germany.

Sand, W., Florian, B., Noël, N. (2009). Mechanisms of bioleaching and the visualization of these by combined AFM & EFM. International Biohydrometallurgy Symposium (IBS). 13. - 17. September 2009, San Carlos de Bariloche, Argentina.

Florian, B., Noël, N., Sand, W. (2009) Visualization of the onset of bioleaching -attachment- by combined atomic force and epifluorescence microscopy. BioHydromet '09. 5. - 7. April 2009. Cape Town, South Africa.

Florian, B., Noël, N., Thyssen, C., Felschau, I., Sand, W. (2010) Control of bacterial metal sulfide leaching. BioHydromet '10. 8. – 9. November 2010. Cape Town, South Africa.

Florian, B., Sand, W. (2011). Inhibition of bacterial pyrite leaching by surfactants. IV International conference on environmental, industrial and applied microbiology Biomicroworld, 14. – 16. September 2011, Torremolinos, Malaga, Spain.

Poster presentations

Florian, B., Noël, N., Bellenberg, S., Rohwerder, T., Sand, W. (2008). Initial colonization and biofilm formation of leaching bacteria on metal sulfides studied in pure and mixed cultures. 12th International Symposium on Microbial Ecology – ISME-12 Microbial Diversity - Sustaining the Blue Planet, 17. - 22. August 2008, Cairns, Australia.

Florian, B., Noël, N., Bellenberg, S., Rohwerder, T., Sand, W. (2008). Attachment of leaching bacteria to metal sulfides elucidated by a combination of AFM and EFM. VAAM Jahrestagung 8. - 11. März 2009 in Bochum, Germany.

Florian, B., Noël, N., Bellenberg, S., Huergo, J., Rohwerder, T., Sand, W. (2009) Attachment behavior of leaching bacteria to metal sulfides elucidated by combined atomic force and epifluorescence microscopy. International Biohydrometallurgy Symposium (IBS 2009). 13. - 17. September 2009, San Carlos de Bariloche, Argentina.

Florian, B., Noël, N., Sand, W. (2009). Biofilm formation in bioleaching – how to optimize the process? 5th ASM Conference on Biofilms. 15. - 19. November 2009, Cancun, Mexico.

Noël, N., Florian, B., Sand, W. (2009). AFM- & EFM-study on attachment of acidophilic thermophiles. 5th ASM Conference on Biofilms. 15. - 19. November 2009, Cancun, Mexico.

Florian, B., Noël, N., Sand, W. (2010). Control of bioleaching or acid mine drainage by understanding biofilm formation. Biofilms IV, Winchester October 2010, England.

Der Lebenslauf ist in der Online-Version aus Gründen des Datenschutzes nicht enthalten.

Hiermit versichere ich, dass ich die vorliegende Arbeit mit dem Titel

„Investigation of initial attachment and biofilm formation of mesophilic leaching bacteria in pure and mixed cultures and their efficiency of pyrite dissolution"

selbst verfasst und keine außer den angegebenen Hilfsmitteln und Quellen benutzt habe, und dass die Arbeit in dieser oder ähnlicher Form noch bei keiner anderen Universität eingereicht wurde.

Essen, im Februar 2012